Adsorption of Milk Proteins

Onto Charged Surfaces

by

Dawn Victoria Brooksbank

Submitted in accordance with the requirements for the degree of Ph.D.

The University of Glasgow

Department of Dairy Science

October 1993

TEXT BOUND CLOSE TO THE SPINE IN THE ORIGINAL THESIS

Abstract

The research in this thesis deals with the influence of charge on the adsorption of milk proteins to surfaces. A variety of charged surfaces were used including negatively charged and zwitterionic liposomes prepared from phosphatidylglycerol and phosphatidylcholine respectively and positively and negatively charged polystyrene latices. Adsorption was determined by measuring the increase in the hydrodynamic radius of the particles by photon correlation spectroscopy and also by solution depletion techniques. In some instances, electrophoretic mobility measurements were also used in order to determine changes in the surface charge of the particle as a result of protein adsorption.

The ionic strength and pH of the buffer were found to be important in the adsorption of protein to liposomes. In the absence of NaCl, adsorption did not occur. At low pH values, addition of both κ-casein and β-lactoglobulin to negatively charged liposomes caused very large increases in size presumably as a result of aggregation. At pH6.2, protein layer thicknesses on the negatively charged liposomes were significantly greater than on the zwitterionic ones due to charge repulsion between the negatively charged surface and the negatively charged regions of the proteins. Removal of the negatively charged phosphate groups which form a cluster in the hydrophilic region of β-casein resulted in a reduction in the thickness of the adsorbed protein layer on the negatively charged liposome but did not have any effect on the thickness on the zwitterionic surface. The thickness of adsorbed layers of α_{s1}-, κ-, and β-casein and β-lactoglobulin on the phosphatidylcholine liposomes were all very similar at around 6nm. Addition of α_{s1}-casein to the negatively charged liposomes appeared to cause aggregation as a result of protein molecules bridging between liposomes.

Attempts to determine the fraction of added protein which bound to the surface

of the liposomes were unsuccessful and therefore, the binding of native, dephosphorylated and methyl-esterified β-casein to small, monodisperse, positively and negatively charged polystyrene latices was studied. As with the liposomes, the thickness of the adsorbed β-casein layer was greater on the negatively charged surface. Removal of the phosphate groups from the protein decreased the layer thickness by about 4nm on the negatively charged surface but had relatively little effect on the thickness on the positively charged surface, once again showing the effect of charge interactions. As with dephosphorylation, methylation also reduces the net negative charge of the protein, but by a different mechanism. This also resulted in a reduction in the thickness of the adsorbed protein layers but only after a significant proportion of the free carboxyl groups had been esterified. Thus methylation of 35% of these groups had relatively little effect on the thickness of the layer on the positively charged latex and no effect on the negatively charged, but esterification of a further 9% (equivalent to two residues) caused a substantial decrease in thickness on both surfaces. These changes are believed to result from alterations in both the charge and hydrophilicity of particular regions of the β-casein molecule. Bridging was found to occur when low levels of native or modified β-casein were added to the positively charged latex. Protein loading was found to range from 2.5 to 5.5mg m^{-2} depending on the nature of the protein and the charge on the surface.

The thickness of adsorbed native and dephosphorylated β-casein layers on the negatively charged latex was found to be influenced by the presence of calcium and increasing ionic strength. Increasing levels of either calcium ions or NaCl in the medium resulted in a very pronounced decrease in the thickness of pre-adsorbed phosphorylated β-casein layers. The changes in dephosphorylated protein layers were less pronounced. The results are discussed in terms of the proposed loop-and-train

configuration of the β-casein at the surface of the latex.

The influence of protein phenotype and the extent of glycosylation on the adsorption of κ-casein was also determined. The more highly glycosylated protein molecules, which also had a higher net negative charge, formed thicker layers on the negatively charged surface. Again, layer thicknesses were less on the positively charged surface, but for each κ-cn phenotype glycosylation increased the thickness, presumably as a result of the increased hydrophilicity of the protein. κ-Casein A, which has one more negative charge than the B phenotype, was found to give a slightly thicker layer on the negatively charged latex. Under certain conditions, adsorbed κ-casein could be cleaved by the enzyme chymosin as shown by the reduction in the size of the coated latex.

Contents

List of figures

List of tables

Acknowledgement

I would like to thank my supervisor at the Hannah Research Institute, Dr. Jeffrey Leaver, for his help and support over the last 3 years. Many thanks to Dr. David S. Horne for his invaluable help with the use and interpretation of photon correlation spectroscopy and electrophoretic mobility data. Thanks are also extended to Mrs. Celia Davidson for her technical help. Thank you to all the staff at the Hannah Research Institute for making my time at the Institute an unforgettable experience.

On a financial note I should like to thank SOAFD for making it possible for me to undertake the project.

Last, but not least, I should like to thank my parents, brother, friends and Ben for their encouragement over the last 3 years.

Author's Declaration

The author confirms that the work submitted is her own work and that appropriate credit has been given where reference has been made to the work of others.

Publications taken from work in this thesis

Published

1. BROOKSBANK, D.V., DAVIDSON, C.M., HORNE, D.S. and LEAVER, J. The Influence of Electrostatic Interactions on Adsorbed Protein Layers. (1993) *Journal of Chemical Society Faraday Transactions*. **89**, 3419-3425.

2. BROOKSBANK, D.V., LEAVER, J. and HORNE, D.S. Adsorption of Milk Proteins to Phosphatidylglycerol and Phosphatidylcholine Liposomes. (1993) *Journal of Colloid and Interface Science*. **161**, 38-42.

In press

1. LEAVER, J., BROOKSBANK, D.V. and HORNE, D.S. Influence of Glycosylation and Surface Charge on the Binding of κ-casein to Latex Particles. *Journal of Colloid and Interface Science*.

Submitted

1. HORNE, D.S., LEAVER, J. and BROOKSBANK, D.V. Electrostatic Interactions in Adsorbed β-casein Layers. *Progress in Colloid and Surface Science*, (Proceedings of VII European Colloid and Interface Science Conference, Bristol, Sept. 1993).

Chapter 1

General Introduction

1.1 Outline

Proteins in foods are the source of amino acids essential to growth and sustenance but in physically manufactured foods they are used to give stability and structure to such foods. Proteins interact with the other ingredients in foods in order to confer stability. Although we are beginning to understand how proteins interact in food systems further information is required in order to maximise their usefulness in the food industry, and in order to predict the properties of particular systems.

The area of interest with which this thesis is concerned is that of protein interactions with surfaces in model food colloid systems and in particular the influence of the charge of both the protein and surface, on these interactions.

The thesis consists of seven chapters. The first constitutes a general introduction to the area of food colloids, whilst the second chapter outlines the structure and physical properties of the proteins used in these investigations. Chapter 3 presents the theory behind some of the techniques employed. Chapters 4-7 detail the results obtained with various natural and modified proteins and discusses the significance of the results.

1.2 Definition of a colloid

Colloids consist of a dispersed phase distributed uniformly in a finely divided state in a dispersion medium. The dispersion medium can be solid, liquid or gas. Examples of colloids include mists and smokes, which are dispersions of fine liquid

droplets or solid particles in gas and are also termed aerosols; milk and mayonnaise, are dispersions of fine droplets of fat in an aqueous phase and are also termed emulsions; butter is also an emulsion but consists of droplets of water in a fat phase; milk is also a gel, which is a dispersion of solid (casein micelles) in a liquid; jellies which are dispersions of macromolecules in liquid and are also termed gels.

Strictly, the definition of a colloid is a system where the dispersed phase lies in the size range 1-1000nm. However, these limits are not rigid, since in some cases, such as emulsions, particles larger than 1000nm may be present.

1.3 Stability of food colloids

A colloid dispersion is stable, if, over a certain period of time, there is only little or no detection of aggregation of the particles. An aggregate is a group of 2 or more solid particles or liquid droplets, held together by unspecified forces. Coagulation and flocculation are terms used to differentiate between compact and loose aggregates. Coagulation produces aggregates with relatively small interparticle distance and is usually irreversible, whilst flocculation produces "flocs" having larger interparticle distances. An additional term is coalescence. This is where two droplets combine to form one larger droplet.

Colloids such as emulsions, need to be stabilised by the addition of an emulsifier. Emulsifiers act by lowering the free energy of the oil/water interface by forming an adsorbed film around the oil droplets. As a result of their amphipathic nature, many proteins are excellent emulsifiers. They are able to bridge across the interfaces by orientating themselves so that the hydrophilic portion of the protein lies in the aqueous phase, and the hydrophobic portion lies in the oil phase.

1.4 Forces involved in colloid stability

The particles in colloidal systems may aggregate *i.e.* stay very close to each other for a much longer time than would be the case in the absence of attractive forces between them. Such aggregation may determine the rheological properties and the appearance of the product, as well as its physical instability. This is reflected in a change in consistency or a loss of homogeneity. Many foods also contain macromolecules (polymers) which may affect aggregation and its rate in a variety of ways.

Whether or not aggregation occurs depends primarily on the interactive forces between the particles. These forces are investigated in colloid science. However, the application of colloid theory to food colloids should be undertaken with care. Colloid theory usually deals with identical, homogeneous, hard spheres. Most foods contain a heterogeneous population of particles ranging in size, shape and deformability. Also food colloids contain proteins which are more complicated than simple polymers. In addition changes may occur, for example, those due to enzymes.

Nevertheless, the application of colloid science can be useful. However, the nature of the system being used must be known first *i.e.* what particles it contains and how they aggregate.

1.4.1 Interaction forces - DLVO theory

For charged colloidal particles the Deryagin-Landau-Verwey-Overbeek (DLVO) theory has proved very useful. This theory considers the free energy, G, required to bring two charged particles from an infinite distance apart to a close distance between their surfaces, h[1,2,3]. There are two components which are additive;

1) electrostatic repulsion between particles, which can be explained as being due to a local increase in osmotic pressure where the ion clouds around charged particles overlap and,

2) van der Waals attraction between identical molecules, and hence particles.

For two identical homogenous spheres of radius, a, in water at room temperature (conditions common in food colloids);

$$G_R \approx 4.3x10^{-9}a\psi_o^2 \log_e(1+e^{-\kappa h}) \qquad (1.4.1)$$

and

$$G_A \approx -Aa/12h \qquad (1.4.2)$$

where, ψ_o, is the surface potential of the particles, often taken as the electrokinetic potential, as this can be obtained more easily, κ is the Debye-Hückel parameter, which is the inverse of the electric double layer. In this case $\kappa \approx 3.3\sqrt{I}$ nm, where I is the total ionic strength (molar). The electric double layer is due to the charge on the colloid surface. Oppositely charged ions (counter ions), are attracted to the particle surface, whereas ions of the same charge (co-ions), are repelled from the surface, so that an ionic atmosphere is formed (Fig. 1.1). A, is the Hamaker constant which depends on the material of the particles and that of the interstitial liquid.

It is therefore possible to calculate the interaction free energy from known or determinable parameters. Fig. 1.2 gives an example. If the minimum near C is deep compared to the average kinetic energy involved in the encounter of two particles (kT), the particles tend to aggregate, *i.e.* particles stay together at the corresponding value of h (secondary minimum). If the maximum near B is not large compared to kT two particles may occasionally move over this energy barrier and become aggregated near,

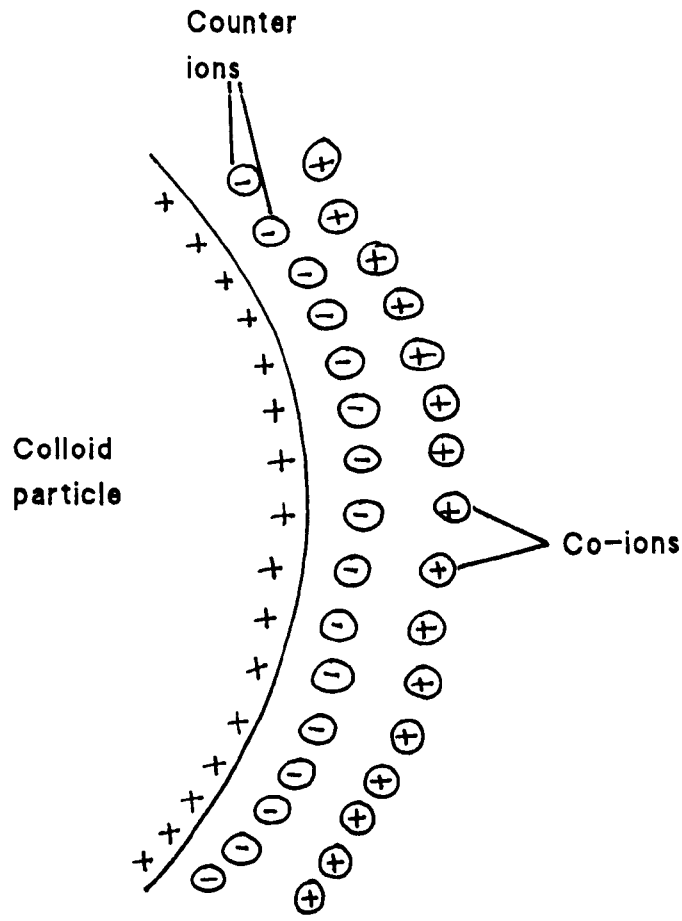

Fig. 1.1. Diagram of the electric double layer at the surface of a colloid particle.

The particle surface has a net charge (+). The ions of opposite charge (counter ions), are attracted to the particle surface where they effectively form a layer. The ions of equal charge to the colloid particle surface (co-ions), are repelled by the colloid particles, but the counter ions will attract the co-ions, so forming a second ionic layer around the colloid particle.

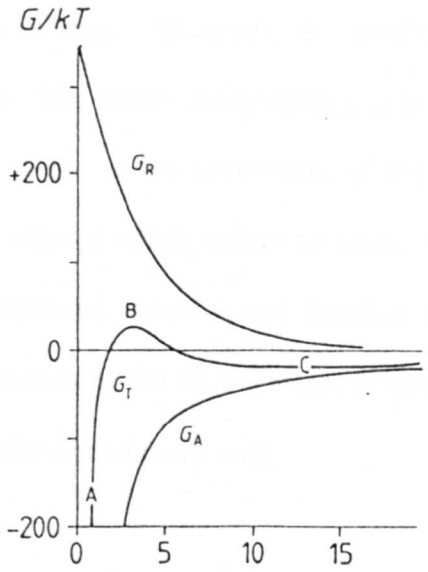

Fig. 1.2. Calculated examples of the repulsive (G_R), attractive (G_A), and total interaction free energy (G_T), as a function of surface separation distance (h), of two identical spheres.

Diagram illustrates electric repulsion and van der Waals attraction. Taken from Walstra[4].

A (in the primary minimum). Lowering the surface potential, *e.g.* by altering the pH, or increasing ionic strength, diminishes the electrostatic repulsion and thereby promotes aggregation.

The DLVO theory has been fairly successful in predicting the aggregation stability of inorganic colloids. However, the predicted effect of particle size is generally not observed. The theory rarely holds true at very small distances, roughly less than 3nm. This is due to the unevenness of the particle surface and also the presence of adsorbed material which cannot be easily accounted for. This adsorbed material may cause additional repulsion and interfere with the determination of the surface potential. Consequently the DLVO theory is rarely exact for food colloids, but has been found to predict trends fairly well.

1.4.2 Steric stabilisation

Polymers present in the continuous (usually aqueous) phase may adsorb onto the particles. If they do not, the polymers usually cause the viscosity of the liquid to be higher. This slows down any aggregation, and may even cause a weak gel to be formed, which will prevent aggregation. Dissolved polymers may also cause aggregation by depletion flocculation. Adsorbed polymers may either prevent aggregation (steric stabilisation) or promote it (bridging flocculation).

Fig. 1.3 shows how macromolecules may adsorb (or be grafted) onto surfaces. Adsorption of the polymer depends on its solubility. The osmotic pressure, Π, of a polymer solution can be used as a guide to polymer solubility. The osmotic pressure is given by;

$$\Pi = RT(c_m + Bc_m^2 + \ldots) \qquad (1.4.3)$$

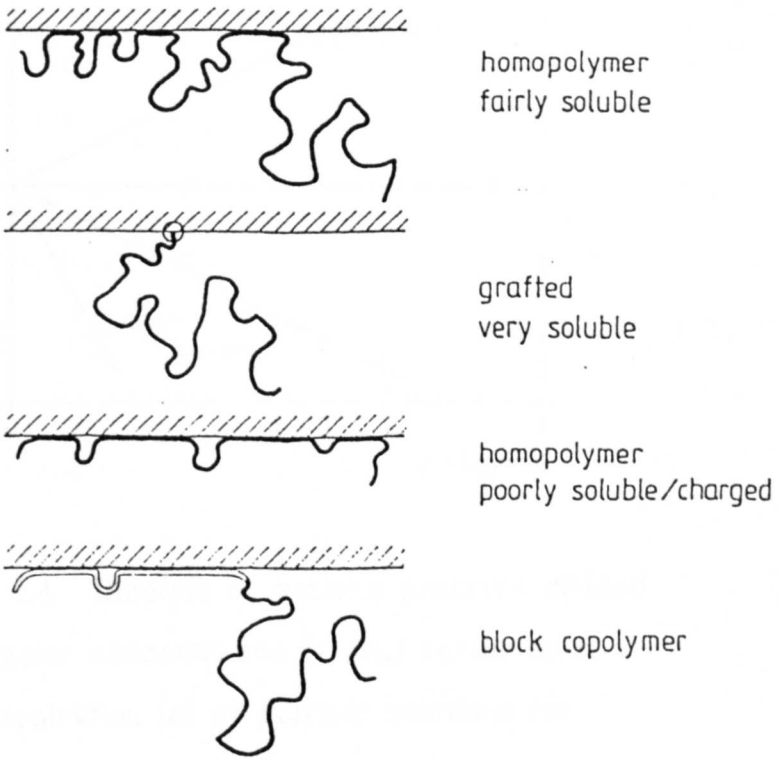

Fig. 1.3. Diagram of the types of protruding macromolecules.

Taken from Walstra[4].

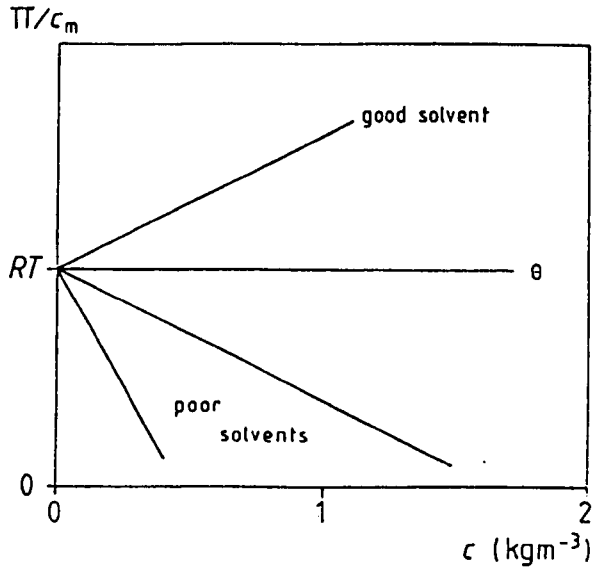

Fig. 1.4. Diagram of osmotic pressure divided by molar concentration (Π/c_m) versus mass concentration (c) of polymer solutions for various kinds of solvent quality.

θ = θ solvent.

Taken from Walstra[4].

where, R, is the gas constant, c_m, is the molar concentration, and, B, is the second virial coefficient, which can be determined fairly easily. Examples are shown in Fig. 1.4. For a good solvent (this curve represents xanthan in water) adsorption is very unlikely. In θ solvents (these occur where forces of attraction between macromolecules are cancelled out by repulsion forces between macromolecules) it is likely, and for poor solvents it is almost certain. In order to have a macromolecule that is both certain to adsorb and also likely to protrude into the solvent, block copolymers are used. Here, part of the macromolecule is poorly soluble and hence adsorbs onto the particle surface, and the other part which is highly soluble, protrudes into the solvent.

Proteins, on the other hand, adsorb in a more complicated way involving various interactions. These include charge-charge (Coulombic), dipole and van der Waals interactions as well as hydrogen bonding. Some portions of the protein will be more attracted to the colloidal surface and other portions will be preferentially attracted to the dispersion medium. As a result the polymer will exist in various orientations. Where the attraction to the particle surface is strongest, the polymer will lie close to the particle forming a "train". In those regions where repulsion from the particle surface is strongest "loops" (within the body of the polymer) or "tails" (if the repulsion occurs at the free ends of the polymer) will be formed.

The adsorbed layers on two colloidal particles can interact in 3 ways;

a) the two layers compress without the layers mixing (interpenetration),

b) the layers interpenetrate but there is no compression,

c) the layers undergo conformational rearrangement without interpenetration or compression occurring.

These options are illustrated in Fig. 1.5.

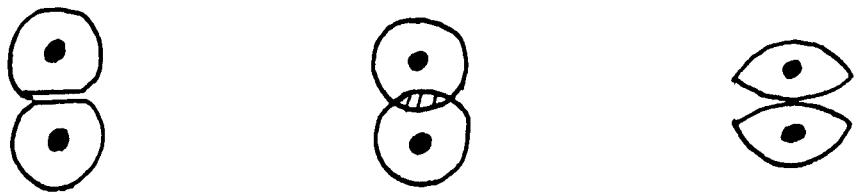

a) b) c)

Fig. 1.5. Different interactions between colloidal particles.

Situation (c) really only occurs with solid particles, and therefore the real situation in food colloids is a mixture of interactions (a) and (b). During collision the loops and tails relax towards their equilibrium configurations, but the distribution of loop size remains constant.

At present there is no comprehensive statistical mechanical theory of steric stabilisation and therefore, a more intuitive method is used. The repulsion between adsorbed macromolecules is mainly entropic and therefore confers a free energy character on steric interaction. The total free energy change is composed of two components, the volume restriction term and the mixing term. These terms are explained in the following sections. For the detailed mathematics concerned in this area, the reader is referred to Dickinson and Stainsby[2]

Volume restriction term

When a surface approaches the protruding macromolecules of another colloid surface, the macromolecules become restricted in their freedom of motion; leading to a decrease in entropy; and hence a repulsive free energy (Fig. 1.6a). A macromolecule

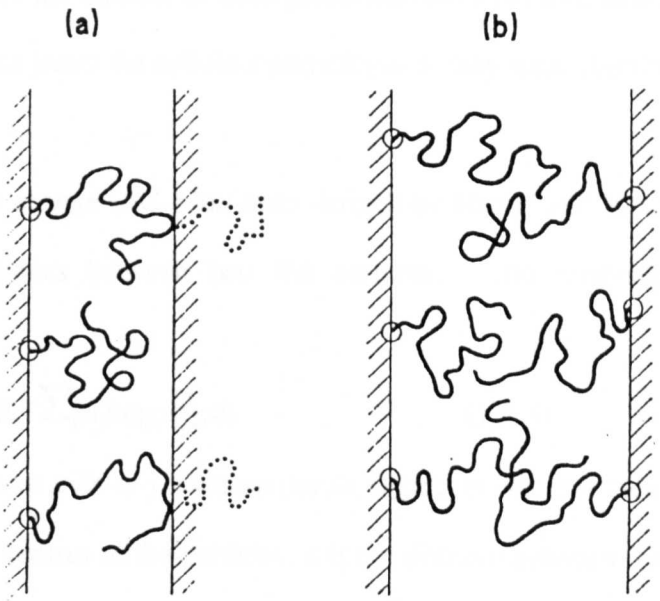

Fig. 1.6. Diagram of the mechanisms of steric repulsion by protruding macromolecules,
(a) volume restriction, (b) mixing.
Taken from Walstra[4].

adsorbed at a surface loses configurational entropy when a second impermeable surface approaches, due to the restricted volume. The entropy change ;

$$\Delta S = kLog_e\{\Omega/\Omega_o\} \qquad (1.4.4)$$

is related to a reduction in the number of configurational states from Ω_o to Ω. k is the Boltzmann constant. This treats the colloidal particles as if they were stabilised by an elastic coating.

The free energy change (ΔG_E) has been derived by Meier[5] and Hesselink[6] by using random-walk statistics between two flat surfaces. The resulting volume restriction term is;

$$\Delta G_E = -2kT\sum_j N_j Log_e R(j,d) \qquad (1.4.5)$$

N_j is the number of loop or tails of j macromolecule segments per unit area and R is the distance between the centres of the particles, d is the distance between the surfaces of the particles and R(j,d) represents the relative loss of configuration for a single loop or tail of j macromolecule segments. This volume restriction term is always positive *i.e.* it causes strong repulsion (unless the macromolecule adsorbs onto the other surface).

Mixing term

Mere volume restriction will, however, rarely occur, since the other surface generally bears macromolecules as well. When adsorbed layers interpenetrate, the increased segment concentration leads to a local osmotic repulsion between the particles. The interpenetration of adsorbed layers corresponds to the mixing of two concentrated macromolecular solutions in the overlapping interpenetration region[7] (Fig. 1.6b). The thermodynamic mixing term (ΔG_M) can then be determined from the

Flory-Huggins theory, assuming that the segment density n° in the overlap region is the sum of the segment densities from each of the colloidal particles. Therefore, from Flory and Krigbaum[8], the free energy of mixing in a volume element δV is;

$$\delta(\Delta G_M) = kT(N_1 \log_e \phi_1 + \chi N_1 \phi_2) \qquad (1.4.6)$$

where, N_1 is the number of solvent molecules contained in δV, ϕ_1 is the solvent volume fraction, and $\phi_2 = 1-\phi_1$ which is the polymer volume fraction. χ is the Flory-Huggins parameter;

$$\chi = (2\epsilon_{12}-\epsilon_{11}-\epsilon_{22})z/2kT \qquad (1.4.7)$$

where, k is the Boltzmann constant, z is the lattice co-ordination number, ϵ_{11} the attractive energy between two solvent molecules, ϵ_{22} the attraction between two solute molecules and ϵ_{12} the attraction between a solvent and a solute segment.

Total interaction energy

The total steric free energy change (ΔG_S) is;

$$\Delta G_S = \Delta G_E + \Delta G_M \qquad (1.4.8)$$

Therefore, if the mixing term becomes sufficiently large and negative to overcome the volume restriction term, attraction between the adsorbed chains can lead to flocculation. This will occur in poor solvents *i.e.* where attraction between segments is greater than the attraction between segments and solvent molecules.

The total interaction energy $\Delta G_T(d)$ between two particles a distance, d, apart is given by;

$$\Delta G_T(d) = U_R(d) + U_A(d) + \Delta G_S(d) \qquad (1.4.9)$$

where, U_R, is the double-layer repulsion term and U_A, is the van der Waals attraction term. It should be noted that these terms are coupled. So that anything that alters the

electrostatics affects $\Delta G_s(d)$ and changes in $\Delta G_s(d)$ affect ζ-potential and hence $U_R(d)$ as well

1.5 Aggregation phenomenon

The food colloids which are of particular interest in this project are emulsions, particularly the oil-in-water (o/w) emulsions. An emulsion may become unstable due to;

a) creaming - movement of droplets under the action of gravity,

b) flocculation - clustering of droplets and,

c) coalescence - spontaneous joining of small droplets into larger ones.

The basic principles underlying these events are briefly explained below.

1.5.1 Creaming

The term "creaming" comes from the spontaneous separation of unhomogenised milk into cream and skim milk. Creaming occurs when the aggregates formed are less dense than the dispersion medium. If the aggregates were more dense, then sedimentation would occur. Both effects are due to the influence of gravity. Creaming is the main process whereby droplets are "removed" from an emulsion, and frequently occurs prior to coalescence. Creaming is inhibited by small droplet size, a highly viscous dispersion medium and a low density difference between the phases. Fat crystallisation may also affect the rate of creaming.

1.5.2 Droplet coalescence

During coalescence two droplets approach each other (a). The surfaces of the

two droplets at the point of contact become thin (b), and then the film bursts to produce one large droplet of lower surface area (c) (Fig. 1.7).

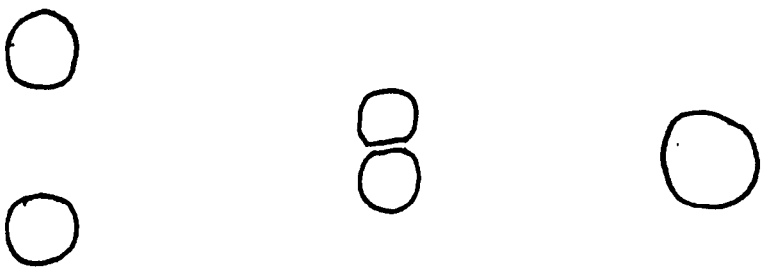

a) b) c)

Fig. 1.7. Diagram of the coalescence between two colloidal particles.

The main barrier to coalescence involves the final stages of thinning and bursting of the film. If the dispersion medium is of high viscosity, as the two droplets approach each other, some of the viscous medium may become trapped between the particles (Fig. 1.8).

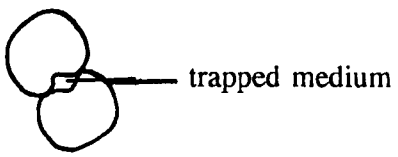

Fig. 1.8. Entrapment of the medium between the two colloidal particles if the medium is a highly viscous one.

The expulsion of this fluid may be a slow process which therefore inhibits coalescence. Thus, the stability of an emulsion to coalescence depends on the resistance to film

thinning and rupture.

1.5.3 Flocculation

Flocculation is the term used to describe the situation where particles aggregate without destroying their individuality. Flocculation is mainly controlled by the nature of the counter ion and under given conditions the effectiveness of the counter ion to cause flocculation is strongly dependent on the valency of this counter ion.

An approximate measure of the influence of an electrolyte on the flocculation of hydrophobic (if in aqueous solution) colloid particles is the critical coagulation concentration (ccc). This is the minimum concentration of counter ions which leads to coagulation under specified conditions of, for example, concentration of colloid particles, rate of addition of counter ions *etc.* The ccc is not always a very reproducible quantity, but it is sufficient to establish the Schultze-Hardy rule. Here, the ccc is determined largely by the valency of the counter ions. As the valency increases so too does the effectiveness in coagulation of negatively charged colloid particles.

There are three types of flocculation;

a) reversible,

b) bridging and

c) depletion.

1.5.3.1 Reversible flocculation

Reversible flocculation may occur under certain conditions in either electrostatically stabilised systems, or in sterically stabilised systems. When two

particles interacting in this way come within range of their mutual attraction, they will tend to form a doublet. This interaction is opposed by Brownian motion of the dispersion medium. Therefore, providing the system is energetically favourable, Brownian motion will act to keep some particles in suspension.

1.5.3.2 Bridging flocculation

Flocculation is not only an electrostatic phenomenon. Adsorption of macromolecules to the colloid particles can also cause flocculation by bridging across two charged particles. Homopolymers adsorbed to the surfaces of closely approaching particles will always make bridges (*i.e.* single molecules become adsorbed simultaneously onto two surfaces) if equilibrium between adsorbed and desorbed homopolymers is attained[9]. However, equilibrium is usually not reached. Since, for bridging to occur the molecules need to be in contact for a relatively long period of time. Brownian motion prevents this from happening.

Bridging does occur if particles covered with adsorbed polymer are mixed with uncovered particles[10]. This occurs if the concentration of the polymer in the solvent is very low, and if very highly surface active polymers are used.

1.5.3.3 Depletion flocculation

Non-adsorbing macromolecules with a radius of gyration, R_g, leave a layer with a thickness approximately equal to R_g around any particle depleted of macromolecules (Fig. 1.9). This causes the osmotic pressure of the system to be higher than in the absence of particles. If the particles come close to each other, the volume of solvent depleted is decreased; leading to a lower osmotic pressure and hence, a decrease in free

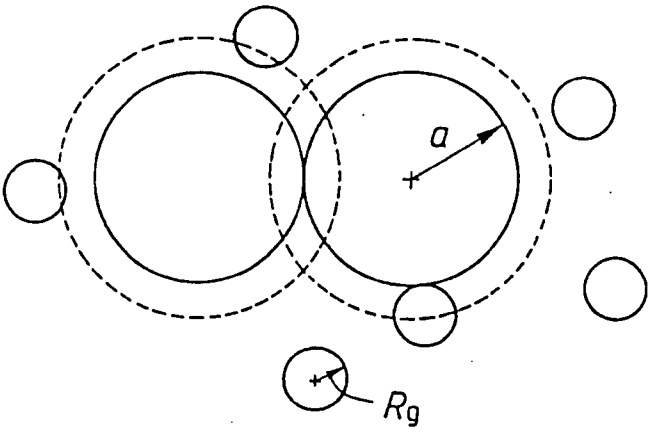

Fig. 1.9. Diagram of the depletion flocculation of macromolecules.

R_g = radius of gyration of a macromolecule.

a = radius of the colloid particle.

Taken from Walstra[4].

energy. This provides a driving mechanism for flocculating the particles. For two hard spheres of radius, a, the interaction free energy is given by[11];

$$G_{dep} = -\pi R_g^2(2a + 4R_g/3)\Pi f(h) \qquad (1.5.1)$$

The function, f(h), decreases from 1 at zero separation distance, to 0 for $h > 2R_g$. So depletion flocculation occurs if R_g is large (*i.e.* high molar mass, good solvent) and if Π is high. For some polysaccharides added to foods, it may be very difficult to determine whether aggregation is caused by (weak) bridging or by depletion[12].

1.6 Protein behaviour in emulsions

In addition to the primary sequence of the amino acid residues which are linked together by peptide bonds, most proteins contain additional components such as lipids, carbohydrates, or specialised groups. Due to the variety of polarity on the amino acids, protein molecules have an amphipathic character. Therefore, adsorption will occur due to removal of non-polar residues from the aqueous environment.

The secondary and tertiary structure of an isolated protein molecule in solution is determined by a delicate balance between intramolecular segmental interactions and interactions between protein segments and water. In oil/water emulsions the non-polar portions of the molecule will be attracted to the oil phase, whilst the polar portions will be attracted to the aqueous phase.

1.6.1 Protein adsorption

Because of their wide range of polarities, proteins are ideal molecules with which to study macromolecular interactions with emulsions. Adsorption of protein onto emulsion droplets results in a protein film being produced.

Depending on the experimental procedure, protein films can be divided into two groups;

a) spread - the protein is literally spread at the o/w interface,

b) adsorbed - protein is adsorbed to the o/w interface from solution.

In dilute spread films the proportion of residues lying on the surface (trains) compared with that solvated by either the oil or water phase (loops and tails) depends on the primary structure of the protein and the experimental conditions. For example, the hydrophobicity of the solvent phase could be changed. Increasing the hydrophobicity leads to an increase in the solubility of the non-polar residues of the protein. In concentrated adsorbed films involving stabilised food colloids, there is a mixture of completely unfolded, partially unfolded and native protein molecules.

The effectiveness of a particular protein as a food emulsifier partly depends on its rate of adsorption at the o/w interface. There are three main stages by which protein adsorbs to the surface[13];

a) diffusion of protein molecules to the surface,

b) spreading and/or unfolding of adsorbed protein molecules and,

c) conformational rearrangement of adsorbed protein molecules.

For further details of the kinetics of these processes the reader is referred to Dickinson and Stainsby[2]. Briefly, the surface concentration increases during process (a), and also in (b), if there is a positive barrier to penetration, but remains constant in process (c). Due to the greater size and complexity of proteins, their adsorption is much slower and more complicated than that which occurs when simple surfactants bind at the oil/water interface.

1.6.2 Irreversibility of protein adsorption

There is some disagreement as to whether, in simple systems, protein adsorption is irreversible or not. Small molecules adsorb at a single site on the particle surface and spontaneously leave the surface a short while after adsorbing. Since proteins adsorb at different points along their polypeptide chains, protein desorption would require the removal of the protein at all these points simultaneously, which is unlikely.

If chemical reactions occur between the protein molecules adsorbed at the lipid surface, then protein desorption ceases. Such chemical bonds include the formation of intermolecular disulphide bonds produced by the disulphide-sulphydryl interchange reaction[14,15].

Experiments with spread and adsorbed films give very different results. This is probably because the experiments are not undertaken in equilibrium conditions. In practice it may take a significant length of time before equilibrium can be reached.

Experiments have shown that protein can be desorbed from the interface using either other proteins[16] or other surfactants[17,18,19,20]. So protein reversibility does seem to occur under certain conditions.

1.6.2.1 Protein displacement from interfaces by surfactants

As a general rule, small amphipathic molecules are more surface-active than proteins in that, at the same concentration (by weight) they lead to a lower interfacial tension at the oil/water interface. It is therefore to be expected that small surfactants will displace proteins from the interface above a certain critical concentration. Competitive adsorption in particular systems is rather sensitive to the nature of protein-surfactant interactions occurring in aqueous solution and at the interface. Protein-

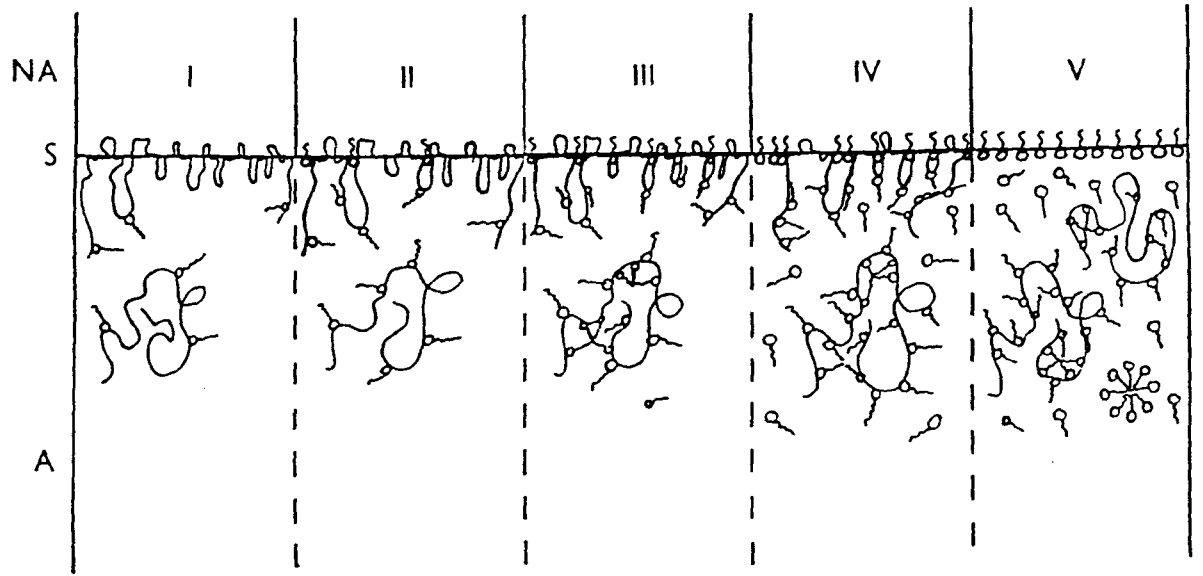

Fig. 1.10. Diagram of protein–surfactant binding and competitive adsorption as a function of increasing surfactant concentration.

The idealised random-chain protein molecules and simple ionic amphiphiles arrange themselves at the surface (S), between the aqueous (A) and non-aqueous (NA) phases. Regions I–V are referred to in the text.

Taken from Dickinson and Woskett[31].

surfactant interactions may be important in the case of latices, since a small amount of surfactant is present in commercially prepared latices. These surfactants will compete with the protein that is subsequently added to the latex suspension.

For a system containing protein plus ionic surfactant, binding can be divided into five regions (I-V in Fig. 1.10). At very low surfactant concentrations (I) the surface tension is essentially the same as that determined with protein alone. The protein predominates at the interface and those surfactant molecules which are present are bound strongly to protein molecules in both the bulk solution and at the interface. Binding is primarily due to electrostatic interactions, but is reinforced by hydrophobic interactions. In region II, the surface tension falls more rapidly with increasing surfactant concentration. It is suggested that there is increasing occupation of surface sites by the adsorption of surfactant molecules in the small gaps between protein train segments caused by the conformational constraints of the adsorbed protein. Because the protein-surfactant complex is more hydrophobic than the native protein, this will also help to reduce the surface tension. Region III, is the intermediate plateau region and extends over a large range of surfactant concentration around the critical micelle concentration (cmc) of the pure surfactant. At some point along this plateau, the surface tension of the mixed protein plus surfactant system becomes higher than that of the pure surfactant. This is despite the fact that the mixed system has more surface-active material. It is presumed that it is more energetically favourable for the surfactant molecules to bind cooperatively on to the protein than it is for them to displace the hydrophobic segments of the protein from the interface. This free energy balance is eventually reversed in region IV, where the protein-surfactant complexes are gradually displaced from the interface. This process may also be, at least partly,

cooperative. In region V, the interface is covered with a surfactant monolayer whilst the bulk solution contains a mixture of surfactant monomers, protein-surfactant complexes and surfactant micelles, with some of the micelles being associated with the protein molecules.

With nonionic surfactants it is generally assumed that the complexes are rather surface-inactive. This is because hydrophobic areas of the protein and nonionic surfactant molecules come together in the binding.

Competition between proteins and small-molecule surfactants can have considerable effect on the behaviour of food emulsions by changing the state of aggregation of the dispersed droplets. For example, bridging flocculation between droplets may be disrupted by using a surfactant to displace protein from the interface[22] which then reduces the emulsion viscosity. Conversely, in whipped toppings displacement of protein from the oil/water interface by addition of low molecular weight emulsifiers leads to an increase in bulk rheological properties caused by partial droplet coalescence at the air/water interface[23].

1.6.2.2 Protein displacement from interfaces by other proteins

Emulsions containing milk proteins are subject to competitive adsorption between disordered polymers (caseins) and globular proteins (whey proteins). Model systems involving β-casein (β-cn), α_s-casein (α_s-cn) and β-lactoglobulin (β-lg) have shown[24,19] that the casein tends to predominate in the adsorbed layer when the two pure proteins are exposed simultaneously to the fresh oil/water interface during emulsification. However, if β-cn is added to an emulsion that has been made with β-lg there is little displacement of the β-lg from the interface and there is a small amount

of additional binding due to β-cn[25]. This contrasts with the addition of β-cn to emulsions made with α_{s1}-cn[26]. Here there is a rapid displacement of α_{s1}-cn. It appears that once globular proteins such as β-lg become established at the oil/water interface, they interact strongly with neighbouring protein molecules[15] which makes them very difficult to displace by other proteins, though they can still be displaced by small surfactants[27,20]. The ability of one protein to displace another is also partly dependent on their relative surface activity. This explains why β-cn displaces the less surface active α_{s1}-cn and also why the reverse does not occur as readily.

1.6.3 Structure of adsorbed films

The structure of adsorbed protein films is more complex than adsorbed layers of small molecules. Graham and Phillips[28,29,30] have extensively investigated the behaviour of a wide range of proteins including the open structured, random coil protein, β-cn and the compact globular protein lysozyme. From their results the structures of these proteins at different surface concentrations has been suggested (Fig. 1.11).

Considering β-cn first, at low concentrations the protein is flattened onto the interface (a). As more protein is packed onto the surface the loop and tail configurations become important (b). As excess protein is added, the layer at the interface remains the same, but multilayers form as more β-cn adsorbs onto the original β-cn layer (c). Analysis of the identity and kinetics of peptide formation resulting from the trypsin-catalysed proteolysis of β-cn stabilized oil/water emulsions[32,33,34] has given additional information on the structure of the adsorbed β-cn. The hydrophilic N-terminal end of the molecule appears to form a loop or tail which projects into the

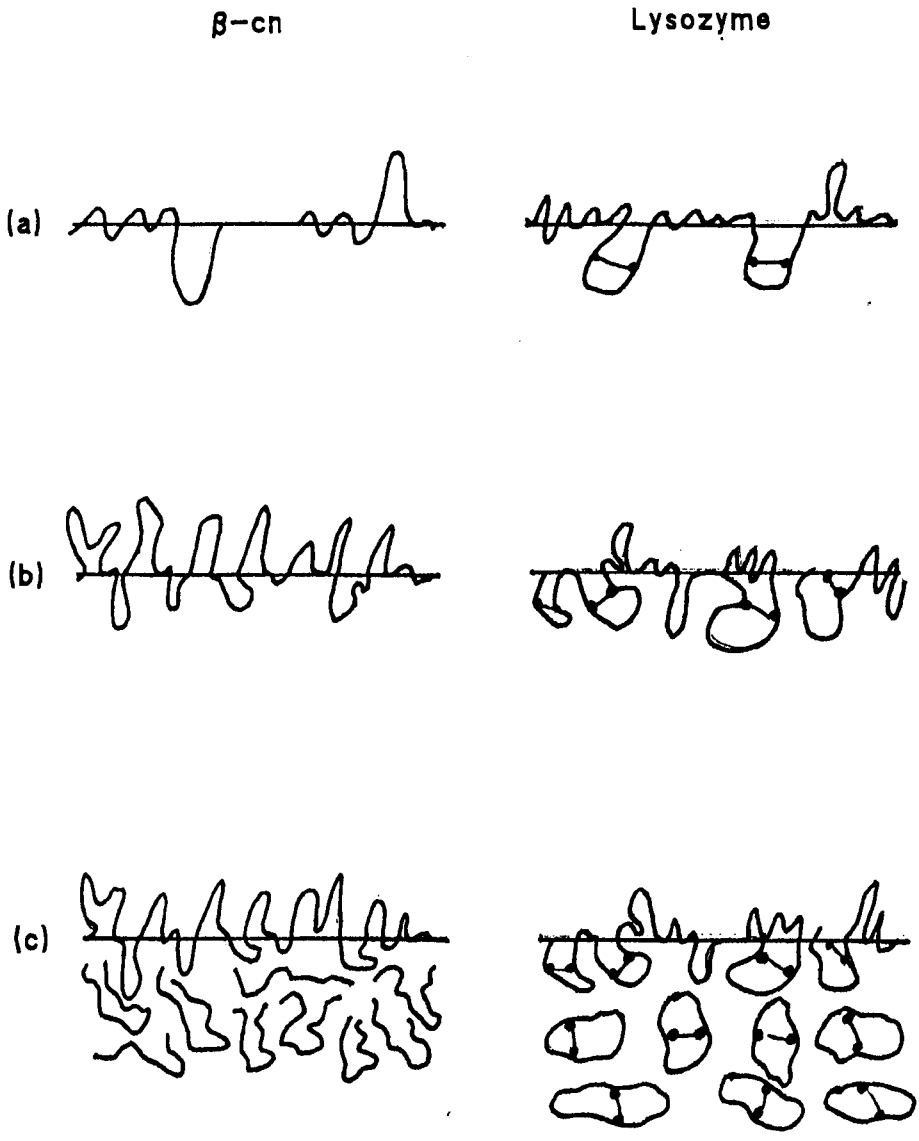

Fig. 1.11. Highly schematic representation of β-cn and lysozyme at the air/water interface at; (a), low, (b), at saturation and, (c), high protein concentrations. •—• represents disulphide bonds. Taken from Dickinson and Stainsby[31].

aqueous phase. Only when most of this region of the β-cn molecule is cleaved is the remainder of the polypeptide attacked by the protease. Furthermore, the nature of the oil phase affects the structure of the adsorbed layer. On the more hydrophilic triglyceride/water interface, the protein is more stretched and more of the trypsin-sensitive sites are accessible than on the more hydrophobic tetradecane/water interface. This has been postulated as being due to some of the less hydrophobic side-chains of the amino acids "dissolving" in the glycerol portion of triglyceride.

Lysozyme molecules have a mainly α-helical structure and contain disulphide bridges. At low concentrations, lysozyme adsorbs with an unchanged configuration (a). As the concentration increases it is suggested that part of the protein becomes denatured and remains adsorbed to the interface, but the rest still in its native form is able to exchange with the protein in solution (b). At excess protein concentrations, multilayer formation again occurs (c).

The actual structure and stability of these protein films will vary depending on pH and electrolyte concentrations, since electrostatic interactions play a vital role in protein adsorption behaviour as is demonstrated in later chapters.

1.6.4 Effect of protein on the stability of dispersions

The way in which adsorbed protein molecules affect the rate of aggregation of colloidal particles depends on the nature and concentration of the protein and also the solvent properties of the dispersion phase.

As protein adsorbs to the particles, the electric double-layer will be disrupted. This will be due to;

a) the protein penetrating the layer (if its electrostatic charge is sufficiently

large),

b) neutralisation of some of the charge in the double-layer by the opposite charges of the protein,

c) exclusion of some of the counter ions from the surface as the protein adsorbs and,

d) trapping of ions within the loop regions of the protein.

These effects change the ζ-potential and electric double-layer thickness.

In a "good" solvent a thick adsorbed protein layer stabilises the emulsion by steric effects. It is the loops and tails that act as steric stabilisers.

1.7 Model emulsion systems

Since it is not possible to study the adsorption of protein onto oil droplets because of the instability of uncoated or partially coated droplets, a variety of model systems have been used to simulate this situation. These include spread monolayers[35,36,37] and solid planar surfaces[38,39] *e.g.* mica and polystyrene latex. This thesis will deal mainly with adsorption to positively and negatively charged polystyrene latices and also to phospholipid liposomes whose surface charge has been varied by using phospholipids with variously charged head groups.

Chapter 2

Milk Proteins

2.1 Introduction

Milk protein is one of the most widely consumed human foods and milk from the Western breeds of dairy cows *Bos taurus*, represents the major source of milk for the food industry, this section will deal solely with the composition of bovine milk. Milk is a multiphase secretion of the mammary gland containing emulsified fat globules, colloidally dispersed casein micelles and dissolved proteins, lactose and salts. Typically the overall composition is 4% fat, 3.5% protein, 4.8% lactose and 0.7% oils. Water represents the dispersion medium. The fat and protein constituents are seasonally variable and reflect breed differences, stage of lactation and feeding regimes[40].

Milk proteins can be divided into two major groups, the caseins and whey proteins. The caseins are a family of related phosphoproteins and contribute about 80% of the total protein content of milk. The majority of the caseins are in the form of large colloidal particles called casein micelles with only about 10% being located in the serum (whey) phase[40]. The family of caseins consist of four members; α_{s1}-casein (α_{s1}-cn), α_{s2}-casein (α_{s2}-cn), β-casein (β-cn) and κ-casein (κ-cn) which are present in the ratio 3:1:3:1 by weight respectively. Micelles require calcium ions in order to maintain structure and the calcium ion concentration in milk is 30mM, of which 27% occurs in micelles[41].

When caseins are removed from skimmed milk (*e.g.* by isoelectric precipitation), the resulting aqueous phase is called whey or milk serum. The protein

present in whey contributes about 20% of the total milk protein[40]. β-lactoglobulin (β-lg) and α-lactalbumin (α-la) make up 70-80% of the whey proteins, the remainder being bovine serum albumin (BSA), immunoglobulins and protease-peptones[40].

2.2 Occurrence of genetic variants

The heterogeneity of milk proteins is further complicated by the fact that they are products of co-dominant allelic autosomal genes. Genetic variants of β-lg were the first to be recognised[42]. Discovery of variants of other gene products followed. Currently there are five known genetic variants of α_{s1}-cn[43,44,45], eight of β-cn[46,47,48,49], four of κ-cn[50,51,52,53,54,55], and six of β-lg[56,42,44]. Examination of the pattern of inheritance of the various casein polymorphs indicates a close linkage of the four gene loci for these proteins[57,58,59]. Thus the four gene products are not observed with random or equal frequencies. For example in western breeds α_{s1}-cn B and α_{s2}-cn A and β-cn A^1 and β-cn A^2 occur more frequently than other genetic variants whereas, κ-cn A and B exhibit a more equal frequency of occurrence. Frequency of occurrence is, however, strongly influenced by breed of cows. Similarly, β-lg A and B appear with equal frequency, whereas the other variants are very rare.

2.3 Identification of milk proteins by gel electrophoresis

Milk proteins are separated from whole milk by various methods, which will not be described here, but usually begin by isoelectric precipitation of the caseins by adjusting skim milk to pH4.6 at 20°C with HCl. Once the proteins have been isolated it is possible to identify, and name them, by measuring their free electrophoretic mobility. The advent of zone electrophoresis in gels made greater resolution possible.

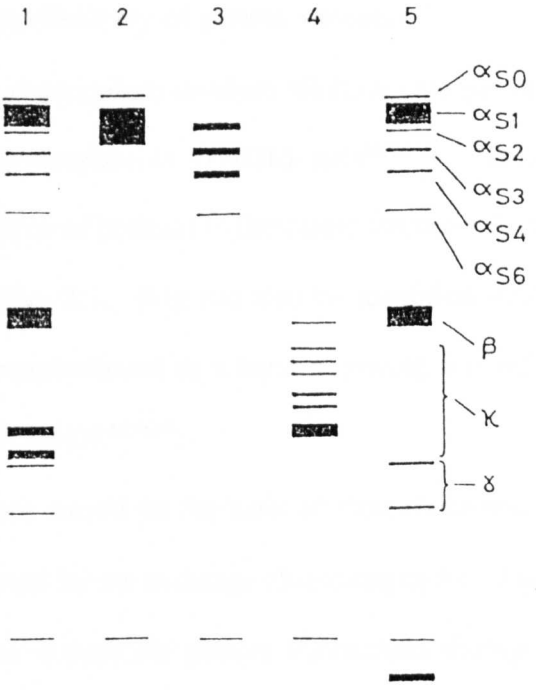

Fig. 2.1. Diagram of the separation of milk proteins on SDS PAGE.

Taken from Swaisgood[63].

Resolution occurs due to both electrophoresis and molecular sieving. Including urea in the gels causes dissociation of the individual proteins[60]. This development provided the impetus for identification, isolation and characterisation of individual components of the casein fraction and the discovery of genetic variants.

The most widely used procedure involves alkaline urea gel electrophoresis in either starch (SGE) or polyacrylamide (PAGE) gels[61,60,62]. These methods are particularly useful for resolution of proteins in the casein fraction. A typical separation is shown schematically in Fig. 2.1. β-lg can also be identified in skim milk in the presence of urea and 2-mercaptoethanol as a band migrating immediately in front of β-cn during alkaline SGE or PAGE[62,64,65].

The caseins have been named on the basis of their electrophoretic separation, the caseins can also be resolved by ion exchange chromatography. Again, for effective separation it is necessary to disrupt the protein interactions during chromatography using urea and 2-mercaptoethanol[66].

2.4 Composition of milk proteins

As a result of the sequencing of the primary structures of the caseins, the composition of these proteins can be presented with much greater accuracy. The amino acid composition of the caseins are not significantly different from those of typical globular proteins. Average hydrophobicities (based on the free energies of transfer of amino acid side chains from water to organic solvent) are only slightly higher than those for the majority of globular proteins which range from 4.18 to 4.60kJ residue^{-1}.

The most unique characteristic of caseins, namely phosphorylation, results from post-translational modification. Each α_{s1}-cn, β-cn and κ-cn molecule contains a

characteristic number of phosphoseryl residues. Thus, α_{s1}-cn B, β-cn A and κ-cn A or B contain 8, 5 and 1 residues respectively. With exception of one residue in α_{s1}-cn D, all of the phosphorylated residues that have been conclusively identified are serines.

In addition to phosphorylation, the κ-cns are also glycosylated. The extent of glycosylation is quite variable, ranging from zero to possibly five sialic acid residues[67]. The carbohydrate moiety of κ-cn from normal milk is composed of three monosaccharides; N-acetylneuraminic acid (NeuNAc), galactose (Gal) and N-acetylgalactosamine (GalNAc)[68,69,70]. These residues usually occur as a trisaccharide;

NeuNAc$\underline{\quad}^{\alpha\text{-}2,3}$ Gal$\underline{\quad}^{\beta\text{-}1,3}$GalNAc$\underline{\quad}^{\beta\text{-}1}$Thr

or as a tetrasaccharide;

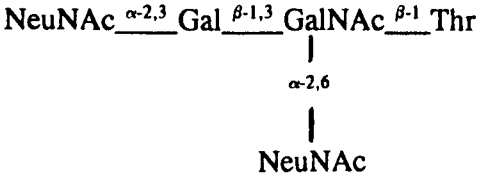

as determined in several laboratories[69,70,71]. The number of these chains attached to the κ-cn molecule can also vary[72].

Another unique feature of β-cn, κ-cn and α_{s1}-cn is the relatively high frequency of occurrence of prolyl residues. These disrupt α-helical and β-structures and often occur in β-turns and are believed to be responsible, at least in part, for the relative lack of secondary structure of the caseins.

Accurate determination of the composition allows certain physico-chemical parameters to be predicted. The predicted values agree well with experimental observations[67] (Table 2.1). The net charge at pH6.6 was calculated because this is approximately the pH of milk. The net charge on these proteins in milk will be altered by the binding of other ions, particularly calcium. κ-cn will also exhibit charge

Protein	*Charge at pH 6·6*	*Isoionic pH*	*Partial specific volume*	*Absorptivity (cm^2/g) 280 nm*	*Molecular weight*
α_{s1}-Casein					
A	−20·0	4·97	0·722	1·13	22066
B	−20·9	4·96	0·725	1·05	23612
C	−20·0	5·00	0·725	1·06	23540
D	−22·6	4·91	0·723	1·05	23722
α_{s2}-Casein A					
$P_{10}(\alpha_{s6})$	−13·2	5·39	0·722	1·11	25148
$P_{11}(\alpha_{s4})$	−14·8	5·32	0·721	1·10	25228
$P_{12}(\alpha_{s3})$	−16·4	5·25	0·720	1·10	25308
$P_{13}(\alpha_{s2})$	−18·0	5·19	0·718	1·10	25388
β-Casein					
A^3	−12·8	5·11	0·742	0·46	23971
A^2	−12·3	5·19	0·742	0·46	23980
A^1	−11·8	5·27	0·742	0·46	24020
B	−10·8	5·35	0·742	0·46	24089
C	−8·2	5·53	0·742	0·46	23939
κ-Casein					
A	−3·9	5·43	0·734	0·95	19037
B	−3·0	5·64	0·734	0·95	19005

Table 2.1. Physico-chemical characteristics of caseins, calculated from composition.

Each molecular weight for κ-cn consists of amino acid residues only. Each trisaccharide chain will add 657Da and each tetrasaccharide chain 948Da, to the molecular weight.

E.g. κ-cn A has 3 tetrasaccharides and therefore, has a molecular weight of 21,881Da.

Taken from Swaisgood[63].

Protein	*Charge at pH 6·6*		*Isoionic pH*		*Partial specific volume*		*Absorptivity*	
	Exp.	*Calc.*	*Exp.*	*Calc.*	*Exp.*	*Calc.*	*Exp.*	*Calc.*
β-Lactoglobulin								
A	−11·0	−11	5·26	5·19	0·751	0·749	0·94	0·92
B	−10·0	−9	5·34	5·28	0·751	0·749	0·94	0·92
C	−7·5	−8	5·33	5·37	0·751	0·749	0·94	0·92

Table 2.2. Physico–chemical characteristics of β–lactoglobulin.

Taken from Swaisgood[63].

heterogeneity according to its content of NeuNAc.

The major gene products of milk occurring in the whey protein fraction are β-lg and α-la. These proteins do not undergo the extent of post-translational processing present in the caseins. Thus they are not phosphorylated and are only rarely glycosylated.

The elucidation of the primary structure has again made it possible to calculate physico-chemical parameters. However, in the case of β-lg there are major discrepancies (Table 2.2). From studying proton binding equilibria it has been found that two β, γ-carboxyls per β-lg dimer do not ionise with the normal pK. These two protons dissociate with an apparent pK of 7.3 following a conformational change of the protein. The unusual titration characteristics of β-lg reflects its stable, compact globular structure.

2.5 Primary structures

Further information on the structural characteristics of proteins is obtained from knowledge of the sequence of residues in the polypeptide chain *i.e.* primary structure. Elucidation of the primary structure should enable the three-dimensional structure to be determined. This is because the primary structure represents the lowest free energy for residue-residue and residue-solvent interactions. Among others, Chou and Fasman[73,74,75] have proposed an empirical method for predicting α-helical, β-structure and β-turns in the sequences of proteins. A combination of sequence and structural information also allows the interpretation and prediction of the location of post-translational modifications.

Fig. 2.2. Primary structure of α_{s1}–casein variants A, B, C, D and E.

Taken from Swaisgood[78].

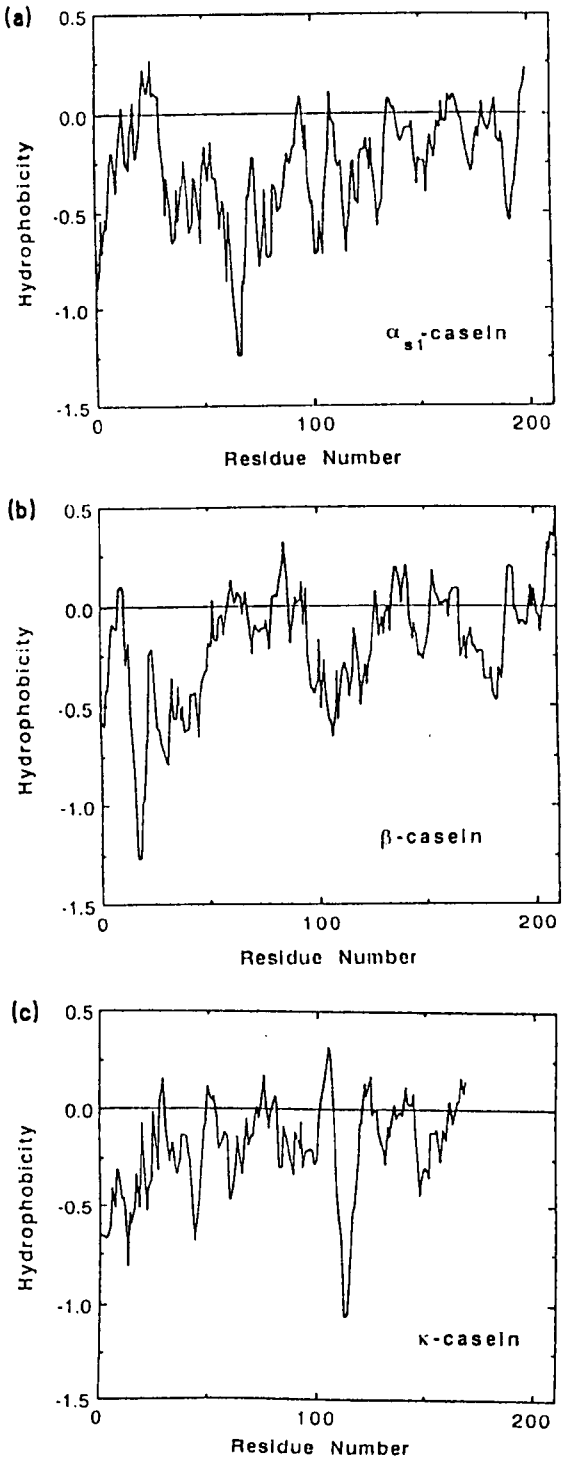

Fig. 2.3. Hydrophobicity plots for (a), α_{s1}–casein, (b), β–casein and (c), κ–casein.

Taken from Dalgleish[77].

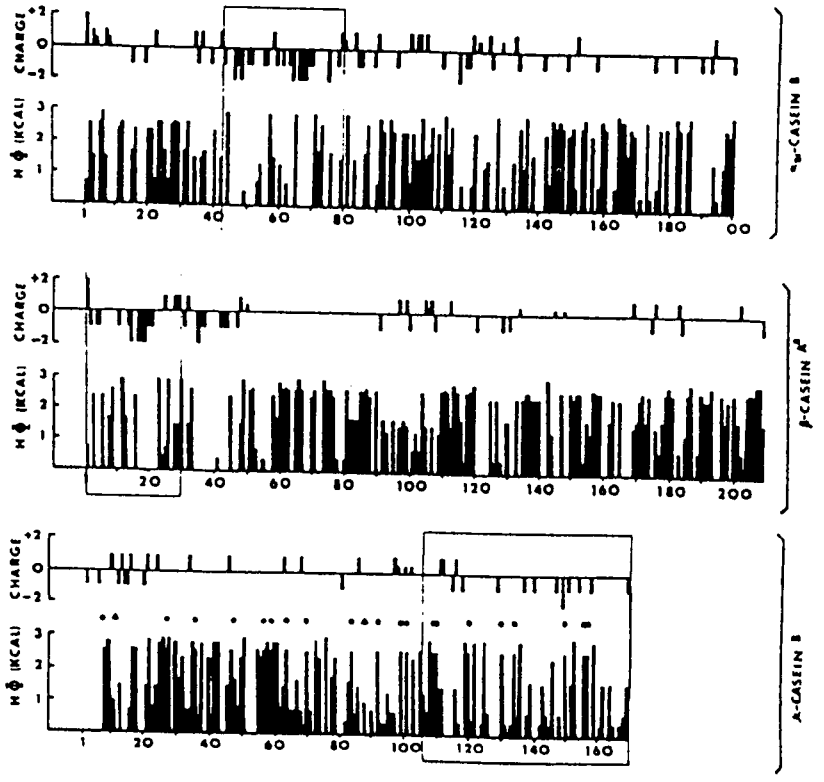

Fig. 2.4. Diagram of the linear chain distribution of charged and hydrophobic amino acid residues in α_{s1}-casein, β-casein and κ-casein.

Taken from Swaisgood[83].

2.5.1 α_{s1}-casein

The primary structures for the genetic variants are shown in Fig. 2.2. From the primary structure it can be seen that like the other caseins, strongly hydrophobic and charged residues are not uniformly distributed along the polypeptide chain. The effect of clustering of similar residues becomes apparent when plots of the hydrophobicity and charge distribution are observed (Figs. 2.3 and 2.4). Three hydrophobic regions, (1-44), (90-113) and (132-199) can be identified. Another region unique to the calcium-sensitive caseins is the region (41-80) which contains the cluster of phosphoseryl residues. At pH6.6 this sequence would have a net charge of approximately -20.6 for the B variant, while the remainder of the molecule would have effectively no net charge. These observations suggest a dipolar-type structure with a globular, rather hydrophobic domain(s) and a highly solvated and charged region which occupies a disproportionately large fraction of the molecular volume.

From early studies of the optical rotatory dispersion (ORD) it was concluded that caseins possess very little secondary structure, particularly α-helix[78]. This is probably true with respect to α-helix. However, α_{s1}-cn may contain some β-structure and undoubtedly a significant proportion of residues occur in β-turns[75]. Caseins have been described as random, structureless, rheomorphic[79] or denatured proteins. A significant fraction of the residues in the hydrophobic domain certainly are unlikely to confer random coil structure on the protein. Future predictions based on the primary structure will probably include β-structure and β-turns in addition to unordered structure.

α_{s1}-Cns are more susceptible to proteolysis than compact, stable globular proteins such as α-la[80]. This difference may be due to the acidic, highly solvated

```
    1
H.Arg-Glu-Leu-Glu-Glu-Leu-Asn-Val-Pro-Gly-Glu-Ile-Val-Glu-SerP-Leu-SerP-SerP-SerP-Glu-

                                                          (Variant C)
21                                                        Ser      Lys
Glu-Ser-Ile-Thr-Arg-Ile-Asn-Lys-Lys-Ile-Glu-Lys-Phe-Gln-    -Glu-   -Gln-Gln-Gln-
                                                          SerP     Glu
                                                          (Variants A,B)
41
Thr-Glu-Asp-Glu-Leu-Gln-Asp-Lys-Ile-His-Pro-Phe-Ala-Gln-Thr-Gln-Ser-Leu-Val-Tyr-

61                    Pro(Variants A², A³)
Pro-Phe-Pro-Gly-Pro-Ile-    -Asn-Ser-Leu-Pro-Gln-Asn-Ile-Pro-Pro-Leu-Thr-Gln-Thr-

                      His(Variants C,A¹, and B)

81
Pro-Val-Val-Val-Pro-Pro-Phe-Leu-Gln-Pro-Glu-Val-Met-Gly-Val-Ser-Lys-Val-Lys-Glu-


101                   His(Variants A¹,A³, B,C)
Ala-Met-Ala-Pro-Lys-    -Lys-Glu-Met-Pro-Phe-Pro-Lys-Tyr-Pro-Val-Glu-Pro-Phe-Thr-
                      Gln(Variant A²)

121 Ser(Variants A,C)
Glu-  -Gln-Ser-Leu-Thr-Leu-Thr-Asp-Val-Glu-Asn-Leu-His-Leu-Pro-Leu-Pro-Leu-Leu-
    Arg(Variant B)

141
Gln-Ser-Trp-Met-His-Gln-Pro-His-Gln-Pro-Leu-Pro-Pro-Thr-Val-Met-Phe-Pro-Pro-Gln-

161
Ser-Val-Leu-Ser-Leu-Ser-Gln-Ser-Lys-Val-Leu-Pro-Val-Pro-Gln-Lys-Ala-Val-Pro-Tyr-

181
Pro-Gln-Arg-Asp-Met-Pro-Ile-Gln-Ala-Phe-Leu-Leu-Tyr-Gln-Glu-Pro-Val-Leu-Gly-Pro-

201                              209
Val-Arg-Gly-Pro-Phe-Pro-Ile-Ile-Val.OH
```

Fig. 2.5. Primary structures of β-casein variants, A^1, A^2, A^3, B and C.

Sites of post-translational phosphorylation are in italics.

Taken from Swaisgood[76].

domain which probably has random coil properties. This would also explain the accessibility of residues in this domain to casein kinases which result in phosphorylation of the protein. In addition, α_{s1}-cn is more susceptible to proteolysis by rennet than β-cn at higher temperatures where β-cn is polymerised. But, at low temperatures, where β-cn is monomeric, it is β-cn that is most susceptible to rennet attack[81,82].

2.5.2 β-casein

Primary structures for five of the genetic variants of β-cn are shown in Fig. 2.5. It is the most hydrophobic of all the caseins. In addition, the highly charged domain is clearly separate from the large hydrophobic domain (Figs. 2.3 and 2.4). Thus, the N-terminal 21 residue sequence would carry a net charge of about -12 at pH6.6, whilst the hydrophobic domain would have no net charge. Consequently, β-cn is a distinctly amphipathic molecule, with a polar domain comprising one-tenth of the chain length, but carrying one-third of the total charge, whereas the nonpolar domain is very hydrophobic, especially in the C-terminal two-thirds of the molecule. β-cn is also characterised by a high frequency ($\sim$0.17) of prolyl residues which would be anticipated to have an effect on the secondary structure.

Much of the discussion pertaining to α_{s1}-cn also applies to β-cn. It seems unlikely that residues in the hydrophobic domain would be completely hydrated, owing to the unfavourable loss of water entropy. β-cn has physico-chemical properties quite different from globular proteins and therefore has been the subject of much investigation. Sequence information has provided predictions on β-cn structure using Chou-Fasman analysis. It was concluded that β-cn consisted of 10% α-helix, 13% β-

sheet and 77% unordered structure[83]. The amount of β-turns was not calculated, which could be important due to the large proportion of prolyl residues present[75]. The picture that emerges from these results is that of an amphipathic molecule with marginal structural stability. The polar domain probably consists of random coil, whereas the hydrophobic domain contains some structural stability.

The action of proteases on β-cn is particularly interesting in view of its primary structure. The apparent greater susceptibility of β-cn in comparison with α_{s1}-cn is most likely caused by the weaker association of β-cn in the micelle, especially at low temperatures[84]. As would be expected, the C-terminal peptides are very hydrophobic and can be extracted with organic solvents[84]. When subjected to a mixture of proteases, the initial rate of hydrolysis of β-cn is similar to that of α_{s1}-cn. However, the extent of hydrolysis is significantly less[80]. This may also be related to its larger hydrophobic domain.

2.5.3 κ-casein

The primary structures of two genetic variants of κ-cn are shown in Fig. 2.6. In comparison with other caseins the most outstanding features of its structure are the lack of phosphoseryl clusters (there is only one serine phosphorylated, residue 149) and the attachment of carbohydrate moieties to threonyl residues. As a consequence, κ-cn does not bind Ca^{2+} to the same degree as other caseins and hence its solubility characteristics are not affected by this ion. Again the κ-cn molecule has amphipathic character[85], with an N-terminal hydrophobic domain and a C-terminal polar domain. There are no cationic residues in the C-terminal 53 amino acids. At pH6.6 the net charge of the κ-cn macropeptide is -10 or -11, depending on the variant. This gives

Fig. 2.6. Primary structures of κ-casein variants, A and B.

Sites of post-translational phosphorylation and glycosylation are in italics.

↓ indicates site of chymosin cleavage.

Taken from Swaisgood[76].

an overall charge on the κ-cn molecule of -3.9 for κ-cn A and -3.0 for κ-cn B. In addition, each sialic acid residue contributes an additional charge, which for three tetrasaccharide chains would yield a total charge of -9.9 or -9.0.

The distinct separation of the hydrophobic and charged domains has been known for some time, due to the specific chymosin-catalysed hydrolysis which releases the macropeptide resulting in the clotting of para-κ-casein. The only bond hydrolysed during the primary action of chymosin is Phe105-Met106 so the resulting macropeptide (106-169) contains all the post-translational modifications and the genetic variation in its sequence[67,86,87]. Release of the polar macropeptide leaves the N-terminal para-κ-casein which is slightly cationic at pH6.6, and has an increased hydrophobicity and a greatly decreased solubility.

A considerable amount of structure is predicted from the amino acid sequence[88], *i.e.* 23% α-helix, 31% β-sheet and 24% β-turns. A highly predicted β-sheet in the region (73-80), which is quite hydrophobic, could participate in the intermolecular interactions leading to curd formation[88]. There are two predicted β-turns either side of the chymosin-sensitive bond and another β-turn (113-116) could cause the sensitive sequence to stand out on the molecular surface, making it especially susceptible to proteolytic attack[86]. Analysis of CD spectra suggests that κ-cn contains more structure than other caseins (14% α-helix, 31% β-structure)[88]. The amount of α-helix is only half that of predicted values but can be increased by increasing the temperature. Also, κ-cn is less susceptible to general proteolysis at pH7.4 than that of α_{s1}-cn or β-cn[80].

Another aspect that is involved in the secondary structure of κ-cn, is the presence of two cysteinyl residues, which are located in the hydrophobic domain. When isolated from milk these residues are in the disulphide form involving

Fig. 2.7. Primary structures of β-lactoglobulin variants, A, B and C.

Dashes indicate that some molecules may have the single sulphydryl group at position 119 and others at 121.

Taken from Swaisgood[83].

intermolecular linkages so that a heterogeneous population of covalent polymers are observed[89]. Existence of the disulphide form in milk would be expected in view of the sulphydryl oxidase activity associated with the skim milk fraction[90]. Thus these residues must be on the surface and accessible for oxidation. This agrees with the predicted structure as Cys11 is in an unordered sequence and Cys88 is in a β-turn region. These observations are consistent with a globular hydrophobic domain possessing a considerable amount of secondary structure.

2.5.4 β-lactoglobulin

The primary structure of β-lg is shown in Fig. 2.7. An important feature is the presence of both disulphide bonds and a free thiol group. The thiol group must be located in a structural region which limits its accessibility to reagents, especially for the case of the C variant[91]. Fig. 2.7 indicates that the thiol is equally distributed between positions 119 and 121[92]. However, this assumption has been questioned[93]. Even so, the molecule presents a unique opportunity for intra- and intermolecular thiol-disulphide interchange, particularly under conditions that increase the accessibility.

Predictions of the amounts of various secondary structures have been made from its sequence[94]. Variable amounts of α-helical structure were predicted, 10-50%, depending on the method used. Better agreement was found for the amount of β-sheet structure, 20-30%, and unordered plus β-turn structure, 50-60%. Since it is a highly structured molecule there is nothing to be gained by observing the hydrophobicity plots. This is because some of the residues will be hidden within the protein molecule when the molecule is in solution. X-Ray crystallography studies have shown three forms of β-lg, lattices X, Y and Z[95]. All three structures show features suggestive of

an α-helix and some β-sheet, but there are no distinct differences. The lattice X forms at pH6.5 which is then converted to Y and Z at pH7.8. The first structure of bovine β-lg to be obtained was that of lattice Y[96]. The structure consists of nine strands of anti-parallel β-sheet, eight of which wrap round to create a flattened, conical barrel, or calyx, closed at one end. There is a three-turn α-helix on the outer surface of the calyx.

2.6 Physico-chemical characteristics of the caseins

Due to homology in their primary structures, the caseins have many features of their physico-chemical properties in common. Therefore, although each protein possesses distinctive characteristics, it is helpful to consider and compare their properties as a unit. Because of their tendency for interaction or self-association it is difficult to find suitable conditions for measurement of characteristics for native monomer forms. Consequently the true characteristics of monomers as they would exist at physiological pH and temperature remains questionable. Even so, it is useful to examine the properties of monomers obtained under the mildest possible conditions.

α_{s1}-Cn dissociates to monomers at low ionic strength, 0.003-0.01, and physiological pH. The intrinsic viscosity is somewhat larger than that expected for a typical globular protein. The three-dimensional shape of the molecule is also questionable. A prolate ellipsoid seems to be unreasonably symmetrical on the basis of other observations, whilst the water associated with a spherical molecule (about 3g H_2O/g) is much higher than for globular proteins. However, the "native" monomer is definitely not a random coil. It only forms a random coil in denaturing solvents. On considering these properties together with the primary structure, it appears that the

α_{s1}-cn molecule contains domains of rather unstable structure, particularly the polar domain which may approach random coil behaviour. Because of this marginal stability and amphipathic nature, the molecular dimensions are sensitive to ionic strength. This instability means that at any point in time, an appreciable fraction of the molecular backbone and side chains will be exposed to water. This requires the hydration of hydrophobic groups which explains the observed atypical hydration and the high affinity of water to the protein.

Hydrophobic interactions seem to play a larger role in the association of β-cn molecules. Consequently β-cn occurs as a monomer at low temperatures, 0-4°C[97]. Under these conditions the hydrodynamic behaviour of β-cn monomer is the most unusual of all the caseins, and is very similar to that for a random coil chain.

So far suitable conditions for examination of a "native" monomer for κ-cn have not been discovered. The interactions between monomers are extremely stable so that at physiological pH, dissociation is not affected by changes in temperature or ionic strength. Native κ-cn monomers are linked together by intermolecular disulphide bonds so that a heterogeneous population ranging probably from trimers to much larger covalent polymers[89,98] of 30-35 monomers[76] are formed. Hydrodynamic data for native κ-cn suggest a spherical polymer with a radius of roughly 9.7nm and a hydration of 3g H_2O/g. This structure probably results from lateral interactions between hydrophobic domains which stabilise the secondary structure in these regions, whilst the polar domains form a highly solvated surface.

Cleavage of the disulphide bonds by reduction or β-elimination at pH12, permits characterisation of the monomer in strongly dissociating solvents[89]. At pH12 the Stokes radius approaches that expected for a random coil structure.

Calcium binding equilibria and the resultant changes in structure are of particular importance to the formation of casein micelles. Because of the acidic peptide regions, including the phosphoseryl residue clusters in the polar domains of α_{s1}-cn and β-cn (as well as α_{s2}-cn), the association of Ca^{2+} with these proteins is unique. Results have shown that the strength of Ca^{2+} binding to α_{s1}-cn increases with increasing ionic strength or decreasing pH[99]. In addition the binding of Ca^{2+} to β-cn, after the first Ca^{2+} ion has bound, is weaker than the binding of α_{s1}-cn[100]. As Ca^{2+} is bound, protons are released and the extent of solvation decreases to plateau levels of 1.7g H_2O/g and 1.9g H_2O/g for α_{s1}-cn and β-cn respectively. Precipitation is initiated in both proteins at levels consistent with Ca^{2+} binding only to phosphoseryl residues. Results also suggest that precipitation of the α_{s1}-cn/Ca^{2+} complex is almost completely determined by the charge of the complex[101]. This is also supported by radioisotope studies[102]. However, in this study there was some binding of Ca^{2+} to κ-cn, even though only one phosphoseryl group is present[102]. This suggests that Ca^{2+} may be binding to a negatively charged cluster.

2.7 Physico-chemical characteristics of β-lactoglobulin

This protein has been the subject of many physico-chemical studies. Only a few of these, relating to the structure of the molecule, will be discussed. At pH values near its isoelectric point up to and including the pH of milk, and at room temperature, each genetic variant exists as a stable dimer of molecular weight about 36,700Da[63].

At pH7, β-lg exists as a dimer of about 36,000Da. The dimensions of the long axis is 6.93nm and that of the short axis, 3.58nm[103,104]. At pH values lower than 3.5 (below the isoelectric point of 5.09 and 5.23 for phenotypes A and B respectively[105]),

the dimer dissociates into two subunits which appear to be identical[103] and this is not accompanied by a change in conformation[63]. At this point there is little difference between genetic variants, but between pH's 3.5 and the isoelectric point, genetic variant influences the association properties. At the pH range 3.5 to just above the isoelectric point and at low temperatures, the β-lg A dimer associates to form octamers of ≈147,000Da. At a concentration of 15g l^{-1} and temperatures above 4.5°C, it appears that significant amounts of tetramer and hexamer must also be present. At higher concentrations or lower temperature the results agree with a simple dimer-octamer model[106]. The octamers have a diameter of about 8.2nm along their long axis[104]. β-Lg B cannot form aggregates greater than a tetramer[107], therefore the tetramer would have a diameter of approximately 6.7nm. Association is attributed to 4 carboxyl groups present at the site of interaction, one of which is probably at residue 64 where variant A has an aspartate and variant B a glycine, resulting in variant A having one more carboxyl than B, and therefore being more surface active[103,106,108]. Consequently the smaller decrease in entropy for β-lg A may result from release of more water molecules as this carboxyl is buried in the interaction site[106]. It also appears that the interaction is less hydrophobic than that of β-cn, for example, since the effect of temperature is the opposite.

In the alkaline region there is a reversible conformational change centred around pH7.5 which exposes and ionises one abnormal carboxyl per monomer[109,110,111,108]. The transition and the abnormally titrating carboxyl are observed in all variants examined *i.e.* A, B and C[111,112]. Tyrosyl and tryptophyl residues become exposed due to the transition. This suggests that these residues are located in the three-dimensional structure near the hidden carboxyl group[108].

Increasing the pH to still higher values induces further structural changes which become irreversible around pH9.5. At this point the β-lg tyrosine residues begin to ionise.

ORD and CD studies indicate a secondary structure consisting of 10-15% α-helix, 43% β-sheet and 47% unordered structure[113,114]. The general agreement is that there is a considerable amount of β-structure but very little α-helix which agrees with predictions from the primary structure[94]. The calyx structure obtained from X-ray crystallography also agrees with this[96]. A more detailed review of β-lg properties has been written by Hambling *et al*[115].

Chapter 3

Physical Techniques

3.1 Introduction

When colloidal particles are immersed in a fluid, they scatter a beam of light (Tyndall effect). The scattering pattern (*i.e.* the intensity of the scattered light as a function of θ, the angle between the incident beam and the scattered beam) depends on the particle size and on the wavelength of light. Therefore, a method of analysing the scattering pattern will provide one effective way of determining the size of the colloidal particles. An alternative method, photon correlation spectroscopy ,which examines fluctuations in light intensity, has only become possible relatively recently due to the introduction of lasers that give coherent, monochromatic, intense and narrow incident beams, together with sensitive and stable photon-detection apparatus and rapid data analysis techniques by computer.

3.2. Photon Correlation Spectroscopy

A typical photon correlation spectroscopy (PCS) apparatus has a laser light source providing an incident beam to be scattered by the sample with the scattered light detected at a given angle away from the light source (Fig. 3.1). It therefore comprises all of the components required in a static light scattering system. Precautions to be observed are the same as those involved in the static or integrated light scattering situations.

Since light is scattered strongly at an interface where a refractive index difference occurs (*e.g.* where there is a change from the cuvette wall to the sample),

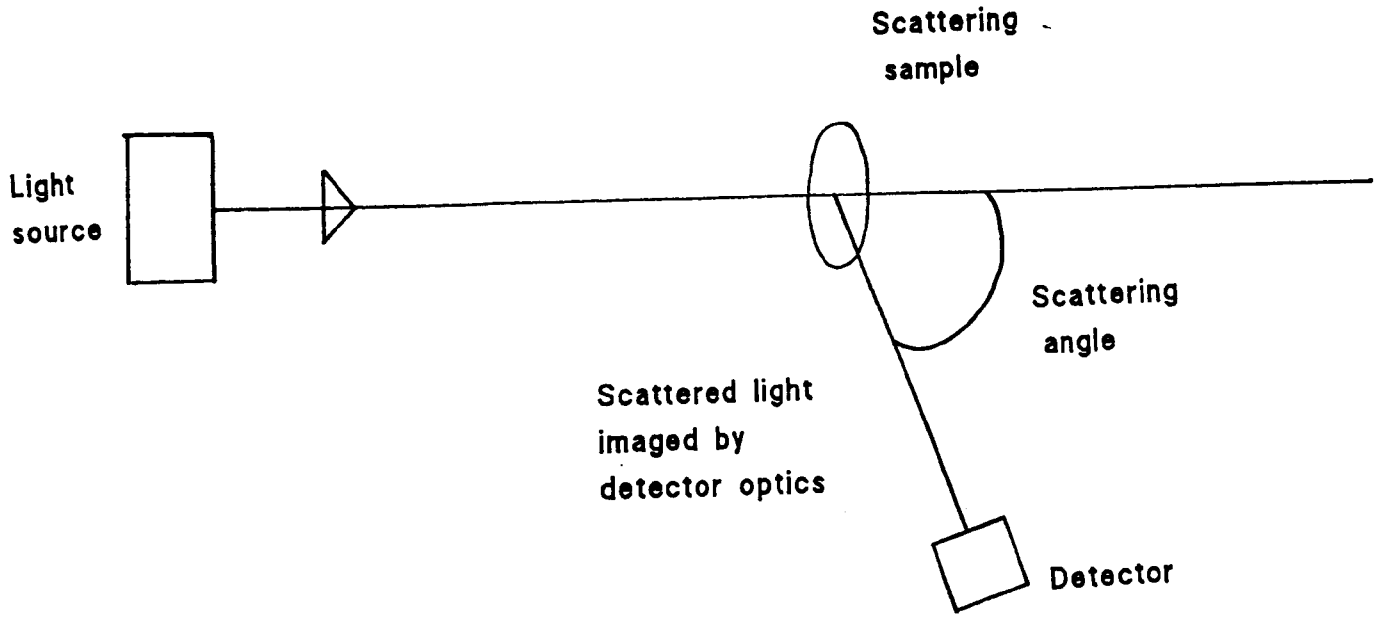

Fig. 3.1. Diagram of the top view of a typical PCS apparatus.

scattered light from the edge of the cuvette must not reach the detector. The scattering angle is often restricted to 90° and this is usually sufficient to prevent this happening. In addition the scattering cuvette is immersed in a "refractive index matching fluid" (usually water) which minimises the change in index at the edge of the cuvette. The water also acts to keep the temperature of the cuvette the same as that of the rest of the measurement cell, which is maintained at a given temperature.

The detector consists of a photon counting photomultiplier that produces an electrical pulse when a photon is detected by the "photocathode". An electron ejected from the photocathode is accelerated in a high voltage field, then falls into a "dynode" that tends to eject more than one electron when struck by a single one. This process is propagated over twelve or more times so that the electron ejected from the original photon is multiplied by 10^7 or more. This electrical pulse is then amplified and converted to a standard "logic pulse" that can be counted and processed by other electronic modules in the system. The detector cannot respond to another photon until the previous output is complete. As a consequence the maximum count rate is around 20 million photons per second. However, photons will arrive at the detector at different times. In order to allow for this, the mean rate should be a factor of 5 or so lower in order to guarantee that the count rate is really proportional to the detected light intensity. The intensity can be altered by changing the aperture in front of the detector. Increasing the aperture increases the number of photons that reach the detector and hence increases the intensity count rate. The scattering sample must be of a sufficient concentration to scatter light, but not so concentrated that the scattered light hits other particles before it reaches the detector (multiple scattering).

3.2.1 The fundamentals of PCS measurement

PCS (also referred to as Quasi-elastic light scattering (QELS)) uses the fact that a photon counting detector can track rapid changes of intensity, if enough photons are present during the "sample time" in which an individual portion of the total intensity is recorded. If those photons detected over an entire "sample time run" are averaged, they would record the sample average intensity as in the previous sample time run, providing all other conditions are kept constant.

The correlator stores successive samples of the signal in "sequential bins" and then multiplies every "old sample" by the current value of the signal as it is measured and these multiples are then added together and stored in a "store channel" (1). Every sample signal is then multiplied by the signal in the bin two bins away and the sum of all these multiples is stored in another store channel (2). Intervals of three bins are then used and the sum of these multiples are stored in another store channel (3). This continues until the interval length is the same as the total number of store channels available (Fig. 3.2).

Each store channel represents a point in a correlation function. The correlation functions are then plotted against the store channel number to give a decay curve. If the sample is monodisperse *i.e.* all of the particles are of the same size, the decay is exponential. The semi-logarithmic plot of InG(t) *vs* sample time gives a straight line is produced, the gradient of which is the diffusion coefficient. In practice the earlier store channels (those calculating small differences in time) are the only ones used. The correlation function decays because particles are moving. When no correlation is seen, particles have moved a distance greater than one wavelength.

The diffusion coefficient, D, can be related to particle size by using the Stokes-

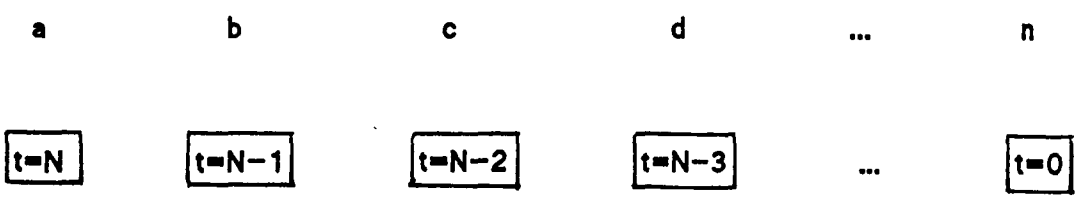

Store channel 1 = [(axb) + (bxc) + (cxd) + ... (...xn)]

Store channel 2 = [(axc) + (bxd) + ... (...xn)]

Store channel 3 = [(axd) +... (...xn)]

Fig. 3.2. Diagram of a simple correlator.

Correlator sums the multiples of the number of counts in each bin by the number of counts in the bin distance N-z away and stores it in a store channel. The same occurs for successively increasing time intervals. Continues until the time interval equals the total number of store channels.

Einstein equation for spheres;

$$D = kt/6\pi\eta R_h \qquad (3.2.1)$$

where, t, is the absolute temperature, k, is the Boltzmann constant, η, the solvent viscosity and R_h, the hydrodynamic radius. R_h, is generally slightly larger than the geometrical radius due to solvation by solvent and some interaction effects. Since size is dependent on viscosity, any change in this parameter must be accounted for. In very dilute systems any addition of small amounts of solute, such as protein, latex or liposomes, will not appreciably alter the viscosity.

The data can be analysed in different ways. Different methods are used because no single method of analysis is applicable in all cases. This is due to there being more than one particle size distribution that corresponds to very similar correlation functions. The method used here is that of cumulants[116]. The cumulant method makes no assumption about the distribution form. It fits a polynomial in channel time (or number) to the Log_e of the normalised correlation function (equation 1.3.2). Cumulant refers to the full measured correlation function being represented by a theoretically infinite series, each term representing a "statistical moment" of successively higher order. These can be interpreted to give information about the shape of the distribution of "decay times" and hence particle sizes. Generally only the first 2 or 3 terms are used. The first moment is used to derive a "z average" mean size and the second the "polydispersity" which is a measure of the width of the distribution;

$$Log_e((G(t)/B)-1) = a + bt + ct^2 + \ldots \qquad (1.3.2)$$

where, G(t), are the measured correlation points, B is the baseline (calculated from the monitor channels), a, b, and c, are the coefficients of the cumulants fit determined by a simple linear-least-squares fit. The coefficient a, is the "intercept", b, the "slope"

(measures the relaxation time for the signal), and, c, the departure from linearity (the curvature of the fit). From these values the diffusion coefficient can be extracted;

$$\tau = 1/b = 2DK^2 \qquad (1.3.3)$$

where, K, is the scattering vector. Polydispersity is then defined as c/2b. It measures the variance of the distribution of decay times and hence provides a measure of the width of the particle size distribution. A monodisperse system, by definition, will have a low polydispersity value, and any large change in polydispersity will indicate aggregation of the system. In these studies any non-time-dependent increase in the z average particle diameter without a corresponding change in polydispersity upon addition of protein, is taken to indicate that protein is adsorbing to the particle (latex or liposome), so forming a layer around the particle.

3.3 Electrophoretic mobility

Another method of characterising protein adsorption to latex particles is that of laser Doppler electrophoresis, which measures the electrophoretic mobility of particles. The Malvern "particle charge" system was used to determine the electrophoretic mobilities. A diagram of the apparatus is given in Fig. 3.3. The system is designed so that two beams of light are focused and cross at a given angle within the volume of an electrophoresis cell (capillary). The light scattered by particles in this cell is then detected by a photomultiplier system, which converts the optical signals into electronic signals that can be analysed to give detailed information about the motions of particles in the electrophoresis cell. If the particles are in motion, *e.g.* when an electric field is applied, the scattered light will undergo a change in frequency due to the Doppler effect. The change in frequency due to Doppler shift is very small. In order to

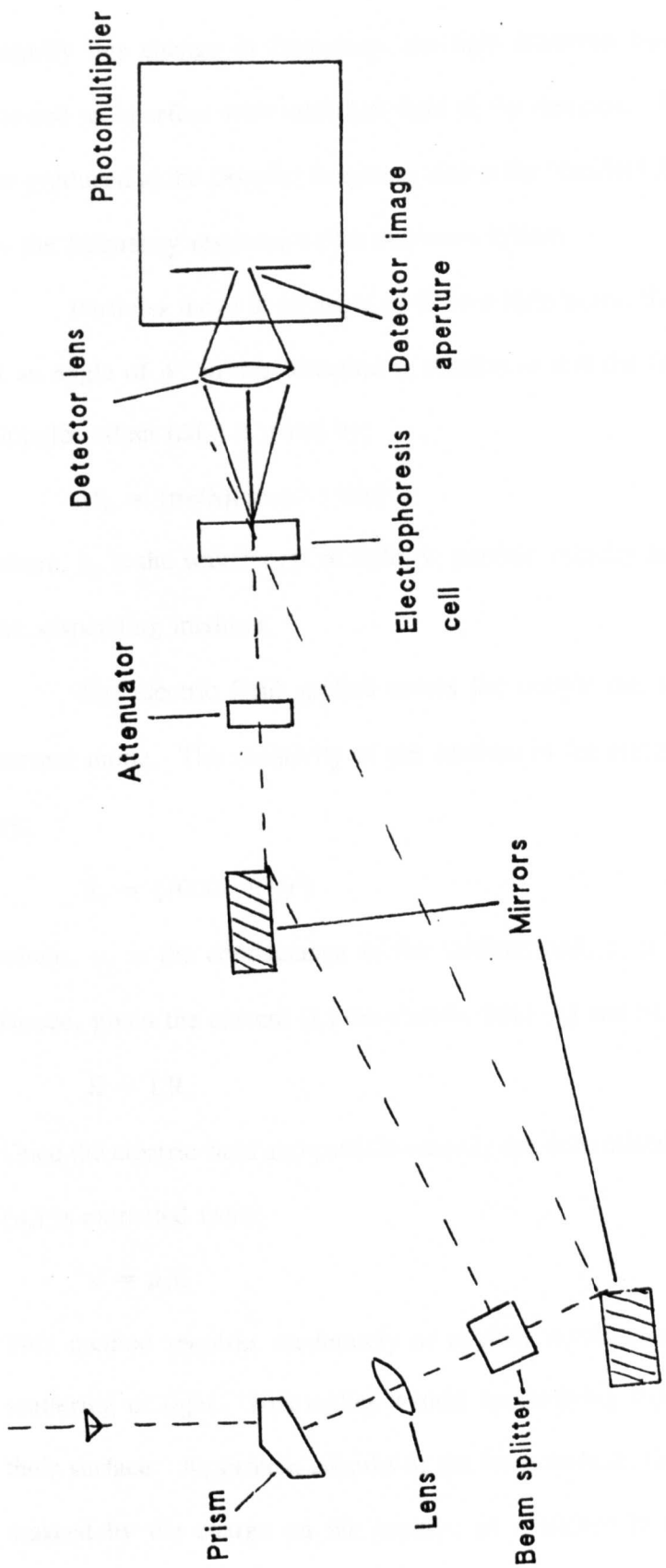

Fig. 3.3. General view of particle charge system.

magnify this change in frequency, the light scattered from the moving particles is allowed to interfere with unshifted light at the detector. As a result, optical "beats" are produced at the Doppler frequency due to the "carrier" frequency being filtered out by the frequency response of the detection system.

Particles move at an angle of θ' to a light beam, the scattered light is detected at an angle of ϕ' to this direction of motion so that the frequency change due to the Doppler effect (Δf_D) is given by;

$$\Delta f_D = (nv/\lambda)(\cos\phi' - \cos\theta') \qquad (3.3.1)$$

where, λ, is the wavelength of light, v, particle velocity and n, the refractive index of the suspending medium.

The electric field applied across the sample can be generated using constant current mode. The resistivity of the medium in the electrophoresis cell (R_c) is given by;

$$R_c = (1000/\gamma)(1/r^2) \qquad (3.3.2)$$

where, γ, is the conductance of the medium and, r, is the radius of the capillary. Hence, given the current (I_c) the electric field (E) can be determined;

$$E = I_c R_c \qquad (3.3.3)$$

Once the electric field and particle velocity are determined the electrophoretic mobility (μ_e) is extracted from;

$$v = \mu_e E \qquad (3.3.4)$$

This method requires moderately or slightly turbid solutions, since it relies on the scattering of light. This makes it ideal for studying latices and the protein bound to their surface. As protein adsorbs to the latex surface, the charge on the latex will be masked by the charge on the protein, so a change in electrophoretic mobility will

occur.

Chapter 4

Adsorption of Milk Proteins to Phosphatidylglycerol and Phosphatidylcholine Liposomes

5.1 Introduction

Phospholipid bilayers are important cell constituents as they form the basic element of the cell membrane. In milk, 21% of the fat globule membrane is composed of phospholipid with protein comprising 41%. Phospholipids, particularly phosphatidylcholine (PC) are added to some processed foods in order to act as emulsifiers. Protein-phospholipid interactions are therefore important with regard to the behaviour of these systems. In addition to forming monolayers at air/water interfaces, phospholipids can be organised into liposomes. These are vesicles in which an aqueous volume is enclosed within a membrane composed of lipid molecules. Usually, the membrane consists of a bilayer of phospholipid molecules whose charged head groups project into the aqueous phase. The charge on the liposome surface can be changed by using different classes of phospholipids. All phospholipids have the same general structure consisting of a glycerol backbone to which is attached two hydrophobic fatty acyl chains, R^1 and R^2 and a charged head group, X[117];

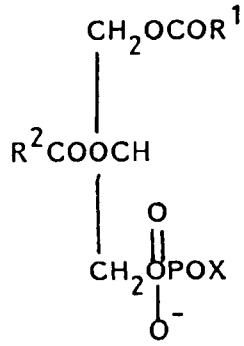

(4.1.1)

Phosphatidylglycerol (PG), a glycerophospholipid, is the major phospholipid present in photosynthetic tissues and in many bacteria. The structure of its head group is[117];

$$-CH_2CH(OH)CH_2OH \qquad (4.1.2)$$

This results in PG having an overall net negative charge. Phosphatidylcholine (PC) is another major phospholipid class and is found in large amounts in plants and in small quantities in some bacteria. The structure of its head group is;

$$-CH_2CH_2\overset{+}{N}(CH_3)_3 \qquad (4.1.3)$$

which results in the molecule having no net overall charge.

Such polar lipids are able to form liquid-crystalline phases. Bonding between the polar head groups result in sheets being formed. These bonds are quite strong when compared with the weak van der Waals forces between the fatty acyl chains. As

a result, before the phospholipid melts completely there is a range of temperatures where the fatty acyl chains are fluid, but the polar head groups are still associated in sheets. Therefore, the overall structure consists of lipid bilayers having disordered chains. Such a structure of short range disorder, but long range order, is referred to as liquid crystalline[118].

When this phase is in aqueous solution above the initial hydrocarbon chain "melting" temperature, water penetrates the polar region and a lamellar-water structure is formed. This consists of water layers alternating with lipid bilayers (Fig. 4.1).

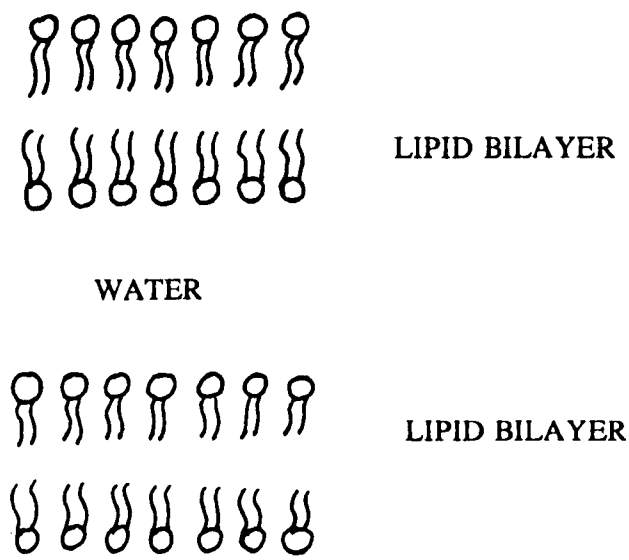

Fig. 4.1. Diagram of lamellar-water structure.

Recent work has suggested that there is a higher degree of chain disorder and entanglement than suggested by the above diagram[119], although this will not affect the

position of the polar head groups. Any proteins binding to the bilayer will attach to the head groups and not to the fatty acyl chains. However, it could be envisaged that any highly hydrophobic regions of the proteins could penetrate the bilayer and interact with the hydrophobic tail regions of the phospholipids (*e.g.* as with intrinsic membrane proteins).

In very dilute suspensions and upon gentle agitation, the lamellar phase can be induced to form liposomes. Here the bilayers are curved into aggregated or hollow vesicles. In dilute systems liposomes take up a spherical shape. These liposomes consist of multiple shells of phospholipid bilayers separated by aqueous layers. Prolonged sonication causes these multilamellar liposomes (MLL) to break up to form homogeneous single spheres consisting of a single bilayer and these are termed unilamellar liposomes (ULL)[120], Fig. 4.2.

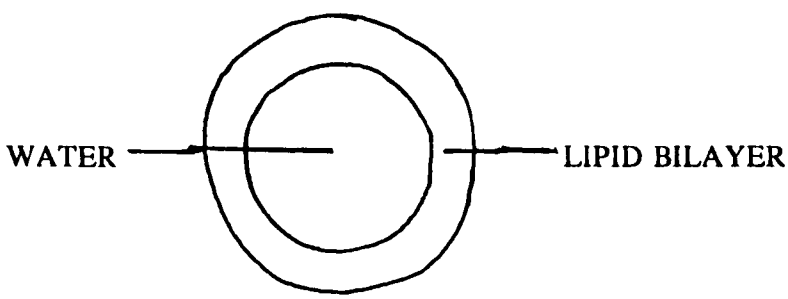

Fig. 4.2. Diagram of the structure of a liposome.

A good deal of research is currently in progress with regard to the potential use of liposomes as a carrier of drugs trapped in the internal aqueous phase. However, the

life span of liposomes within the body is variable. Adsorption of blood proteins from the blood serum onto the surface of liposomes has been demonstrated[121] and this may influence the stability of individual liposome preparations.

Polystyrene latex has been used to study the interaction of proteins with charged surfaces[122,123,39,124]. The attraction of polymer latices is that they can be prepared reasonably "clean" (free from surface-active impurities) and monodisperse.

Many aspects of adsorption at solid surfaces apply equally to liquid interfaces, however, two specific areas of difference can be identified. First, there are electrostatic interactions between charged protein residues and fixed charges on the particle surface (*e.g.* on polystyrene latex there are sulphate groups from the polymerization initiator). The protein interacts with the electrical double-layer around the particle. This alters the ionic distribution in the diffuse layer, which modifies the dissociation of titratable groups on the latex surface and on the protein. Secondly, the solid phase is relatively impenetrable. This means the tendency for protein molecules to unfold and expose their apolar residues to the non-aqueous phase is not so strong as at liquid interfaces. Therefore, they do not necessarily provide the most realistic models for food systems involving proteins and phospholipids. This is partly because polystyrene latices are solid, impenetrable spheres and also because the detergent that may be present with the latex may compete with the protein molecules in binding to the latex surface. Therefore, the examination of the binding of milk protein to small ULL was used as an alternative model to the latex particles. This chapter deals with the interaction of a number of the major milk proteins with small ULL, and also investigates the influence of charge and pH on these interactions.

4.2 Materials and methods

L-α-phosphatidyl-DL-glycerol (PG) and L-α-phosphatidylcholine (PC), both from egg yolk, were purchased from Enzymatix Ltd, Cambridge, UK and Sigma Chemical Company Ltd., Poole, Dorset, UK respectively. Caseins were purified chromatographically from bulk skimmed milk[66]. The A and B phenotypes of β-lg were purified from homozygous β-lg milks by method Ia of Armstrong *et al*[125], with the purified protein being freeze-dried rather than crystallised. β-cn was dephosphorylated using potato acid phosphatase obtained from Sigma[126].

Liposomes were prepared by drying 50mg of a chloroform solution of the phospholipid onto the walls of a round-bottomed flask, under vacuum for 2hr. Saline (0.9%; 25ml), previously purged with nitrogen and warmed to 25°C, was added and the contents mixed on a vortex mixer until all the lipid was removed from the flask walls. The suspension was then placed in a 100ml conical flask and sonicated under nitrogen for 1hr in a sonicating water bath. After standing for 2hr at 25°C to allow the liposomes to anneal, the suspension was centrifuged at 91,000g and 25°C for 2hr. The supernatant, which contained the small ULL, was decanted from the pellet and after filtering through a 0.2μm filter, was stored under nitrogen at 4°C until required. Liposomes were only used the day following their preparation.

The concentration of lipid in the supernatant fraction was determined by measuring its phosphorus content by a sulphuric acid digestion procedure[127]. Lipid was extracted from the aqueous suspensions by adding 1ml of the liposome preparation to 4ml of chloroform/methanol (2:1 v/v). The chloroform layer was collected and assayed for lipid phosphorus. The degree of oxidation of the phospholipids in the liposome preparation was determined spectrophotometrically at 233nm[128].

The average hydrodynamic diameter of the liposomes was determined by photon correlation spectroscopy (PCS) using a Series 7032 Multi 8 Correlator (Malvern Instruments Ltd., Malvern, Worcs. UK). Measurements of the dynamics of scattered light were made at 90°, average diffusion coefficients being determined by the method of cumulants[116], and particle diameters were calculated from these using the Stokes-Einstein relation for spheres. Aliquots of the proteins in saline were added to the liposome suspensions and incubated for at least 30min. at 20°C before determining the hydrodynamic diameter of the coated liposomes. Adsorbed layer thicknesses were determined by subtracting the uncoated liposome radius from that of the protein coated liposome particle. For each suspension, five determinations of particle radius were made and these were averaged to give the value for that suspension.

4.3 Results

4.3.1 Analysis of liposome preparation

Mean concentrations of the phospholipids in the ULL preparations were 1.08 $\pm$ 0.07mg ml^{-1} for PG and 1.00 $\pm$ 0.09mg ml^{-1} for PC. This was equivalent to a yield of 54 and 50% respectively. Typically, the PG liposomes had a mean diameter of 80nm and the PC liposomes, 150nm. The relative degree of error in measuring the increase in diameter of the particles as protein molecules adsorbed to the surface was therefore less with the PG liposome preparations than it was with PC. This explains the reduced scatter in the measurements of the increase in diameter as a result of protein binding to PG liposomes. Liposomes are naturally a polydisperse system. The filtering of the liposomes through a 0.2μm filter eliminates the large particulate matter. The resulting liposome suspension has a relatively high polydispersity of 0.1-0.4

compared to 0.02-0.05 obtained with polystyrene latex. Conventionally a system is considered polydisperse above values of 0.3. The values obtained for this parameter do not vary during normal adsorption studies and are consistent between preparations and with time. So it appears that the liposome preparation method produces a reasonably monodisperse suspension of liposomes. The total available liposome surface area in these studies was approximately 0.2 to 0.3m^2 ml^{-1} and the volume fractions of the solution occupied by the PG and PC liposomes were typically 0.0012 and 0.0028 respectively. The extent of oxidation of the lipids in the liposome preparations was low at 0.3% for PG and 0.08% for PC liposomes.

Attempts to separate bound from unbound protein by filtration or size exclusion chromatography, in order to determine the proportion of added protein which was bound to the surface, were unsuccessful. Since it was not possible to determine the amount of adsorbed protein, and since the available surface area would be important with respect to protein coverage, the increase in protein layer thickness was plotted as a function of added protein expressed as μg or mg of protein per square metre of available liposome surface.

4.3.2 Influence of ionic strength

Sodium chloride (0.9% *i.e.* 154mM) was found to be essential for binding of protein to both types of liposome. This level of NaCl had been used previously by workers investigating liposome preparations[129,130,131], presumably because it is the physiological concentration of NaCl. In the absence of salt, no increase in diameter was detected as the protein concentrations increased.

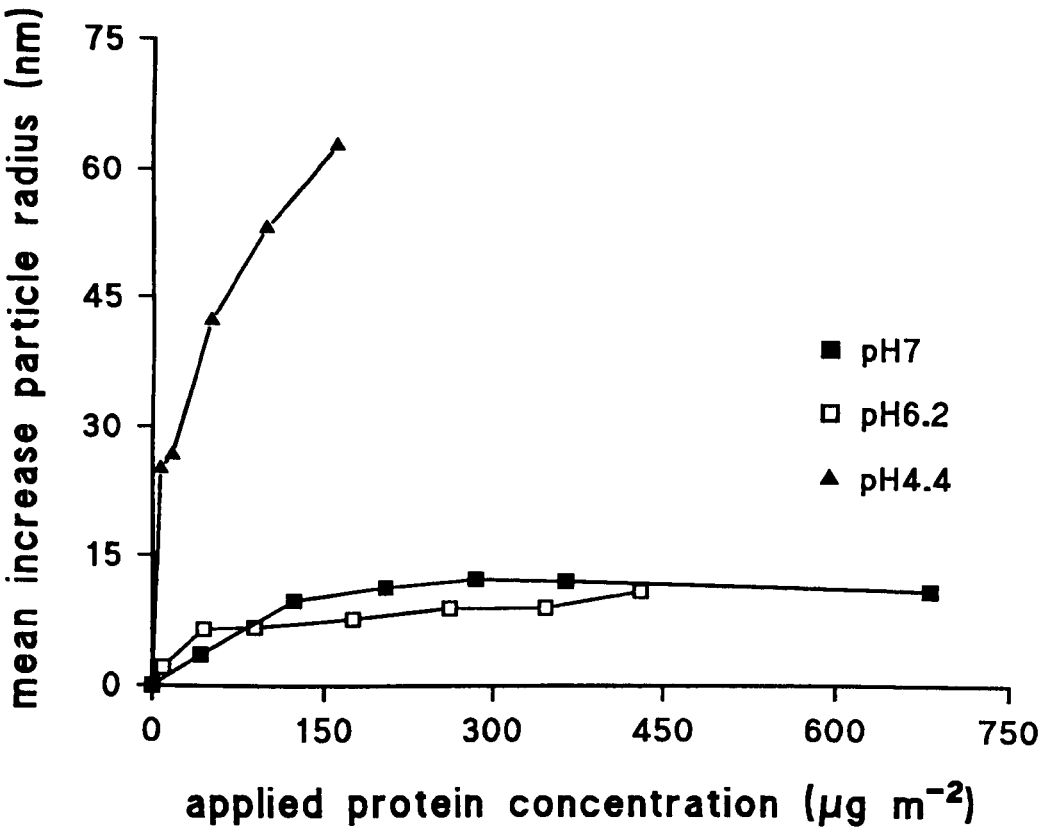

Fig. 4.3. κ–cn binding to PG liposomes at pH7, pH6.2 and pH4.4.

4.3.3 Effect of pH

In liposome suspensions in which isotonic saline was used as the hydration buffer, the pH was typically 6.2. To try and simulate these conditions, the pH of liposomes already present in 50mM bis-tris-propane (BTP)/0.9% NaCl pH7.0 was adjusted to pH6.2. Fig. 4.3 shows the effect on κ-cn binding in these conditions. There appears to be only a slight difference in the binding affinities between these two pHs, suggesting that the protein is probably binding in its native form. This is not true when the pH is reduced further, to pH4.4. The increase in radius at pH4.4 is much greater than at pH7.0, and is probably indicative of aggregation.

pH4.4 is too close to the isoelectric points of α_{s1}-cn and β-cn. Attempts to bind these proteins failed as they precipitated out of the stock solution. At pH9.0 no binding was observed with α_{s1}-cn, β-cn, κ-cn or β-lg. In the case of β-lg this was probably due to denaturation which occurs more rapidly at pH9.0[132]. In the presence of acetate buffer (pH4.4) the adsorption of both β-lg A and β-lg B is enhanced (Fig. 4.4). At pH7, addition of β-lg B resulted in a thicker adsorbed protein layer (8nm) when compared with β-lg A (4nm), although the concentration of protein required to reach the maximum layer thickness for both phenotypes was similar. This difference is significant since both results carry a standard error of approximately $\pm$1nm.

4.3.4 Adsorption of β-cn

Increase in particle size as a result of adsorption of native, fully phosphorylated β-cn to PG and PC liposomes is shown in Fig. 4.5. The maximum layer thickness on the PC liposomes was about 6nm whereas that on the PG liposomes was 11nm. The layer thickness on the PG liposomes is almost identical to that of β-cn on negatively

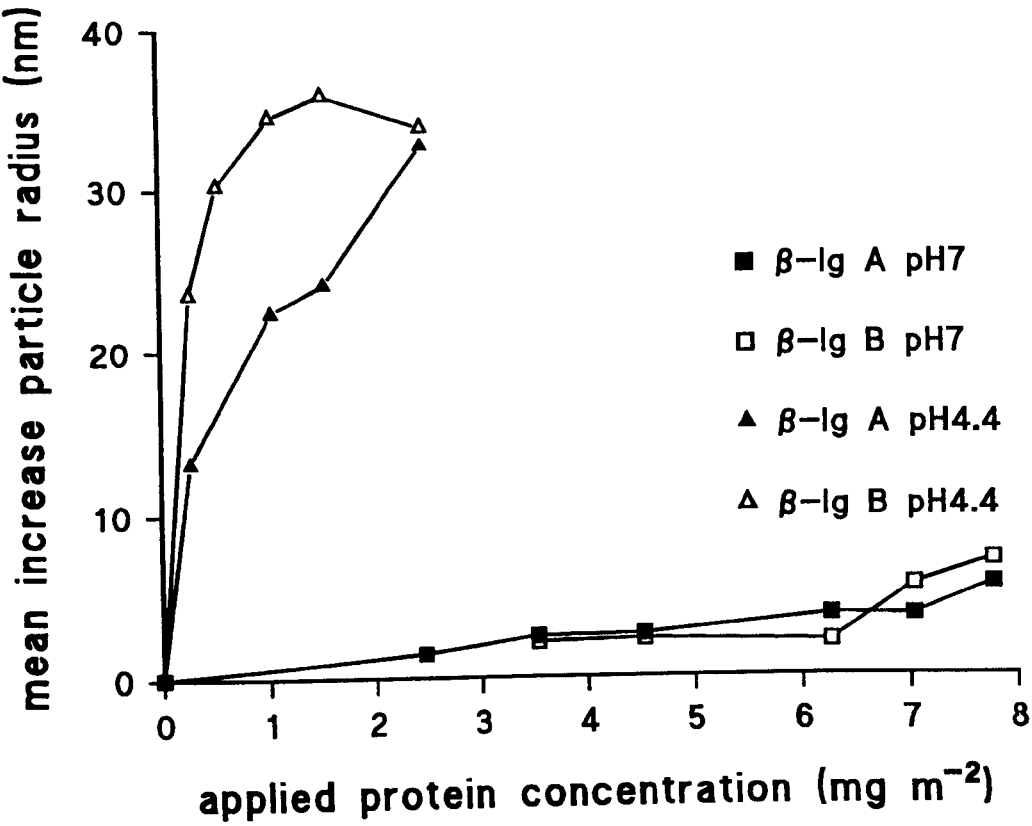

Fig. 4.4. β–lactoglobulin A + B binding to PG liposomes at pH7 and pH4.4

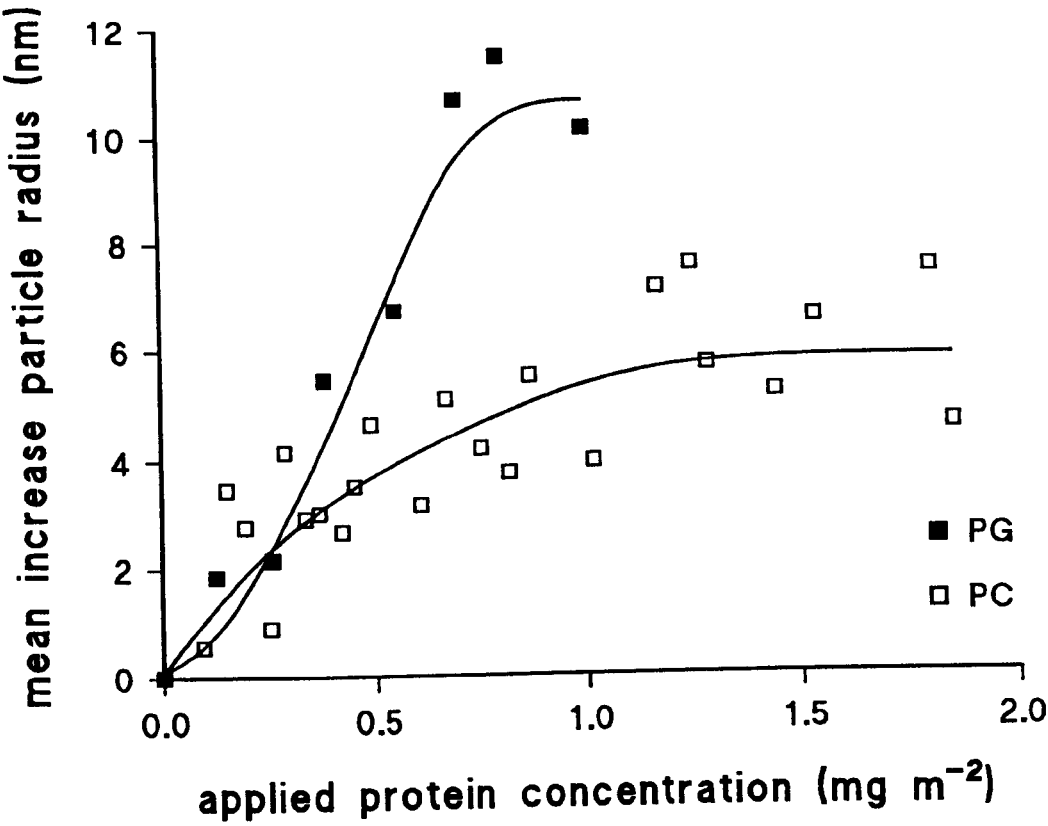

Fig. 4.5. β–cn binding to PC and PG liposomes.

Points shown are the results of different liposome preparations (5 for PG and 7 for PC).

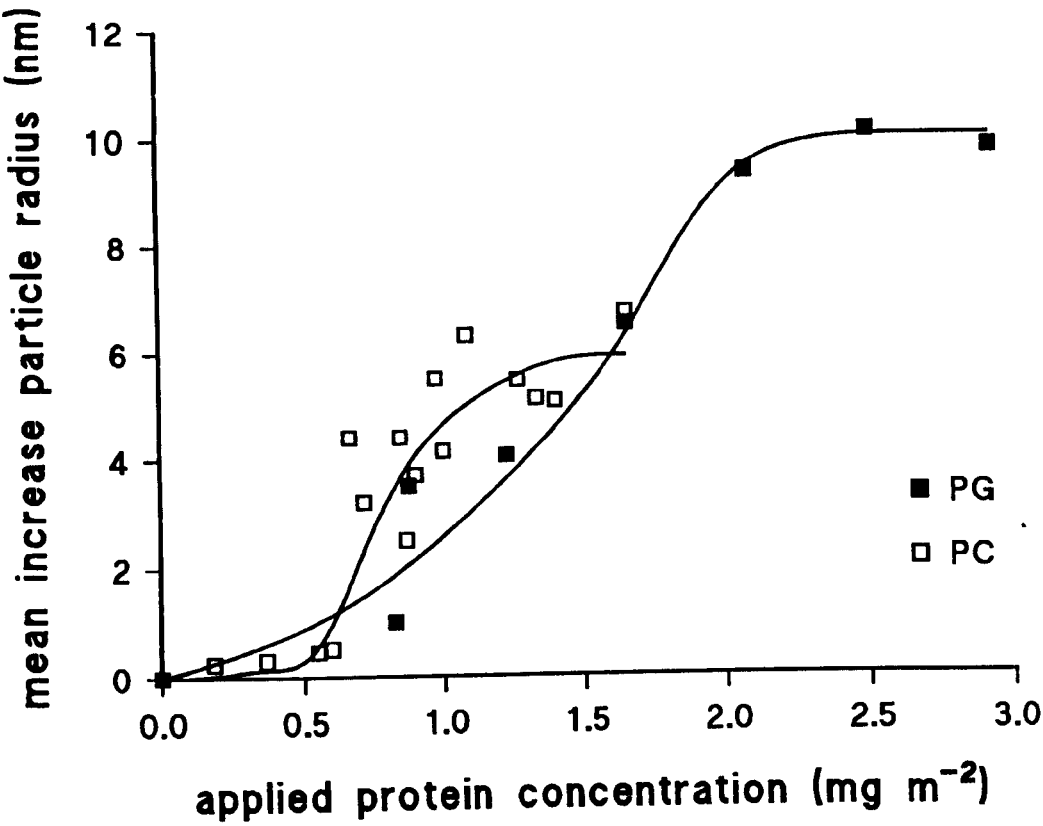

Fig. 4.6. Dephosphorylated β–cn binding to PC and PG liposomes.

Points shown are the results of different liposome preparations (4 for PG and 6 for PC).

charged latex as measured by PCS by Mackie *et al*[39], but 4nm less than that measured by Dalgleish[122] and Leaver and Horne[124] on the same type of latex. However, the addition of 154mM (0.9%) NaCl to these β-cn/latex suspensions caused a reduction in the layer thickness to about 10 to 11nm[124] (see Chapter 5). Some of the negative charge on the β-cn is due to the phosphoserine residues which form a cluster between residues 15 to 19. These phosphate groups can be removed by treating the protein with the enzyme potato acid phosphatase. When the binding of this dephosphorylated protein was measured (Fig. 4.6), the adsorbed thickness on the PG surface was found to be slightly less (by about 0.5 to 1.0nm) than that of phosphorylated β-cn. This decrease in the thickness of the protein layer as a result of dephosphorylation, was less than the 4nm reported by other researchers using negatively charged latex[122,39]. But again, in the presence of 154mM NaCl, the difference in the layer thicknesses of native and dephosphorylated β-cn on negatively charged latex is reduced to 1 to 2nm (see Chapter 5). The thickness of the adsorbed protein layer on PC liposomes was the same for both the native and dephosphorylated forms. The shape of the plot of the increase in radius as a function of the concentration of added dephosphorylated β-cn was considerably more sigmoidal than that for native β-cn on both surfaces.

4.3.5 Adsorption of α_{s1}-cn

The binding of α_{s1}-cn to the two types of liposomes is shown in Fig. 4.7. At low concentrations of the protein, the increase in the radius of both PC and PG liposomes was very similar. Above a protein concentration of about 20μg ml^{-1}, the particle radius of the PG liposomes began to increase more rapidly, probably signifying aggregation, reaching a plateau value of about 50nm compared with 7nm on the PC

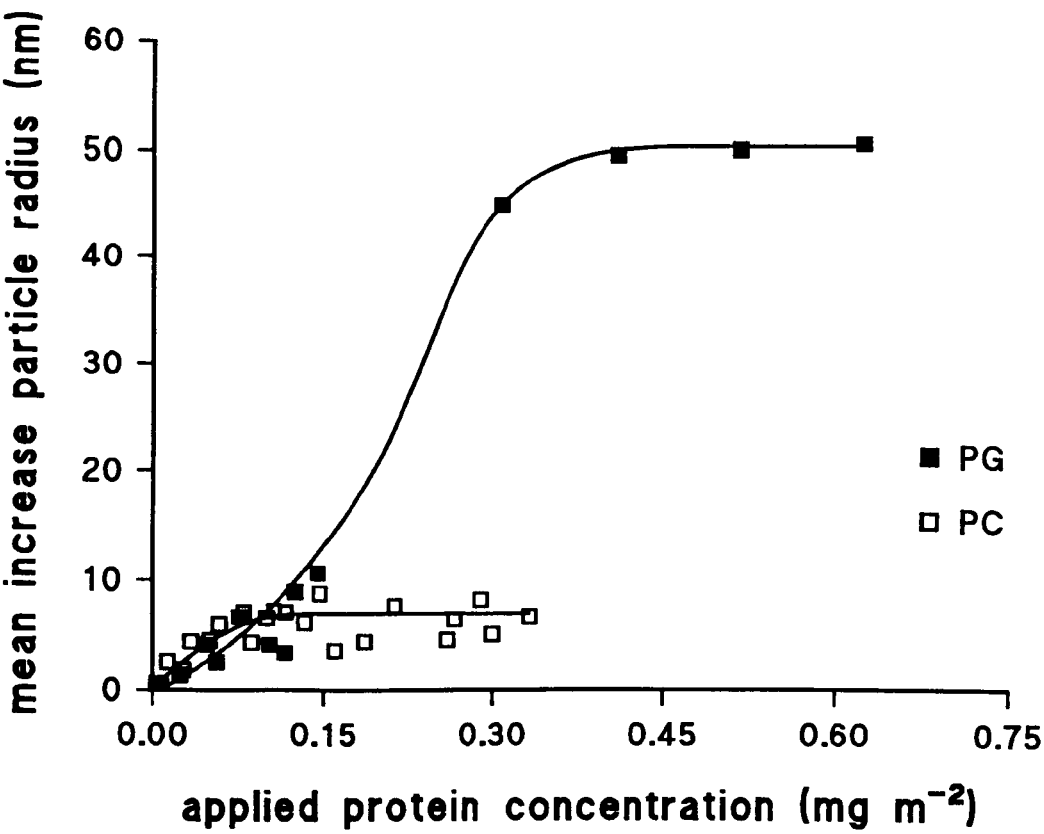

Fig. 4.7. α_{s1}-cn binding to PC and PG liposomes.

Points shown are the results of different liposome preparations (6 for PG and 8 for PC).

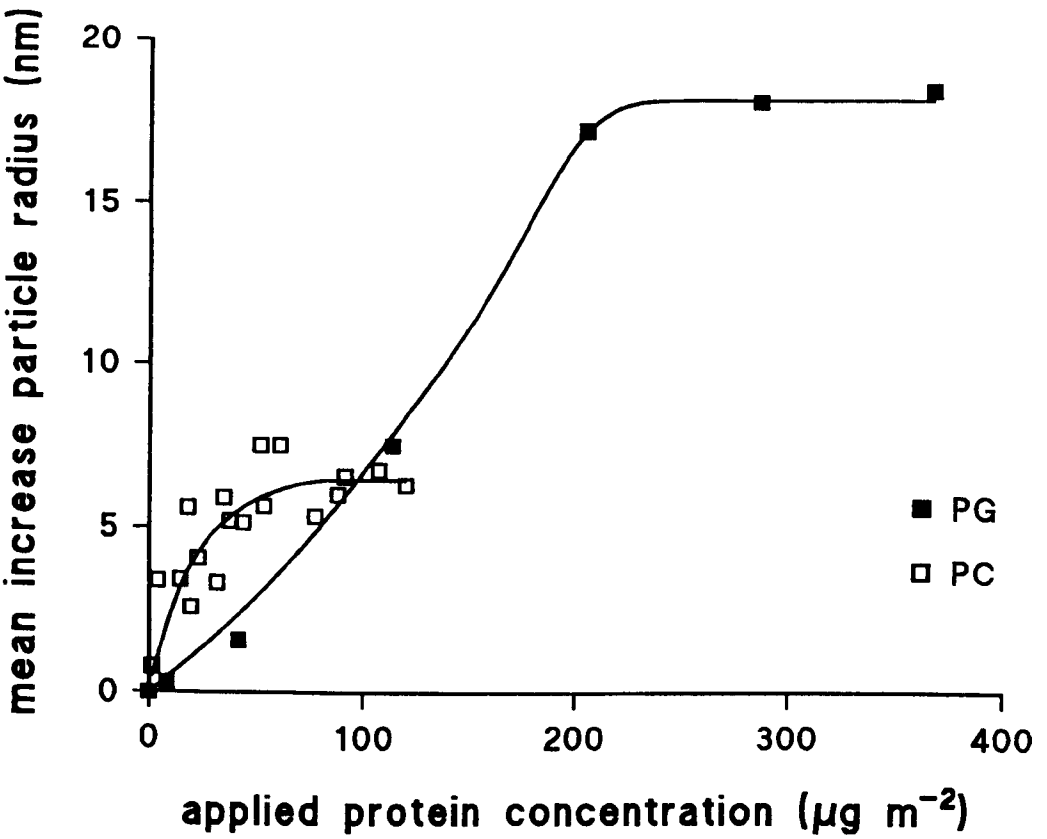

Fig. 4.8. κ–cn binding to PC and PG liposomes.

Points shown are the results of different liposome preparations (3 for PG and 6 for PC).

liposomes. Dalgleish[122], reported a layer thickness of 10.5nm for α_{s1}-cn on negatively charge latex, which increased to 11.5nm when urea was added to the buffer, presumably as a result of urea causing unfolding of the protein structure. The same author also detected aggregation of the latex particles at low protein levels in the presence of 50mM NaCl, but this was overcome at higher protein concentration.

4.3.6 Adsorption of κ-cn

The increase in the radius of PC and PG liposomes with increase in the applied κ-cn concentration at pH6.2 is shown in Fig. 4.8. The maximum layer thickness was greater on PG liposomes than on PC (18.0 and 6-7nm respectively). At low protein concentrations the diameter of the PC liposomes increased more rapidly than that of the PG. Whether this was due to differences in the affinity of the κ-cn for the two surfaces, and hence in the amount of protein bound, or to differences in the orientation of the protein on the surface is not known.

The thickness of the κ-cn layer on PG liposomes was found to be time dependent (Fig. 4.9). In general, at higher protein concentrations the adsorbed layer thickness decreased with time, whereas it increased at low protein concentrations. This may indicate that initially there is a relatively rapid adsorption of the protein molecules to the surface, which is followed by a slow rearrangement.

The age of the κ-cn solution was found to be important with respect to adsorption behaviour. On addition of freshly prepared κ-cn to PG liposomes a layer 8nm thick was formed. However, when the same protein solution was used 3days later, very little binding occurred (Fig. 4.10). This may be due to stable aggregates, which had a lower affinity for the liposome surface, forming in the stock solution.

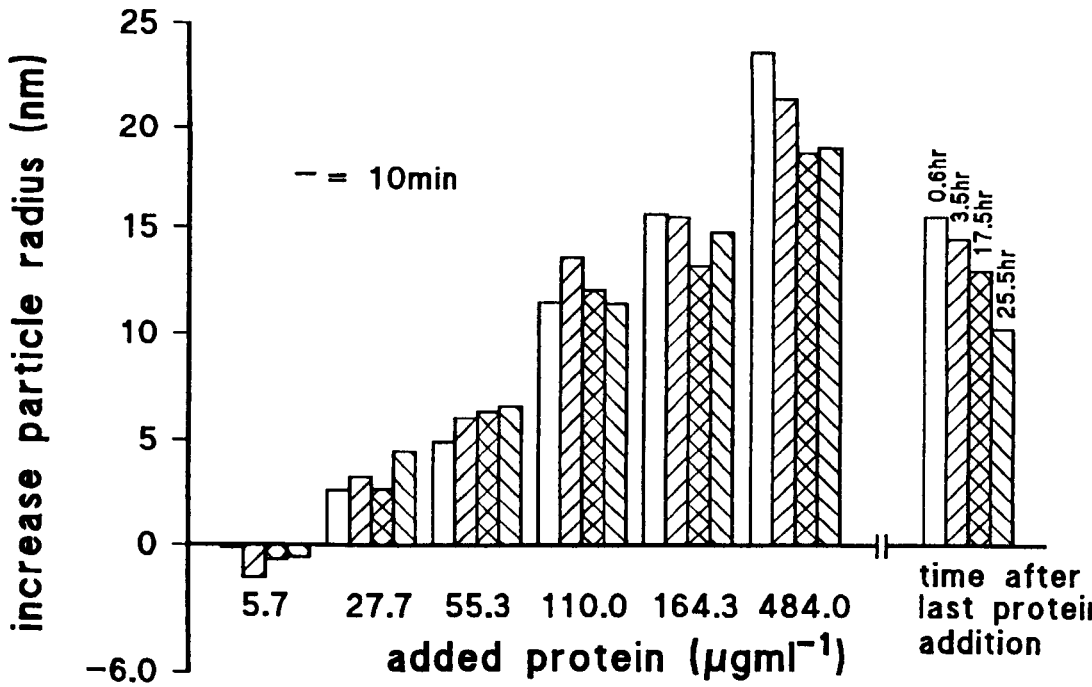

Fig. 4.9. Effect of time on κ−cn binding to PG liposomes.

Each protein concentration is added sequentially to the previous sample and sized continually for 40min. Sizes every 10min. are recorded on on the bar chart. Standard errors range from +/−1 to +/−2nm.

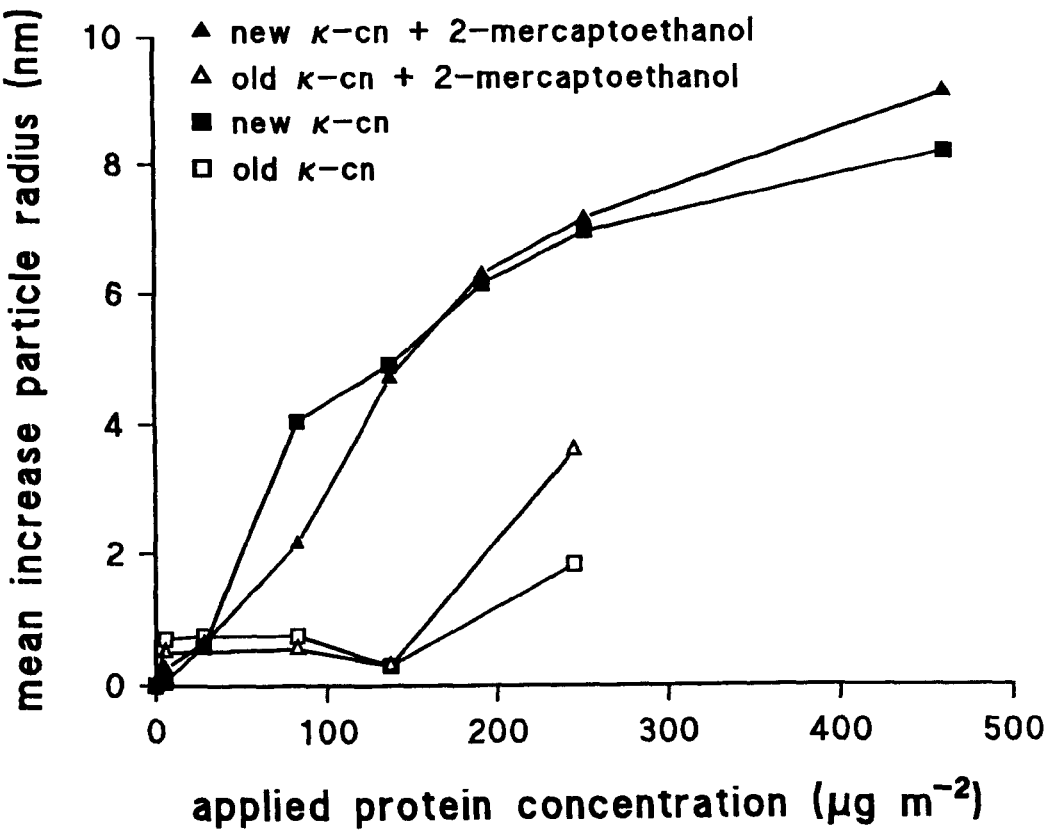

Fig. 4.10. Effect of κ–cn age and 2–mercaptoethanol on κ–cn binding to PG liposomes in 50mM bis–tris–propane pH7.0.

This was supported by the observation that although addition of 2-mercaptoethanol to a fresh solution of κ-cn did not change the binding curves, it did increase the layer thickness of 3 day old κ-cn, but not to the levels of fresh κ-cn. This suggests that the formation of the aggregates may be, in part, irreversible. The layer thickness of freshly prepared κ-cn on PG liposomes in Fig. 4.10 was about 10nm less than in Fig. 4.8. In Fig. 4.8 the liposomes were prepared in 0.9% saline pH around 6.2, however, in Fig. 4.10 50mM bis-tris-propane/0.9% saline, pH7.0, was used as the suspension buffer. This slight change in pH coupled with the buffer salts is probably responsible for this. Because earlier studies had shown that the layer thickness was altered by the choice of suspension buffer it was decided to remain with one suspension solution throughout (0.9% saline).

κ-cn coated PG liposomes were treated with trypsin. The concentration of trypsin used was similar to that used by Dalgleish and Leaver[34] to hydrolyse β-cn on coated latex. From earlier experiments it appeared that trypsin works better on freshly coated liposomes, than if the liposomes were coated with κ-cn the day before. This could be due to protein molecules "settling-down" on the liposome surface with time. The trypsin sensitive bonds may, therefore, become masked resulting in the trypsin molecules being unable to reach the bonds in order to cleave the protein. When trypsin was added to κ-cn coated PG liposomes (Fig. 4.11) a fall in radius of about 9nm occurs followed by aggregation. The initial drop in radius does not fall to that of the uncoated liposomes, but leaves a protein layer about 9nm thick.

4.3.7 Adsorption of β-lg

The binding of both the A and B variants of β-lg to the liposomes at pH6.5 was

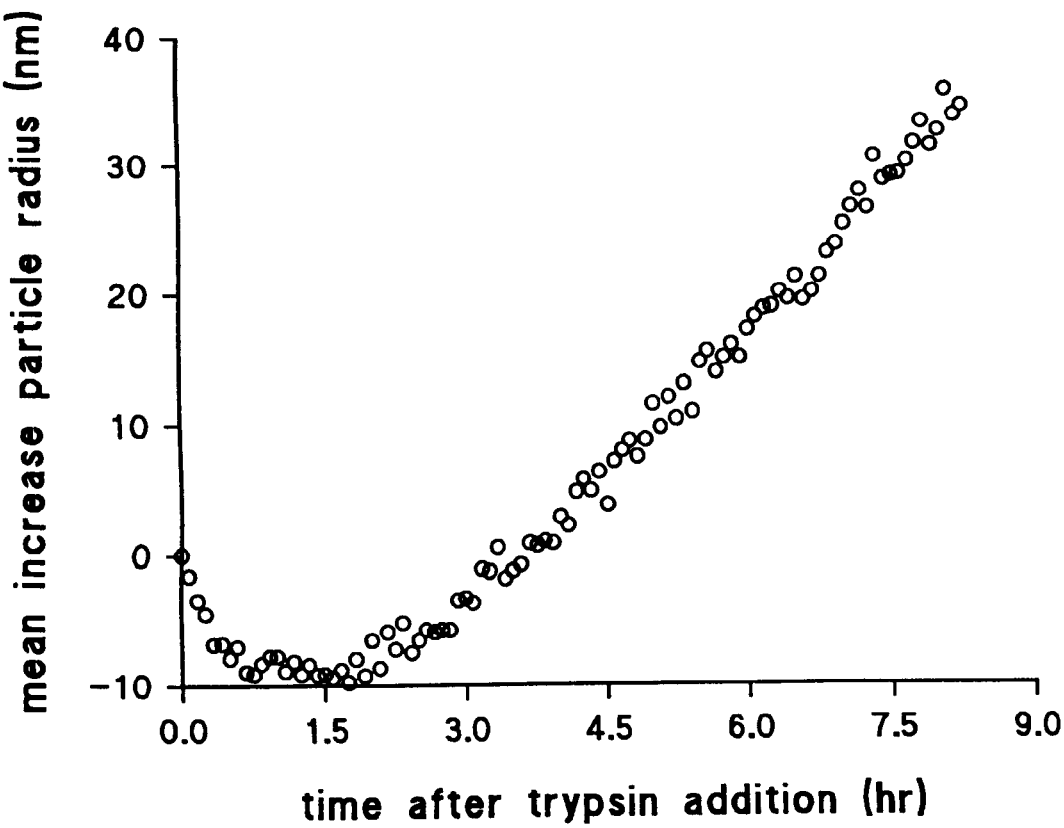

Fig. 4.11. Effect of trypsin on κ−cn coated PG liposomes.

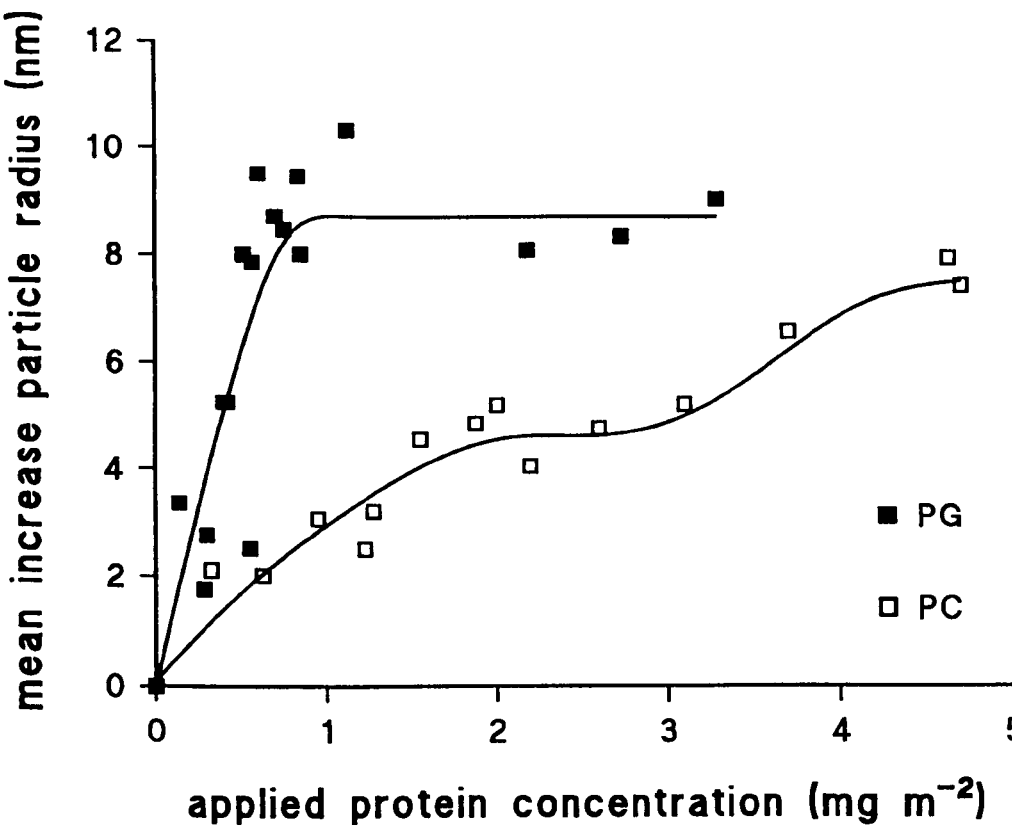

Fig. 4.12. β–lg A binding to PC and PG liposomes at pH6.5.

Points shown are the results of different liposome preparations (5 for PG and 6 for PC).

similar. The plot of the increase in radius of the PC liposomes with protein concentration (Fig. 4.12) had a stepped appearance. The first plateau corresponded to a protein layer 4nm thick and the second plateau of 7.5nm at higher protein levels. No stepping was observed with the PG liposomes where a single plateau at a layer thickness of 8-9nm was determined.

4.4 Discussion

In these studies of the interactions between surface active proteins and liposomes, it was important to keep the levels of lipid oxidation low. This is because the oxidised products may compete with the proteins for the surface and will tend to destabilise the phospholipid bilayer. Preparation of liposomes by bath sonication under nitrogen was found to be more effective at minimising the amount of oxidation than was probe sonication.

The failure to detect any increase in diameter of the liposomes in the absence of salt suggests that the initial charge-charge repulsion between the proteins and liposome surface was diminished at high salt concentration, allowing hydrophobic interactions to dominate.

The differences in the shapes of the plots of increase in particle diameter as a function of added casein for the two types of liposome and also in the thickness of the adsorbed protein layers, can largely be explained on the basis of the net charge on the liposome surface and the distribution of charge on the protein molecules. Above pH4.4, PG possesses a net negative charge[133], whereas the zwitterionic PC has no net charge. β-Cn is the most hydrophobic of the caseins and has a pronounced amphiphilic structure with a hydrophilic N-terminal region and a relatively hydrophobic C-terminal

region. The 21 residues in the N-terminal domain have a net negative charge of -12[63]. The remainder of the molecule has no net charge. Therefore, it would be expected that electrostatic charge repulsion would lead to thicker layers on the PG liposomes as the N-terminal region is pushed away from the surface. There is increased sigmoidicity in the plots of the increase in diameter of both of the liposome preparations as a function of the concentration of added dephosphorylated β-cn. This may have been due to the removal of some of the negative charge permitting the protein molecules to pack closer together, before electrostatic repulsion on adjacent protein molecules pushes them out into the aqueous phase to their maximum extent.

The increase in diameter in the PG liposome preparation at higher concentrations of α_{s1}-cn was too great to be accounted for merely by extension of the protein from the surface. Protein bridging between liposomes is the most likely explanation. As with the other caseins, the charged amino acids of α_{s1}-cn are not uniformly distributed throughout the molecule[63]. However, unlike β-cn and κ-cn, the highly charged region is located in a more central position. At pH6.6, the region comprising residues 41-80, which also contains the phosphoseryl cluster, would have a net charge of about -20. The remainder of the molecule will have no net charge. On the PC surface the α_{s1}-cn apparently behaves like the other caseins with the unordered casein molecule lying relatively close to the surface. On the negatively charged PG surface, however, charge repulsion would result in the negatively charged region of the protein being displaced from the liposome surface. It apparently remains attached by one or both ends of the molecule. As protein loading increases either one of the ends is displaced from the surface by competition with other casein molecules, or the concentration of the free ends reaches a level at which they will link to other

liposomes and form stable clusters. This is indicated by the large increase in particle size.

κ-cn also has an amphiphilic structure with a hydrophobic domain in the N-terminal region and a C-terminal polar domain[63]. No positively charged amino acids are found in the C-terminal 53 amino acids. The net charge of the C-terminal portion at pH6.6 is -10 or -11. The sialic acid residues are bound to κ-cn in the polar domain and each residue contributes an additional negative charge. Therefore, for three tetrasaccharride chains there would be an overall net charge of -16 or -17. Hence, it would be expected that electrostatic repulsion would be greater between the negatively charged C-terminal tail and the negatively charged PG head groups. This would result in the charged κ-cn "tail" being pushed further from the liposome surface.

The time dependent decrease in the thickness of the adsorbed κ-cn layer and the relatively high layer thickness on PG liposomes, could have been due to adsorbed κ-cn molecules rearranging and settling down onto the negatively charged surface. Multimeric κ-cn (formed through disulphide bridging between molecules) may also rearrange after adsorption to the liposome surface.

The fact that 2-mercaptoethanol causes no appreciable difference in the binding of fresh κ-cn to PG liposomes, suggests that κ-cn may be binding in a monomeric form. 2-Mercaptoethanol reduces disulphide bonds, so preventing bridging between κ-cn molecules. Therefore in the presence of 2-mercaptoethanol κ-cn should be binding as monomers. Some of these disulphide bonds may be on the inside of the κ-cn complex and so protected from the action of 2-mercaptoethanol, which would explain why the addition of 2-mercaptoethanol to aged κ-cn only slightly increases the thickness of the κ-cn layer. Larger, more stable aggregates may be present in aged solutions

which cannot be disrupted by 2-mercaptoethanol.

Lowering the pH of binding causes aggregation when κ-cn is added to PG liposomes. The isoionic point of κ-cn is approximately pH5.5[63], therefore, at pH4.4 the κ-cn molecule will be largely positively charged. This will result in greater attraction towards the negatively charged PG. This may result in the κ-cn acting as a bridge between liposome molecules, which would then result in a larger particle size.

When trypsin was added to κ-cn coated PG liposomes, the radius of the coated liposomes decreased. This was followed by an increase due to aggregation. Trypsin hydrolyses proteins at lysine and arginine residues, of which κ-cn has a total of 14. The fact that the size of the particles does not decrease to that of the uncoated liposomes could be due to aggregation beginning before the hydrolysis of all the protein molecules is complete, or some peptides may remain bound to the liposome surface. As κ-cn is hydrolysed, the more hydrophobic peptides will remain bound to the liposomes, whereas the hydrophilic peptides will migrate into the aqueous phase. As proteolysis proceeds the surface of the liposomes will become more hydrophobic and so aggregate.

In contrast to the random coil structure of the casein molecules, β-lg has a highly folded, globular structure. Addition of β-lg to liposomes also caused aggregation at low pH values. This agrees with Cornell's[134] work on interactions between β-lg and the negatively charged lipid, phosphatidic acid. At pH4.4 β-lg exists as polymers with β-lg A forming octamers with a diameter of about 8.2nm along the long axis[104], whilst β-lg B only forms tetramers with a diameter of 6.7nm. As a consequence, it is these polymers which bind to PG liposomes. A maximum increase in radius of approximately 8.2nm for β-lg A and 6.7nm for β-lg B, would be expected if a monolayer of aggregates is formed. In both cases the increase in radius is much

larger *i.e.* approximately 32nm for β-lg A and 35nm for β-lg B. This suggests that either multilayers of the polymerised β-lg are coating the liposomes, or that β-lg induced aggregation of liposomes is occurring. Binding of β-lg to PG at pH4.4 which is below the isoelectric point of the protein at 5.1, probably results from electrostatic attraction between the positively charged protein and negatively charged PG surface, as concluded by Cornell[134].

Contrary to the results of Cornell[134] at pH7.0, β-lg also bound to PG liposomes. This discrepancy could be due to the difference in the lipids used (Cornell used phosphatidic acid), which may make a difference at pH7.0, but not at pH4.4. At pH6.2, β-lg exists as a dimer with a long axis of 6.93nm and a short axis of 3.58nm[103,104]. If the β-lg molecules were initially adsorbed onto the PC surface with the long axis parallel to the surface, this would result in a layer thickness of around 4nm. As the amount of added protein increases, these molecules may then reorientate such that the long axis was perpendicular to the surface. The measured layer thickness of 7.5-8nm is within experimental error of the expected value of 6.93nm. There was no indication of this stepping on the PG liposomes. The final layer thickness of around 8nm suggests that the protein molecules were orientated perpendicular to the surface at all protein concentrations. As with the binding of casein molecules, this may have been due to charge repulsion between, in β-lg, the liposome surface and negatively charged regions of β-lg. The charge distribution is more difficult to predict due to its globular structure. Examination of the distribution of charge does not show the existence of any specific, highly charged regions[63]. An alternative explanation for the stepping behaviour is the formation of multilayers of protein on the surface. In the absence of measurements of the protein surface loadings, this cannot be ruled out. But

even assuming that all of the added protein is adsorbed to the liposome surface, multilayer formation must be occurring at relatively low surface loadings.

This study has clearly shown the role which charge plays in adsorption behaviour in the liposome-protein system. This may be important not only with respect to the long-term stability of colloidal food systems but also in the use of liposomes as drug carrier systems in the body. In the latter case, there will be a tendency for injected liposomes to adsorb proteins from blood serum. As this work shows, the composition and hence the charge on the liposome surface may influence the behaviour of the adsorbed protein. This may explain, in part, why different formulations of liposomes have differing life-spans in the blood stream. Similarly, the types of phospholipid, pH and the ionic strength of foods in which they are found, may influence the long-term stability of these colloidal systems.

The refractive index of the water-filled liposomes was significantly less than that of the solid latex particles usually used as model systems in protein binding studies. As a result, the amount of light scattered by the liposomes was also less. In addition the volume fraction of the liposomes used in these studies was 50 to 100 times greater than that of latex particles used in similar studies. Even though this is still only 10% of that of a real colloidal food system such as milk, the maintenance of single scattering conditions makes it a more suitable model system when the ability of proteins to bridge between individual particles is being considered. However, the failure to separate bound from unbound protein means that surface loading of protein cannot be determined. In addition, liposome preparation was a very time consuming process. Therefore, subsequently, work concentrated on the determination of protein binding to latex particles.

Chapter 5

Influence of Electrostatic Interactions on Adsorbed β-cn Layers

5.1 Introduction

Information on the thickness and structure of adsorbed protein layers can be used to make predictions about the stability of the emulsion system[37]. Proteins carry an electric charge which can result in intra- and intermolecular electrostatic interactions. These interactions will influence the binding of the protein and the adsorbed layer thickness.

These interactions can be influenced in various ways. Binding of one protein can be influenced by competitive adsorption with another protein[15] or other surfactants[18]. The binding of cations to α_s-cn and β-cn has been shown to reduce the solubility[135] and therefore, emulsifying properties of these proteins.

Modification of proteins effects their emulsifying and solubility properties. Chobert *et al*[136] showed that ethyl-esterification lowered the solubility and emulsifying properties of β-cn, whilst ethyl-alkylation increased the emulsifying properties. Galactosylation also increases the emulsifying activity of β-cn[137].

This chapter studies the effects which modifying β-cn so as to reduce its net negative charge, have on the binding of the protein to negatively charged polystyrene latex. This involves the enzymatic removal of the cluster of phosphate groups on the serine residues in the N-terminal region of the molecule. In addition, the effect of ionic strength on the adsorbed protein layers was also investigated. Also reported are parallel measurements of particle electrophoretic mobility and protein adsorption

isotherms, under the same experimental conditions. These will provide a comprehensive picture of the adsorbed protein layers.

5.2 Materials and methods

Polystyrene latex (nominal diameter 91nm) and potato acid phosphatase were purchased from Sigma Chemical Company Ltd., Poole, Dorset, UK. Stock latex suspensions were used as supplied, without treatment to remove any stabilising surfactants.

Bovine β-cn was purified from bulk milk by ion-exchange chromatography[66]. β-cn was completely dephosphorylated using potato acid phosphatase[126], obtained from Sigma.

5.2.1 Latex binding studies

Stock latex and protein solutions were prepared in imidazole/HCl buffer (20mM, pH7.0). Latex was diluted to 1μl ml^{-1} in imidazole/HCl buffer. Stock calcium solution was prepared from calcium chloride hexahydrate, the Ca^{2+} content being determined by titration with a standard solution of ethylene diamine tetra-acetic acid using a calcium selective electrode (Radiometer, Copenhagen). Aliquots of protein were added to the latex suspension and left for 20min. before sizing. The concentration of the stock protein solutions were measured spectrophotometrically using known absorbance coefficients.

The hydrodynamic radii of the latex particles before and after treatment with protein, were measured using photon correlation spectroscopy (PCS). Adsorbed layer thicknesses were determined by subtracting the uncoated latex radius from that of the

protein-coated particle. For each suspension five determinations of particle radius were made and these were averaged to give the value for that suspension. In all cases standard deviations of these averages were about 1 % of uncoated latex radius. In cases where aggregation was occurring at low applied protein concentrations, separate latex suspensions were prepared for each different applied protein concentration.

5.2.2 Adsorption isotherms

The amounts of protein adsorbed to the latex were determined by centrifuging the suspension at 30,000g for 2hr. at 20°C to pellet the latex. The protein content of the supernatant was then determined by the Bradford method[138]. This was converted to a surface coverage measurement by dividing by the total available surface area of latex.

5.2.3 Electrophoretic mobilities

These were deduced from the Doppler shift in frequency of the light scattered by the particles in an electric field using a "particle charge" system. Dispersions of protein-coated latices were prepared as for PCS, except for the addition of sodium chloride at a concentration of 50mM. The salt was required in order to provide an ionic environment in which the particles could respond.

5.3 Results

5.3.1 Adsorption isotherms

The measured adsorption isotherms for native and fully dephosphorylated β-cn onto polystyrene latex at 20°C and pH7.0 (20mM imidazole/HCl buffer) are shown in

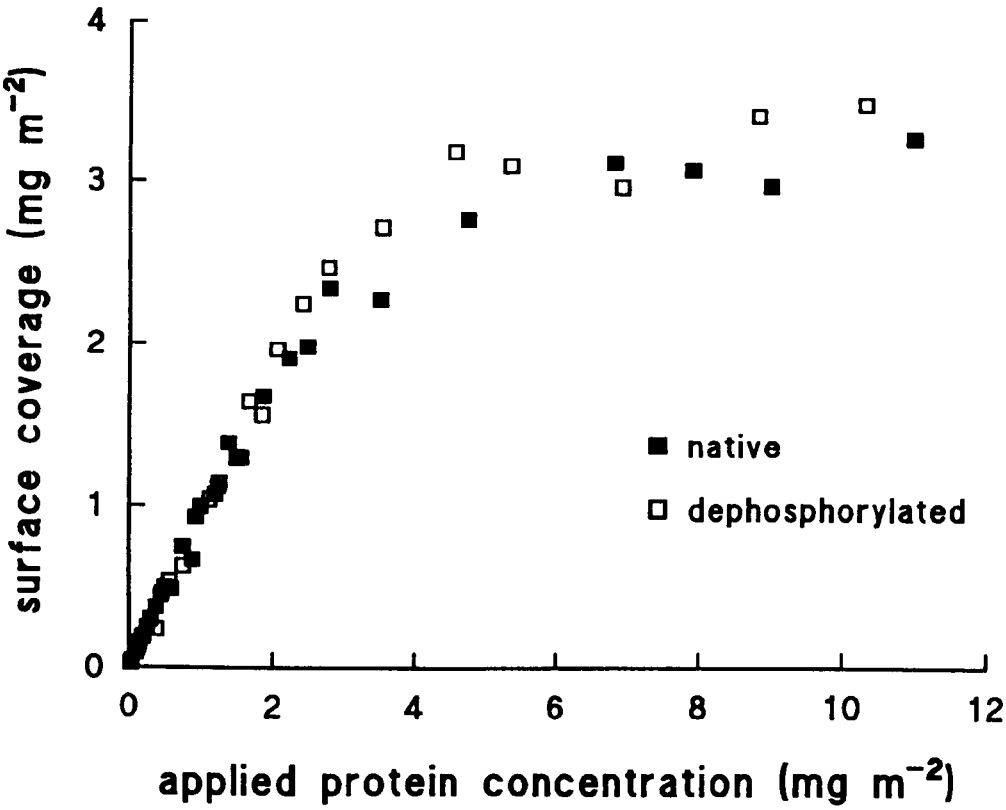

Fig. 5.1. Adsorption isotherm for β–cn on latex.

Fig. 5.1. Isotherms are plotted as a function of the applied protein concentration, defined as the concentration of protein supplied per unit area of available latex surface. The adsorption isotherm for native β-cn resembles that of Mackie *et al*[39], though the applied protein levels used here extend to higher values in the plateau region in order to guarantee that saturation coverage has been reached.

The adsorption isotherms for both native and dephosphorylated β-cn are of the "high-affinity" type, surface coverage rising linearly with unit gradient in the lower range of applied protein. Both isotherms reach plateau values in the range of applied protein between 4 and 6mg m^{-2}. The adsorption of dephosphorylated β-cn apparently continues to increase linearly with applied protein concentration to higher surface coverages than native β-cn. This may indicate a slightly higher affinity for the latex or possibly a higher packing density on the surface with the dephosphorylated protein. The latter possibility is also indicated by the plateau values for the surface coverage. These average at 3.3mg m^{-2} for dephosphorylated β-cn and 3.1mg m^{-2} for native β-cn. Tighter error bars are required before a definitive answer can be supplied.

The close similarity in the adsorption behaviour of the two proteins suggests that the affinity of the β-cn for the polystyrene surface was largely unaffected by the removal of the cluster of phosphate groups from the N-terminal of the protein. This suggests that this region of the molecule does not bind to the latex surface. The values for the saturation surface coverage for native β-cn on polystyrene latices agree well with most previously published values[139,39], the exception being the large value of 6mg m^{-2} obtained by Dalgleish *et al*[140], who expressed concern about possible losses of protein through binding to the filters used in the filtration procedure to separate the latex-protein complex from unbound protein.

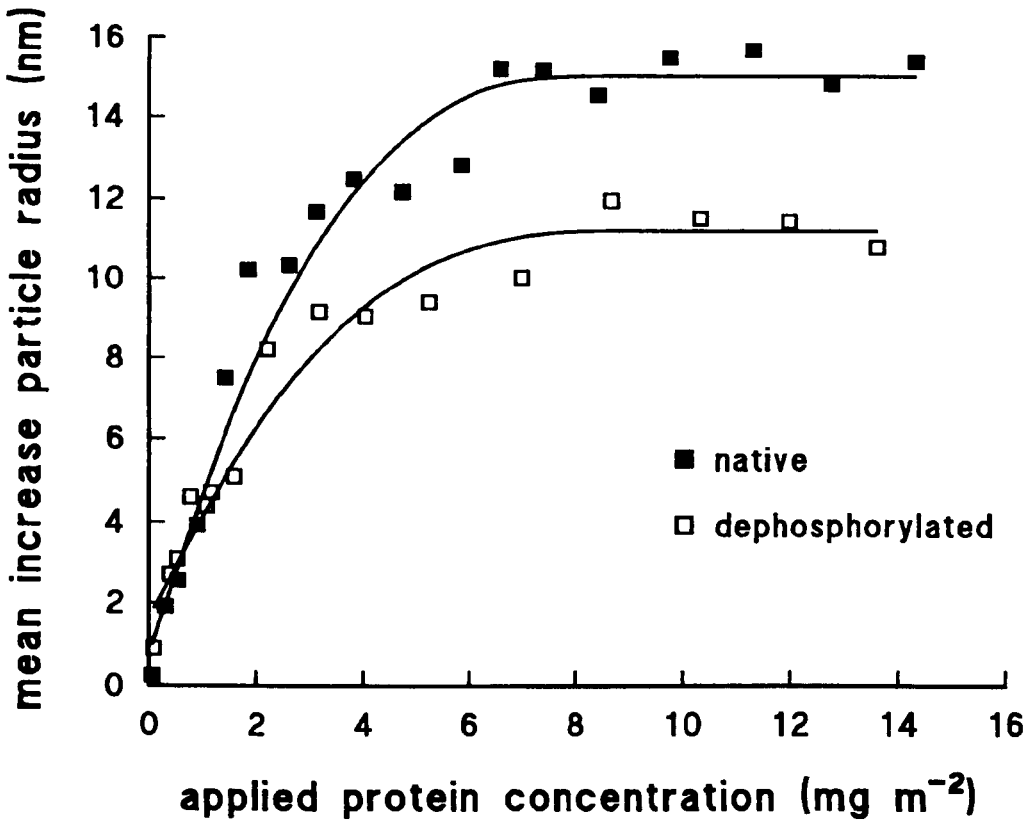

Fig. 5.2. β–cn adsorption to latex.

5.3.2 Adsorbed layer thickness

The increase in the hydrodynamic radius of the latex particle in the presence of native and dephosphorylated β-cn is shown in Fig. 5.2. As the applied protein concentration was increased, there was a smooth increase in the measured radius of the latex/casein complex. For the native casein, this increase in radius levels off at 15.0nm, whilst for dephosphorylated β-cn there is a plateau at 11.3nm. These plateau values are interpreted as representing the hydrodynamic thickness of an adsorbed monolayer of protein around the latex particle, and not artefacts caused by limited aggregation of the latex/protein complex, as demonstrated by previous researchers[140,39,122]. The values for layer thickness of both native and dephosphorylated β-cn are almost identical to those of Dalgleish[122] under the same solution conditions. However, results for native β-cn are 3nm greater than the value obtained by Mackie *et al*[39]. Again it is noted that the applied concentration range used is twice as great as that used by Mackie *et al*[39]. A layer thickness of around 12nm is achieved in the region of adsorption density that they considered to correspond to a plateau. The results reported here agree with this, but further thickening of the native protein layer was seen at slightly higher applied protein levels before a constant thickness was reached over a reasonable range of protein concentration. Mackie *et al*[39] may have reached an intermediate layer thickness where the protein molecules undergo rearrangement prior to any observed increase in layer thickness.

The results for dephosphorylated β-cn do not show the sigmoidal dependence on protein concentration observed by Dalgleish[122]. There was no apparent induction stage at low protein concentrations. Instead there was the same linear increase in radius as was found for native β-cn. Plots for both proteins superimpose in this area

of the graph. The author has no definitive explanation for this difference, though it may be due to the β-cn phenotype used. In these studies β-cn B was used, but β-cn purified from bulk milk was used by Dalgleish, which would contain phenotypes A and B.

5.3.3 Effects of NaCl addition

The above studies of layer thickness were carried out at low ionic strength. This was to maximise the possible effects of electrostatic interaction between the highly charged N-terminal region of β-cn and the negatively charged latex surface. When similar measurements were carried out in buffer containing 50mM NaCl, aggregation was observed at low applied protein concentrations (<2mg m^{-2}). These surface coverages were lower than the plateau values of Fig. 5.1. This bridging flocculation has been observed in previous studies with β-cn[139,122]. At higher applied protein concentrations (>4mg m^{-2}), this aggregation does not occur, and a plateau value for the increase in particle radius is achieved. For native β-cn the presence of 50mM NaCl produces a slight decrease in layer thickness to 12.9nm, but for dephosphorylated β-cn, the layer thickness remains the same, within experimental error, at 11.0nm.

In the next experiment, measurements of layer thickness were made on latex suspensions as a function of applied protein concentration. First measurements were taken in salt-free buffer and again following the addition of sufficient NaCl solution to each protein/latex suspension to give a final concentration of 25mM. In the absence of NaCl, the layer thickness for the individual aliquots of applied protein was close to those in Fig. 5.2, for native and dephosphorylated β-cn. When NaCl was added, bridging flocculation was again observed at low applied protein concentrations. As

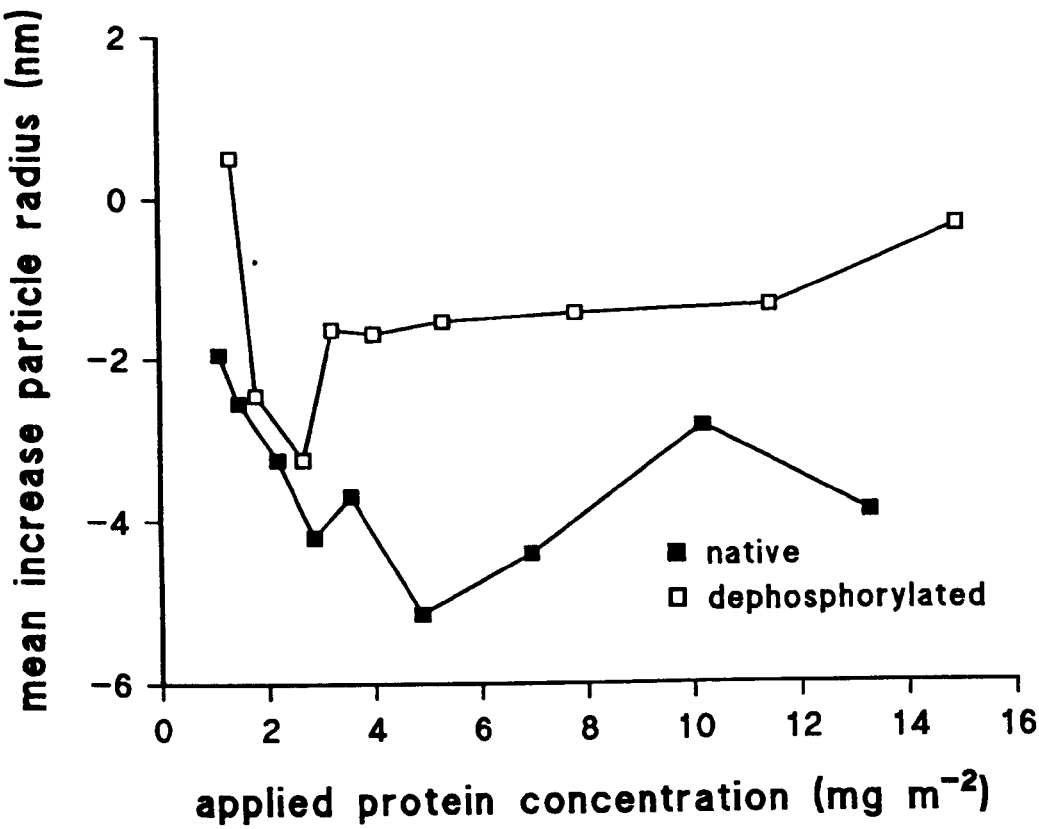

Fig. 5.3. Effect of adding NaCl at a level of 25mM on the thickness of pre-adsorbed β-cn layers.

applied protein concentration increased aggregation was no longer obvious, and decreases in adsorbed layer thickness occurred (Fig. 5.3). Before complete surface coverage is achieved (<3mg m^{-2}) both protein layers show similar decreases in thickness on exposure to NaCl. With complete coverage, the dephosphorylated protein partially recovers. The layer thickness becomes less responsive to the effects of NaCl addition, producing an average decrease of approximately 1.5nm over the region of saturated surface coverage. Over the same range of applied protein concentration the total contraction of native β-cn remained at 3.6nm. Therefore, the more highly charged protein is more responsive to changes in ionic strength, as it produces a larger decrease in layer thickness as the ionic strength is increased.

The final experiment on the effects of NaCl concerned the influence of NaCl concentration on the thickness of a pre-adsorbed layer of native β-cn at a single applied protein concentration of 9.2mg m^{-2}. This protein concentration is high enough to ensure saturation coverage, and is also well above the levels where bridging flocculation might be expected when NaCl is added. Adding NaCl to this system produced decreases in the adsorbed layer thickness (Fig. 5.4). The effect of increasing ionic strength decreased as NaCl concentration was increased. At still higher NaCl levels there was an increase in layer thickness. This indicates an increase in the size of the coated latex particles and the onset of salt-induced aggregation. The maximum decrease in thickness obtained before aggregation was 4-5nm.

5.3.4. Effects of Ca^{2+} addition

Addition of $CaCl_2$ at a fixed level of 5.33mM, caused the layer thickness at all protein concentrations, to be thinned (Fig. 5.5). Native β-cn was affected more than

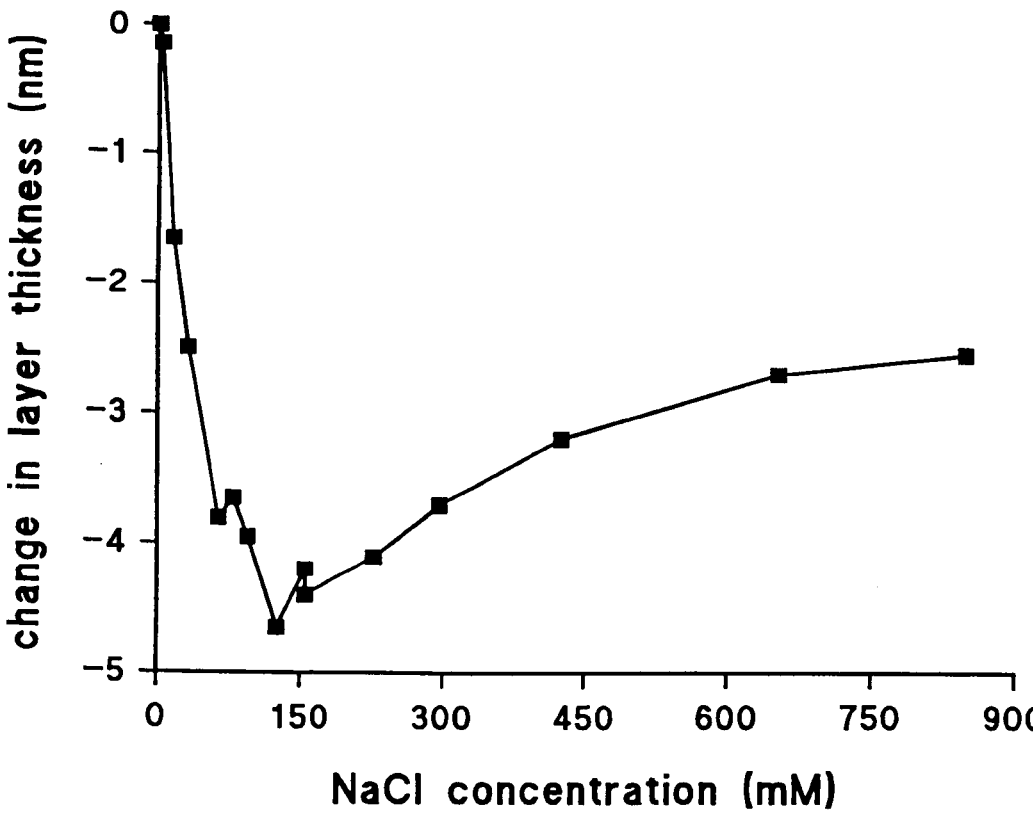

Fig. 5.4. Effect of NaCl on latex coated with native β−cn.

Latex coated with β−cn at saturation coverage (applied protein concentration 9.2mg m^{-2}). The change in radius from zero salt is plotted as a function of NaCl concentration.

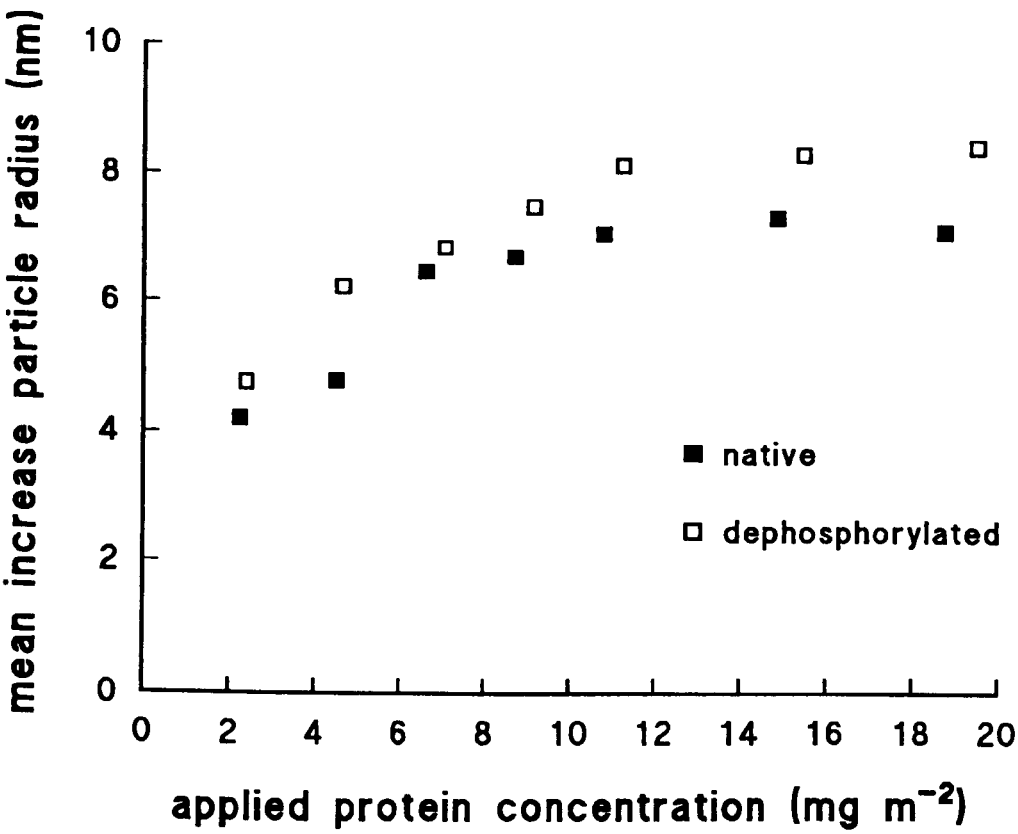

Fig. 5.5. β–cn adsorption to latex in the presence of 5.33mM Ca^{2+}.

Ca^{2+} added after formation of protein layer.

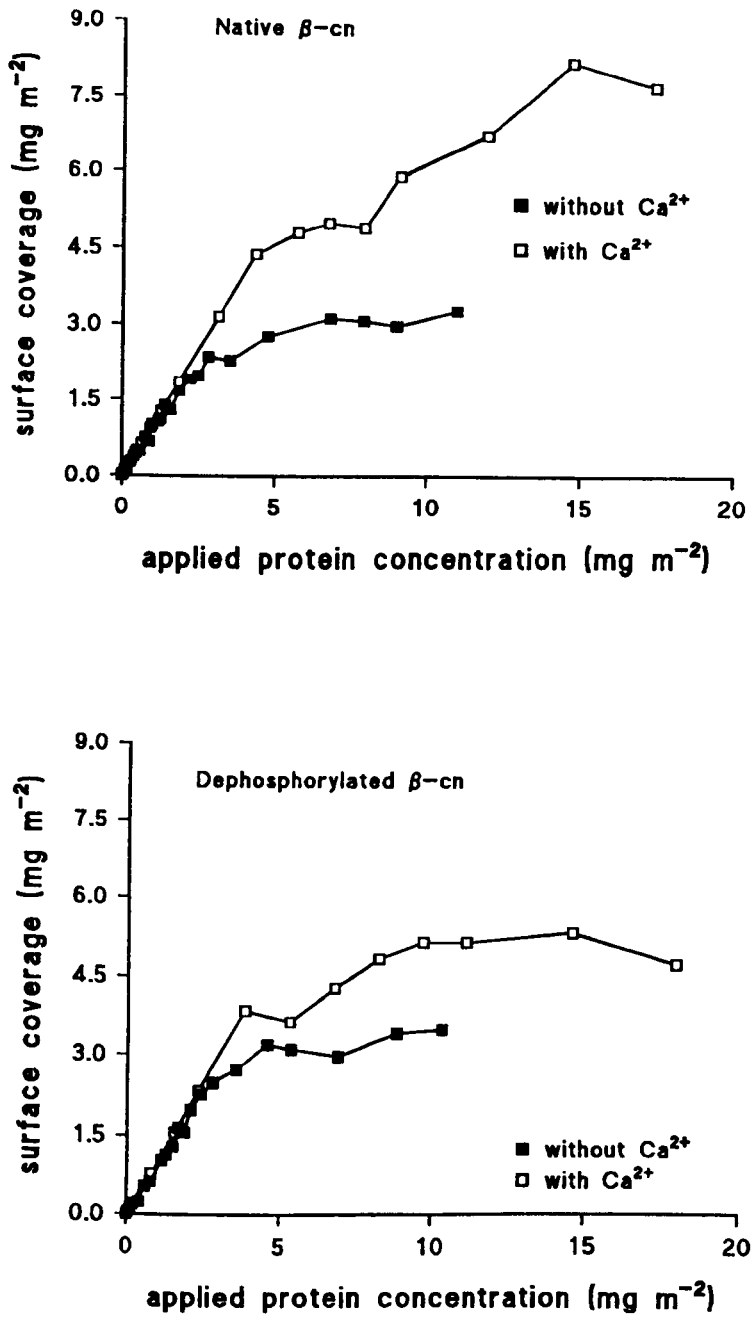

Fig. 5.6. Adsorption isotherms for native and dephosphorylated β–cn with and without Ca^{2+}.

Ca^{2+} added to uncoated latex before the addition of protein.

dephosphorylated β-cn, so that both protein layers showed similar thicknesses of 7-8nm at their plateau levels (compare with Fig. 5.2).

Adsorption isotherms at 5.33mM $CaCl_2$, showed that the thinner layers were not due to protein desorption (Fig. 5.6). At low protein concentrations, all of the protein continued to be adsorbed. The attainment of plateau in the adsorption isotherm shifted to higher values of applied protein for both native and dephosphorylated β-cn. Saturation surface coverage values were also higher at 5.0mg m^{-2}.

Further measurements of layer thickness and surface coverage were made as a function of $CaCl_2$ concentration. The applied protein concentration was fixed at 15mg m^{-2} to ensure saturation of protein adsorption. The variation in protein layer thicknesses for both native and dephosphorylated β-cn are shown in Fig. 5.7. Also plotted are the variations in thickness observed for native β-cn at a lower protein concentration of 6mg m^{-2}.

In the absence of Ca^{2+}, the dephosphorylated protein gave a layer thickness of 10nm compared to 11.8nm for native β-cn at 6mg m^{-2} applied protein and 13nm at 15mg m^{-2} (compare with Fig. 5.2). The bound layers of both proteins were affected by the addition of Ca^{2+}. The effect was more marked with native β-cn (Fig. 5.7). The lowest Ca^{2+} concentration used induced the sharpest drop in layer thickness. The dephosphorylated β-cn layer contracted to just under 8nm (a drop of 2nm) and then declined slowly to approximately 7nm as the Ca^{2+} content was raised to 12mM. The native β-cn layer also contracted to 7.5-8nm in the presence of 0.67mM Ca^{2+} (a drop of 4-5nm). Again, as the Ca^{2+} level was increased, thinner layers were observed with native β-cn and a minimum layer thickness of 6nm was obtained. As Ca^{2+} levels increased further, the layer thickness began to increase (above 6.7mM Ca^{2+} for higher

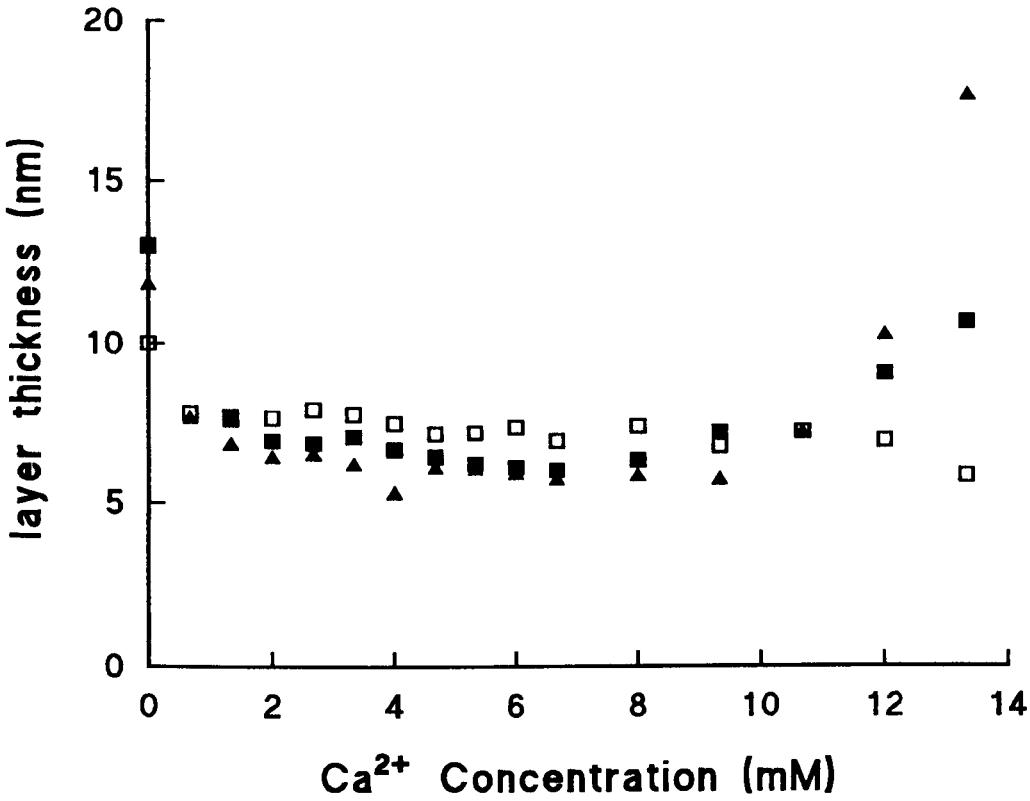

Fig. 5.7. Influence of Ca^{2+} addition on radius of pre-adsorbed layers β-cn.

Radius is plotted as a function of Ca^{2+} concentration for dephosphorylated β-cn layer at an applied protein concentration of 15mg m^{-2} (■), and for two native β-cn coverages of 6mg m^{-2} (▲) and 15mg m^{-2} (□) applied protein.

protein concentration and 10mM for the lower). This is consistent with Ca^{2+}-induced aggregation of the coated latex particles. When Ca^{2+} was added to uncoated latex, increases in radius were observed at all Ca^{2+} levels from 1mM onwards. With Ca^{2+} levels <4mM, the increases in radius were constant over the time over which the samples were observed. This indicates limited aggregation. Above 4mM Ca^{2+}, the radius continued to increase with time and the rate of increase grew as the Ca^{2+} concentration was increased.

Further measurements of surface coverages at the same applied protein concentrations as above, confirmed that including Ca^{2+} did not cause protein desorption. There was no drop in surface coverages when Ca^{2+} was added, which shows that protein desorption was not the source of the decrease in layer thickness. There was an increase in surface coverage which could be due to Ca^{2+} binding reducing the size of the β-cn molecules so that more could adsorb onto the surface.

5.3.5. Electrophoretic mobilities

Electrophoretic mobilities were determined at 25°C in 20mM imidazole/HCl buffer pH7.0, containing 50mM NaCl. Measurements for both native and dephosphorylated β-cn are plotted in Fig. 5.8 as a function of applied protein concentration. The adsorption of protein lowered the particle mobility as the latex/protein complex took on the charge of its coating. Thus the less highly charged dephosphorylated β-cn produced the larger decrease. At saturation coverage of the native protein, the value of $2.4 \times 10^{-8} m^2$ Vs is obtained. This is close to the mobilities obtained by Dalgleish *et al*[140] and Dickinson *et al*[141], for both polystyrene latex particles and oil/water emulsion droplets coated with β-cn.

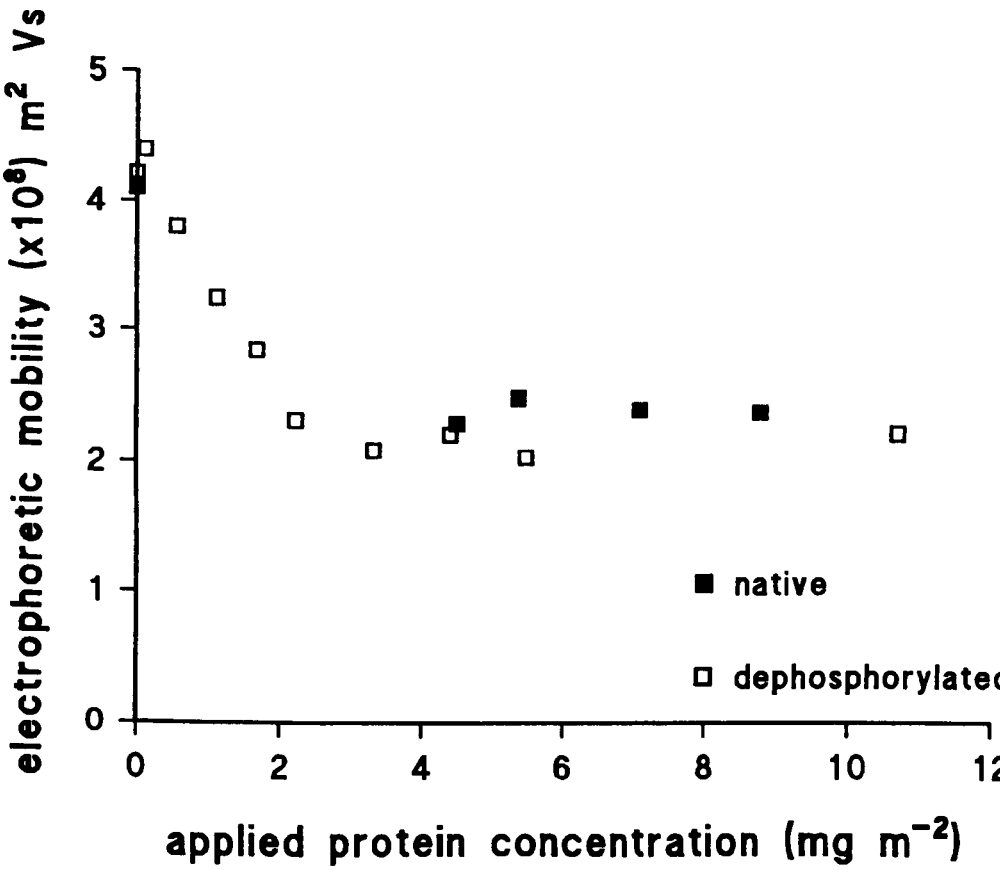

Fig. 5.8. Electrophoretic mobilities of casein–coated latex particles as a function of applied protein concentration.

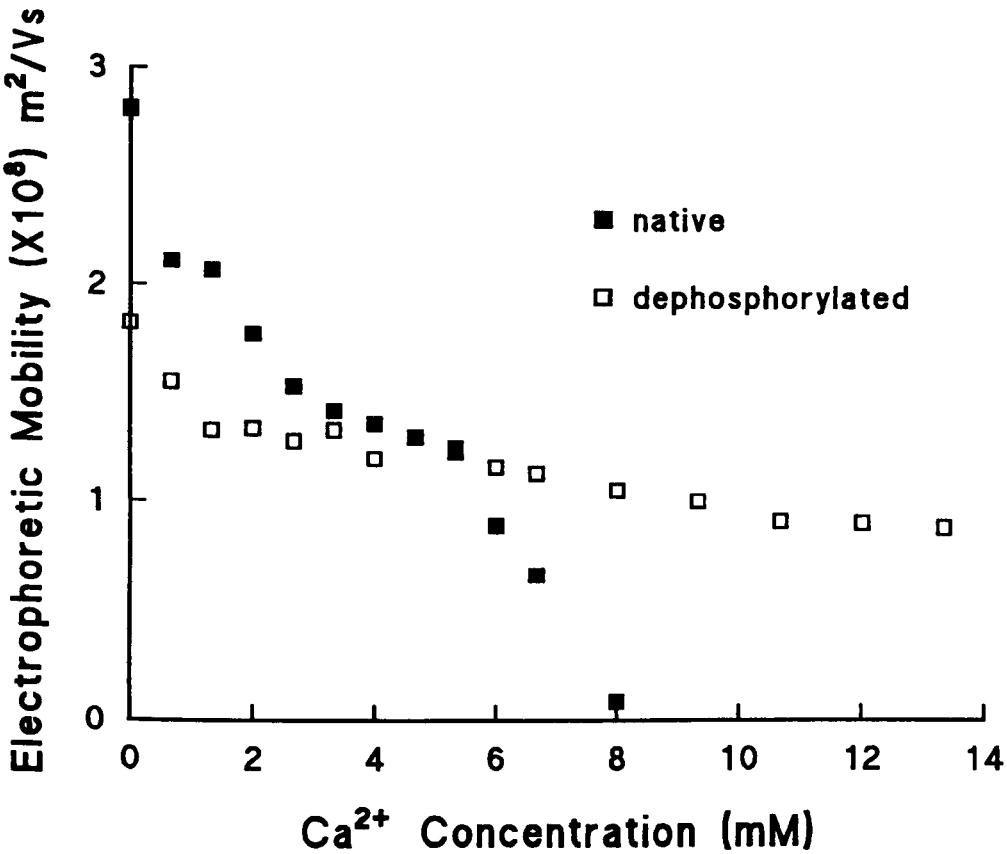

Fig. 5.9. Electrophoretic mobilities of β–cn coated latex particles in the presence of Ca^{2+}.

Mobility is plotted as a function of Ca^{2+} concentration. Measurements were made at an applied protein concentration of 5mg m^{-2}.

The same Ca^{2+} concentrations used in the layer thickness studies were used in electrophoretic mobility studies (Fig. 5.9). All solutions contained 50mM NaCl and measurements were made at an applied protein level of 5mg m^{-2}, which corresponded to the plateau in the adsorption isotherm in the absence of Ca^{2+}. From Fig. 5.9 it is clear that Ca^{2+} was more effective in reducing the electrokinetic potential of the latex particles coated with native β-cn, than with those coated with the dephosphorylated protein. The decrease in mobility in the dephosphorylated system, as Ca^{2+} increased, was more shallow than that for the native protein. Native β-cn mobility started from a higher value and declined so rapidly as to overtake the dephosphorylated β-cn mobility. Further evidence of differences in the effects of Ca^{2+} on these systems were seen at high Ca^{2+} levels (>9mM). In this region the gradual decline in mobility continued for particles coated with dephosphorylated β-cn . However, the mobilities of native β-cn coated particles became very low and erratic. This was presumably due to the aggregation occurring via an isoelectric precipitation mechanism.

5.4 Discussion

The milk protein β-cn is one of the most widely studied in terms of its adsorption behaviour at oil/water interfaces. Research on this topic has recently been summarised by Dickinson[37]. The adsorbed protein can be represented by a loop-and-train model, with train segments lying along the interface and loops and tails protruding into the aqueous phase. Evidence for this model comes from a range of sources.

First, direct information on the structure of β-cn[142] and on the thickness and structure of adsorbed β-cn layers at the air/water and oil/water interfaces has been obtained from neutron reflectivity measurements[143]. The segment density profile

calculated from this data indicates a dense inner layer some 2nm thick and has a volume fraction of about 0.9 and a tenuous outer layer some 6-8nm thick, volume fraction 0.15. Such overall layer thicknesses agree well with the hydrodynamic layer thicknesses obtained here and in other studies[122,39] of β-cn adsorption on latex particles.

This two-layer model fits the loop-and-train picture. It is also consistent with the earlier speculated conformations based on the accessibility of digestion sites in the adsorbed β-cn molecule to the proteolytic enzyme trypsin[32,33,34]. Those studies revealed that the N-terminal region of β-cn was much more susceptible to proteolysis than was the rest of the molecule. Peptides 1-25 and 1-28 were more readily cleaved from the adsorbed molecule. The rapid release of these peptides was found to be correlated with observed changes in the hydrodynamic radii of the latex/casein complex and casein-coated emulsion droplets following the addition of trypsin[34]. Tryptic attack caused the adsorbed layer thickness of native β-cn on latex to rapidly decrease by about 10nm, but still left a layer 3-5nm thick on the latex particle.

The distribution of hydrophobic residues along the polypeptide chain is not uniform, but favours the idea of a loop-and-train model. The first 40-50 residues of the N-terminal polypeptide are predominantly hydrophilic. Therefore, it is feasible that this part of the molecule extends into the aqueous phase and can be assigned the role of the loop. This view is supported by its ready accessibility to trypsin.

The results of the experiments reported here not only provide further evidence for the loop-and-train model, but also add more detail to this picture. The ideas are best outlined by referring to the cartoon drawing (Fig. 5.10). This represents a β-cn molecule adsorbed onto polystyrene latex. Since an individual casein molecule is so much smaller than a latex particle, the surface of the latex can be regarded as a plane.

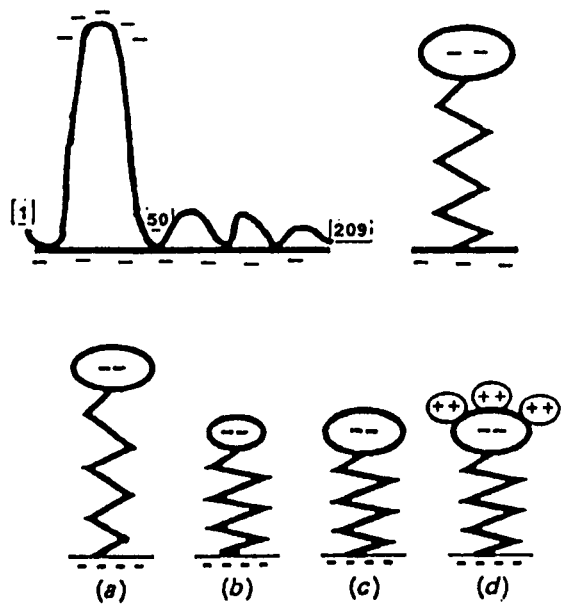

Fig. 5.10. Diagram of the loop–and–train configuration postulated for adsorbed β–cn on latex.

Top diagram, the numbers in squares on the first diagram are the amino acid residue numberings along the single chain protein sequence. It is suggested that this configuration is equivalent to the blob and spring shown alongside, the negatively charged blob or head group repelled by the negatively charged surface and constrained by the spring. In the series (a) to (d) the size of the blob reflects the charge it carried and the extension of the spring the hydrodynamic layer thickness. In (c), the head group is effectively larger due to the addition of NaCl. In (d), the double positive charges represent bound Ca^{2+} ions.

The latex surface carries sulphonic acid groups and so has an overall negative charge. β-cn can bind to the latex surface by hydrophobic interactions and also by plus/minus salt bridges, which partly neutralise the surface charge of the latex. The high concentration of negatively charged amino acids in the chain positions 15-25 allow this portion of the loop-train to be regarded as a negatively charged "head". This will be repelled from the latex surface by electrostatic forces, but will be restrained from moving completely into solution by the extended, stretched "spring" section. This "spring" is the amino acid chain that connects the "head" to the surface-bonded train.

When β-cn is dephosphorylated, the cluster of negatively charged phosphate groups are removed from residues 15-19. When compared to native β-cn, dephosphorylated β-cn produces a minimal change in surface coverage. Hence, the train bonding and latex surface charge are unaffected, but the reduction in the charge of the "head" segment decreases the electrostatic repulsion between surface and "head". This allows the spring to relax back towards the surface (Fig. 5.10b) and a thinner layer is observed.

Similarly when the ionic strength of the buffer is increased (by adding NaCl), the range and effectiveness of the repulsion between "head" and surface are diminished. This enables the spring section to relax which again reduces the adsorbed layer thickness (Fig. 5.10c). In this limited series of experiments, the plateau thickness varies inversely with the square root of the ionic strength (Fig. 5.11). This is most apparent for the native protein data. For the dephosphorylated β-cn the data is much more sparse. Results indicate that the response to ionic strength is much less, lying largely within experimental error, but tending towards a thinner layer as ionic strength increases. The lower gradient in the plot of thickness versus $I^{-½}$ for dephosphorylated

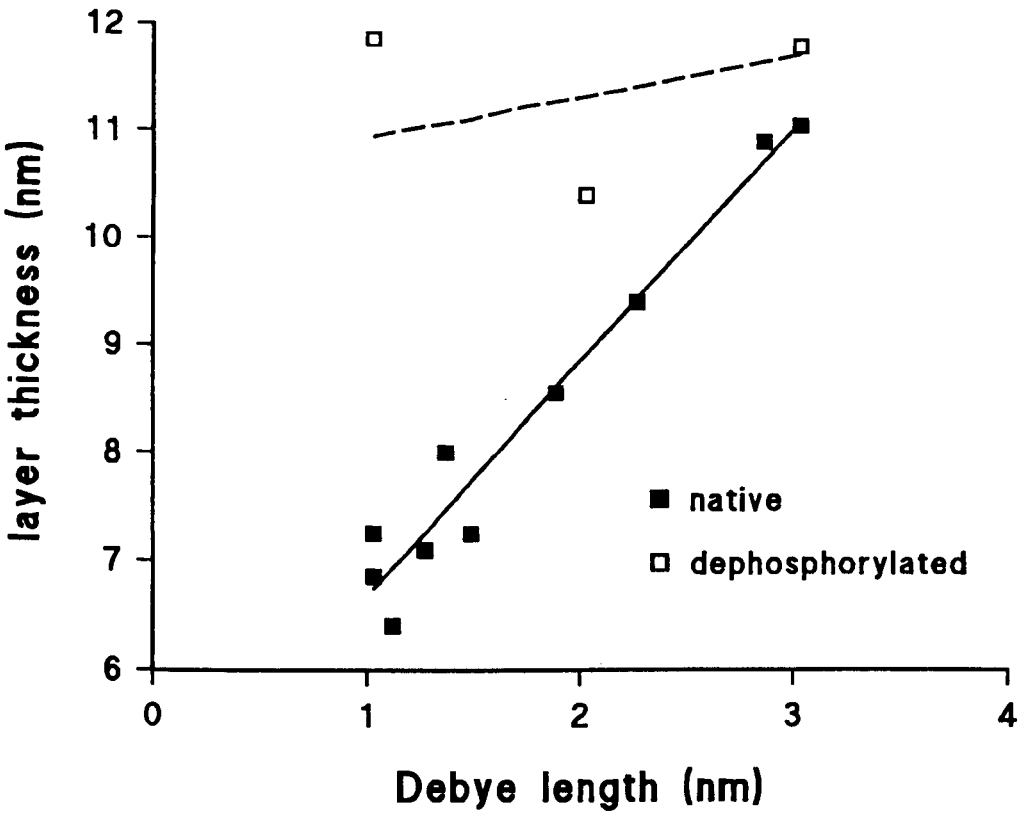

Fig. 5.11. Relationship between hydrodynamic layer thickness of adsorbed β–cn layer at saturation coverage and Debye layer thickness.

Debye layer thickness calculated as reciprocal of Debye Hückel parameter, κ where $\kappa = 3.288\ I^{-1/2}$ in units of nm^{-1} when appropriate values of the universal constants are substituted to give the numerical pre–factor and where I is total ionic strength of system (temp. = 25°C). Plot of native β–cn uses data from Fig. 5.4.

β-cn, is as would be expected from lowered repulsion by the charge-reduced head group.

As shown in Fig. 5.7, the plateau layer thickness obtained with adsorbed native β-cn is extremely sensitive to the presence of Ca^{2+} in the buffer solution. The dephosphorylated protein layer is less sensitive. The response to Ca^{2+} is too great to fit with the $I^{-½}$ dependence noted above, so this Ca^{2+} sensitivity is more than a simple ionic strength effect. It is suggested (Fig. 5.10d), that the layer thinning results from specific binding of Ca^{2+} to the negatively charged "head". This again reduces the electrostatic repulsion between "head" and surface, which then permits the "spring" to relax. The evidence for this comes from the fact that dephosphorylated β-cn is less sensitive to Ca^{2+} than the native form, so Ca^{2+} is probably binding primarily to the phosphate residues in the "head" region. Further evidence of specific binding effects comes from the electrophoretic mobility plots of the protein/latex complexes as a function of added Ca^{2+} (Fig. 5.9). For dephosphorylated β-cn, a shallow dependence of Ca^{2+} is observed. With native β-cn there is a much higher initial mobility, as expected for a more highly charged species. But, this then descends much more sharply as Ca^{2+} content increases, and crosses the line of the dephosphorylated β-cn plot. If changes in mobility were due to the same mechanism, mainly increasing ionic strength, then parallel plots would have been expected.

It is interesting that the minimum layer thickness measured for the native β-cn/latex complex prior to Ca^{2+}-induced aggregation (Fig. 5.7) is approximately 6nm. This is nearly identical to the "brush" thickness for the protein tail calculated to be 6.4nm by Mackie *et al*[39] using a model proposed by de Gennes[144,145]. If it is proposed that there is neutralisation of protein charge, or at least isoelectric behaviour, then the

β-cn tail apparently behaves as an uncharged homopolymer. The observed extension in the absence of neutralising Ca^{2+} ions suggests a repulsive force other than excluded volume (a steric effect) controlling this extension. The effects of calcium, ionic strength and protein charge indicate that this force is electrostatic in nature.

It is clear from these results that the conformation adopted by the bound caseins is a function of the ionic composition of the aqueous phase, and that an adsorbed molecule responds to such changes in its environment when able to do so. In monitoring and recording these changes, definitive information is provided on the precise structure of the protein film. The results also highlight the role of electrostatics in controlling intramolecular interactions and protein layer thickness.

Chapter 6

Influence of Surface Charge and Protein Modification on Adsorbed Protein Layers

6.1 Introduction

The proteins in milk, whether used collectively in milk powders, or individually as caseins and whey proteins, display a wide range of functional properties, and are used in many food products because of these properties. Caseins and caseinates are commonly used where solubility, heat stability and surface-active properties (emulsifying, foaming) are required[146,147]. Heating induces physicochemical changes in whey proteins and induces complex formation with κ-cn in micelles. Thus, specific "preheat" treatments (85-100°C for 30min.) are used in the preparation of non-fat dry milk to achieve optimum properties *i.e.* inactivation of loaf depressing factors for bread making/bakery purposes[148]. In order to study these functional properties, the effects of chemical modification of the proteins on their functional properties has been studied, especially with β-lg[149,150].

The majority of studies on food protein structure-function properties have involved alkylation and acylation of the epsilon amino group of lysine residues[149,136,150], although modification of ω-carboxyl groups of aspartyl and glutamyl residues has also been investigated[136,151,150]. These types of modification can directly affect the net charge and charge-density of the protein molecules. In addition they often result in conformational changes and alterations in intra- and intermolecular interactions which also modify the effective hydrophobicity of the proteins.

In this chapter, the effect of methyl-esterification of β-cn will be investigated. Esterification of carboxyl groups may be accomplished by suspending the protein in the appropriate alcohol (in this case methanol) with an acid catalyst[152,153]. The carboxyl groups of aspartate and glutamate residues can be blocked by amidation or esterification. As with enzyme-catalysed dephosphorylation, esterification reduces the net negative charge on the proteins. The free carboxyl groups are relatively uniformly distributed throughout the protein, whereas the phosphates are all located in the N-terminal region. Therefore, the effects on the esterification of the protein may well be different. Any effects due to methyl-esterification are viewed in conjunction with the effects of surface charge. This is investigated by using different latices. A positively charged amidine and the negatively charged polystyrene latex, LB1 are used. Also reported are parallel measurements of particle electrophoretic mobility and protein adsorption isotherms, under the same experimental conditions. These will provide a comprehensive picture of the adsorbed protein layers.

6.2 Materials and methods

Positively charged amidine polystyrene latex (nominal diameter 76nm) was obtained from Interfacial Dynamics Corporation, Portland, Oregon, USA. Negatively charged LB1 (sulphonated) latex (nominal diameter 91nm) was purchased from Sigma Chemical Company Ltd., Poole, Dorset, UK. β-cn preparations whose free carboxyl groups had been methyl-esterified to different extents were a gift from T. Haertlé at INRA, Laboratoire d'Etude des Interactions des Molécules Alimentaires, Nantes, France. Bovine β-cn was purified from bulk milk by ion-exchange chromatography[66]. β-cn was completely dephosphorylated using potato acid phosphatase obtained from

Sigma[126].

6.2.1 Latex binding studies

See section 5.2.1. The absorbance coefficients for native β-cn were used for the methyl-esterified β-cn since nothing was known about the effects on the coefficient due to methyl-esterification.

6.2.2 Adsorption isotherms

See section 5.2.2. To correct for possible interference in the protein determination methyl-esterified β-cn was used to calibrate the Bradford assay instead of native β-cn.

6.2.3 Electrophoretic mobilities

See section 5.2.3.

6.3 Results

β-cn was esterified in the presence of methanol to produce methylated β-cn. β-cn has 23 carboxyl groups which are all susceptible to esterification. These consist of the 18 glutamic acid and 4 aspartic acid residues plus the free C-terminal carboxyl group. In two protein preparations, 35% and 44% of these carboxyl groups were methylated. A third sample of 69% methylated β-cn was insoluble at pH7 and so was not investigated further. It has been reported that additional methylation may occur due to substitution during the esterification process[154]. Solubility of the methylated protein was poor at pH7.0 and decreased with increasing methylation[136]. This is due

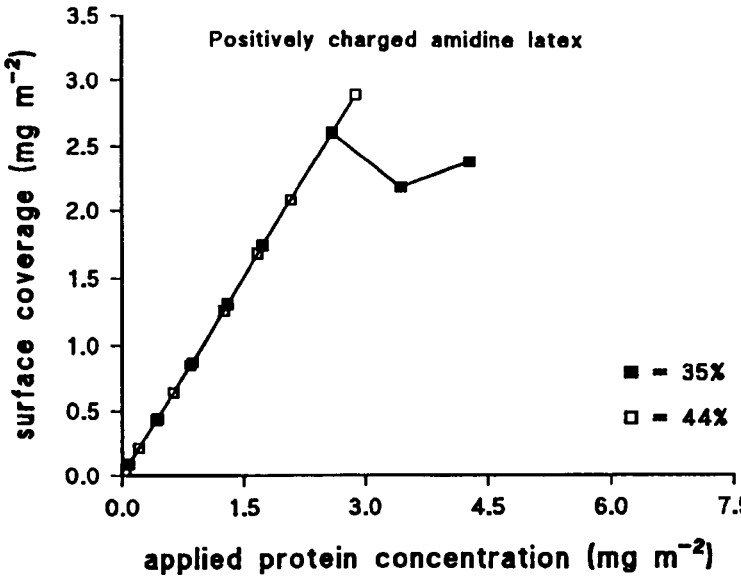

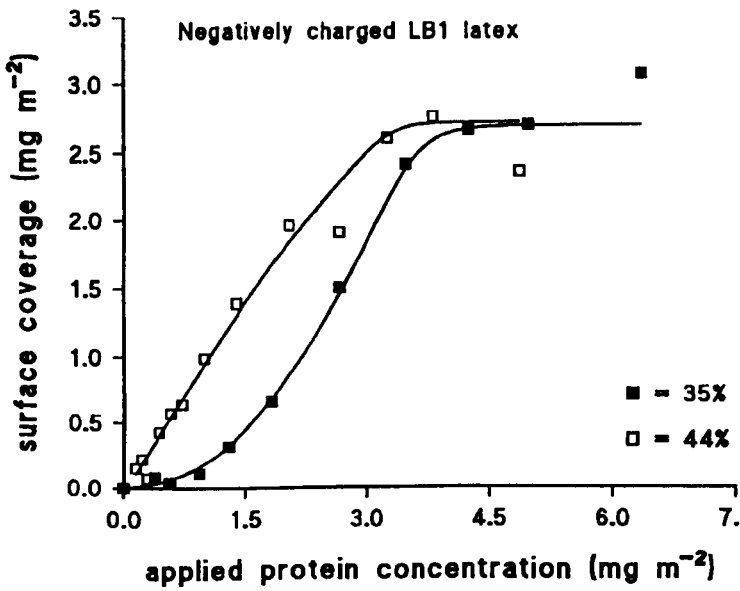

Fig. 6.1. Adsorption isotherm for β–cn at various degrees of methylation on negatively and positively charged latex.

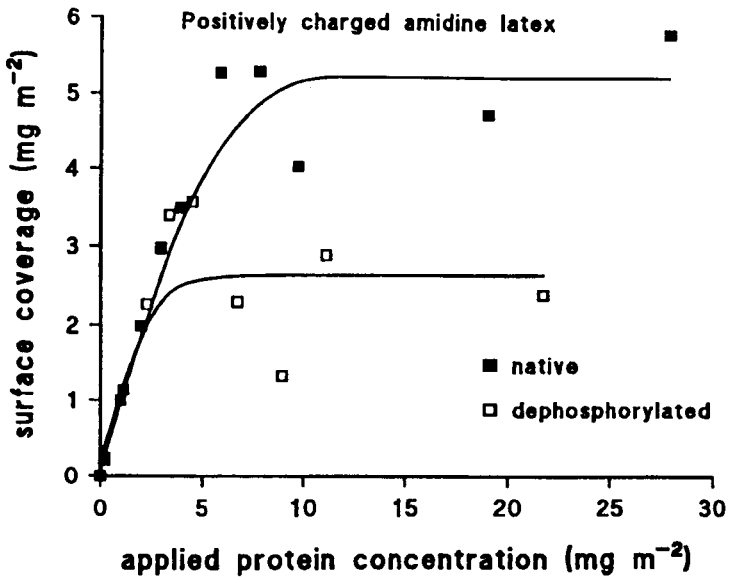

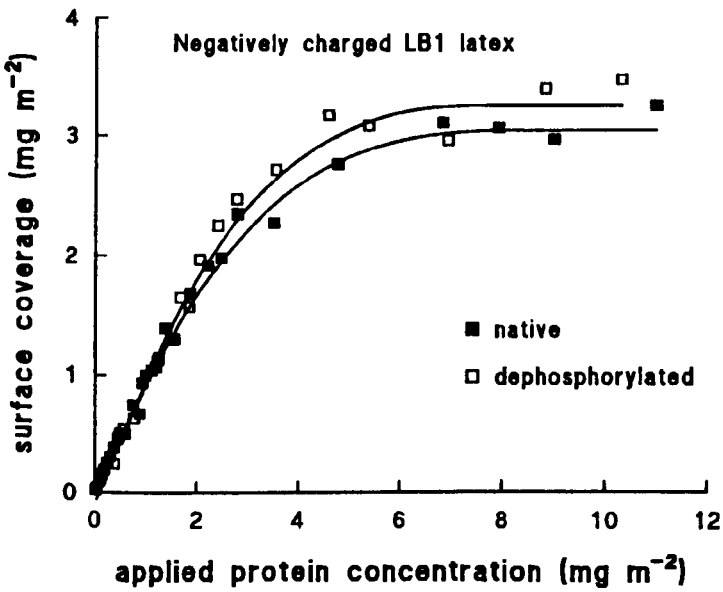

Fig. 6.2. Adsorption isotherm for β–cn on positively and negatively charged latex.

Results on LB1 latex from Fig. 5.1 of chapter 5.

to the increasing hydrophobicity resulting from methylation of the protein.

6.3.1 Adsorption isotherms

The adsorption isotherms for the 35% and 44% methylated β-cn onto polystyrene latices at 20°C and pH7.0, are shown in Fig. 6.1. These results are compared with those of native and dephosphorylated β-cn in Fig. 6.2. On the negatively charged latex the final surface coverage values of both methylated samples are 2.8mg m^{-2}, which were similar to the value obtained with native β-cn (3.0mg m^{-2}). At low concentrations of added protein, the 44% methylated β-cn bound more strongly than did the 35% methylated form. The adsorption isotherm of the 35% methylated protein had a sigmoidal appearance compared with the hyperbolic shape of the native and 44% methylated forms. This was unexpected since the native and 44% methylated β-cn both show high affinity for the surface (*i.e.* at low applied protein concentrations all of the applied protein molecules bind to the latex). It would therefore be expected that the 35% methylated β-cn should also have high affinity for LB1 latex as well. The maximum surface coverage levels were attained at a slightly lower applied protein concentration with the 44% methylated protein. The similarity in the adsorption behaviour of the 44% methylated protein and native β-cn, suggests that the affinity of β-cn for the negatively charged latex was similar. When the proteins were added to the positively charged amidine latex, surface coverages continued to increase as more protein is added. The maximum surface coverage of the 35% methylated protein was approximately 2.3mg m^{-2}. No plateau level was reached with the 44% methylated protein. At higher applied protein levels the surface coverage of the 35% and 44% methylated samples continued to increase rapidly. This suggests either that the protein

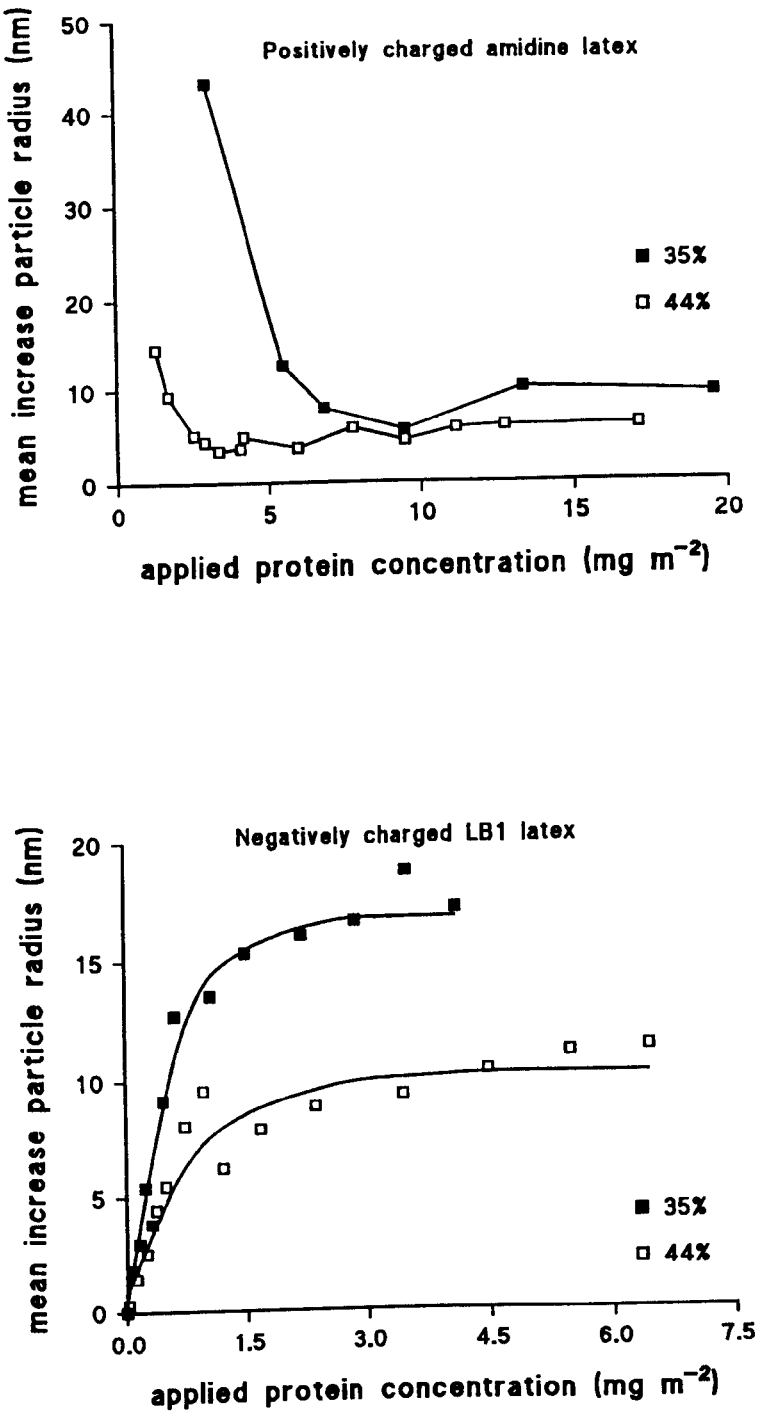

Fig. 6.3. Methylated β–cn adsorption to positively and negatively charged latex.

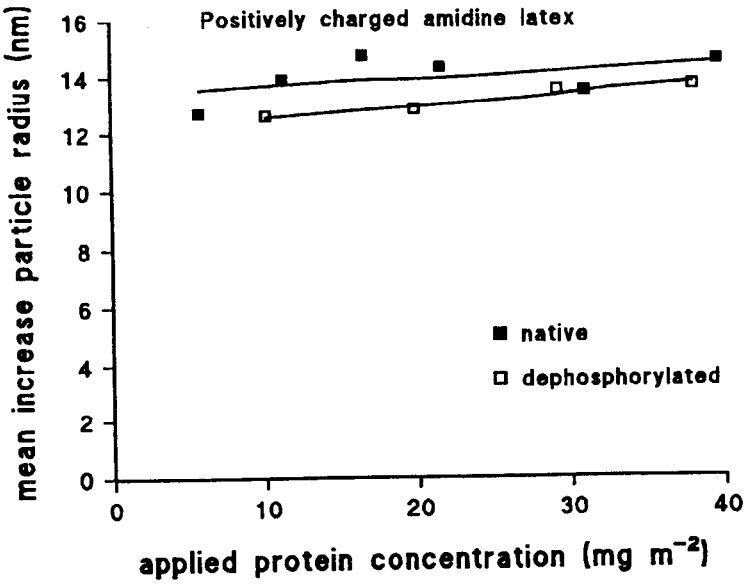

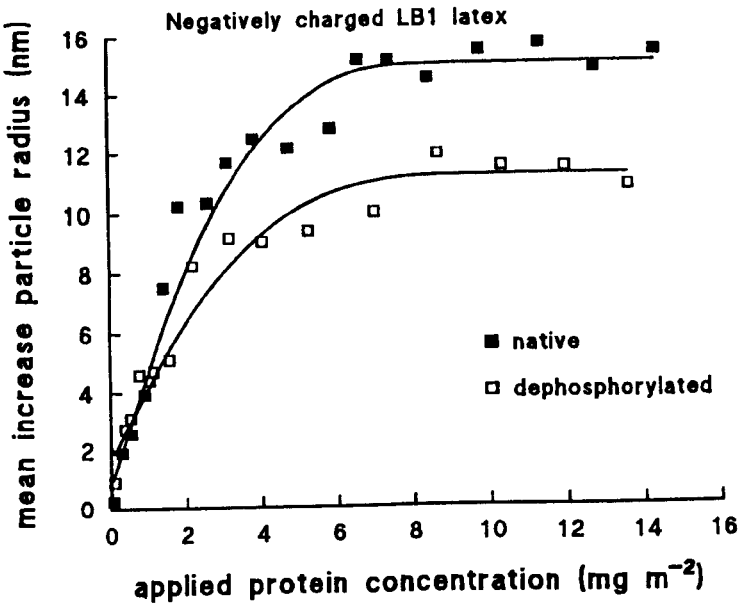

Fig. 6.4. β–cn adsorption to positively and negatively charged latex.

Results for LB1 latex were as Fig. 5.2 of chapter 5. Results on amidine latex are those after aggregation has been overcome.

was adsorbing as aggregates at higher protein levels, or that the proteins were reaching their limits of solubility, and were therefore pelleting with the latex during centrifugation. The latter possibility is favoured since, as the amount of methylation increased it became more difficult to dissolve the protein before adding it to the latex.

6.3.2 Adsorbed layer thickness

The increase in the hydrodynamic radius of the latices as a result of adding the 35% and 44% methylated β-cn is shown in Fig. 6.3. These plots are compared with the results obtained with native and dephosphorylated β-cn (Fig. 6.4). On the negatively charged latex there was a smooth increase in radius as more methylated protein was added to the latex. The maximum layer thickness of the 35% methylated protein was some 6nm greater than with 44% methylated β-cn (16nm compared with 10nm). The layer thickness of native β-cn lies between the two methylated forms, and that of the dephosphorylated β-cn is the same as the 44% methylated form (Table 6.1).

Addition of low concentrations of all the proteins resulted in aggregation (as indicated by the large increase in particle size), when added to positively charged amidine latex (Fig. 6.5). Similar results occurred with native and dephosphorylated β-cn. This aggregation was probably due to protein molecules bridging between latex particles. These aggregates could not be disrupted by adding more protein, probably due to the tight binding of protein to the latex surface. This is supported by the fact that larger initial aliquots of protein produce no aggregation, and similar layer thicknesses to those on LB1 latex were observed. As the amount of methylation increased, less protein was required to overcome this bridging. This suggests that the less highly methylated fraction had a greater affinity for the positively charged latex.

Protein	System	Native	Dephos.	35% met.	44% met.
Layer Thickness (nm)	LB1	15.0±0.5	11.0±1.0	16.0±2.0	10.0±1.0
	LB1 + 50mM NaCl	12.9±1.0	11.0±1.0	9.0±1.0	9.0±1.0
	Amidine	14.0±1.0	13.0±2.0	10.0±2.0	6.0±1.0
Surface Coverage (mg m^{-2})	LB1	3.0±0.4	3.4±0.5	2.7±0.5	2.8±0.4
	LB1 + 50mM NaCl	6.0±1.0	7.5±2.0	4.0±1.0	NR
	Amidine	5.2±1.0	2.5±0.8	2.4±0.3	NR

Table 6.1. Layer thickness and surface coverage of native and modified β-casein on latices.

met. represents methylated β-casein. Dephos. represents dephosphorylated β-casein. NR represents plateau not reached at the concentrations used. Results in the presence of NaCl for native and dephosphorylated β-casein are taken from chapter 5.

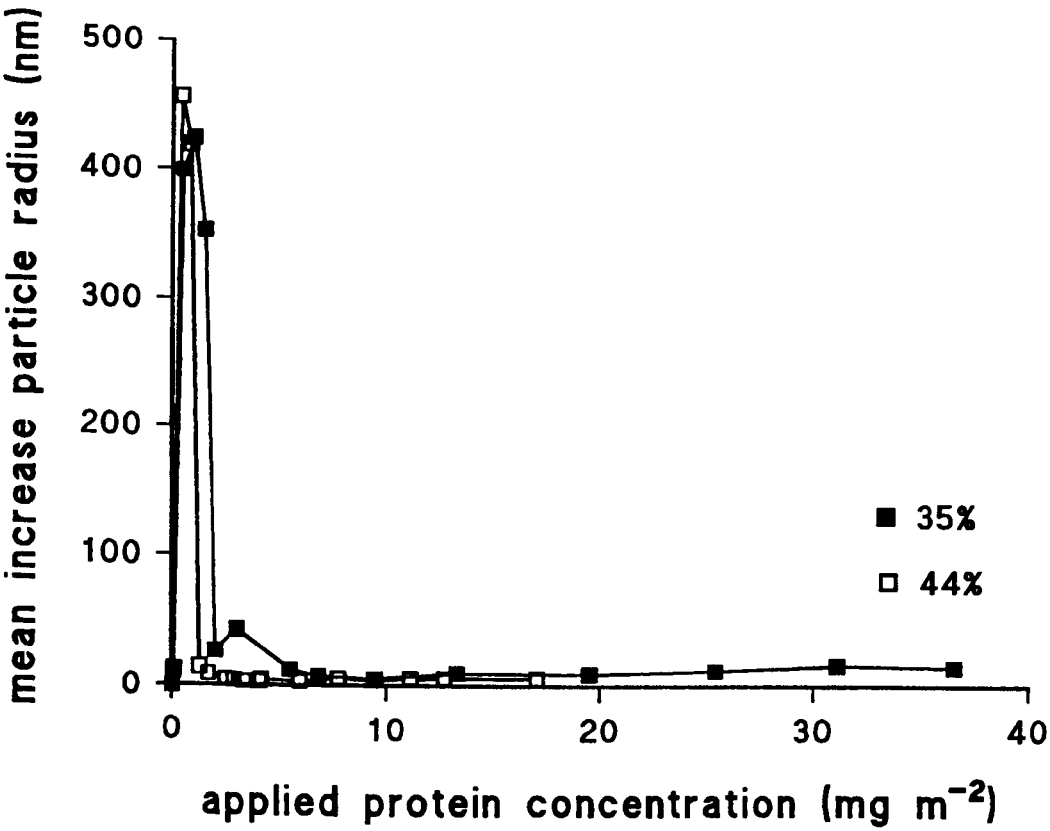

Fig. 6.5. Methylated β–cn adsorption to amidine latex.

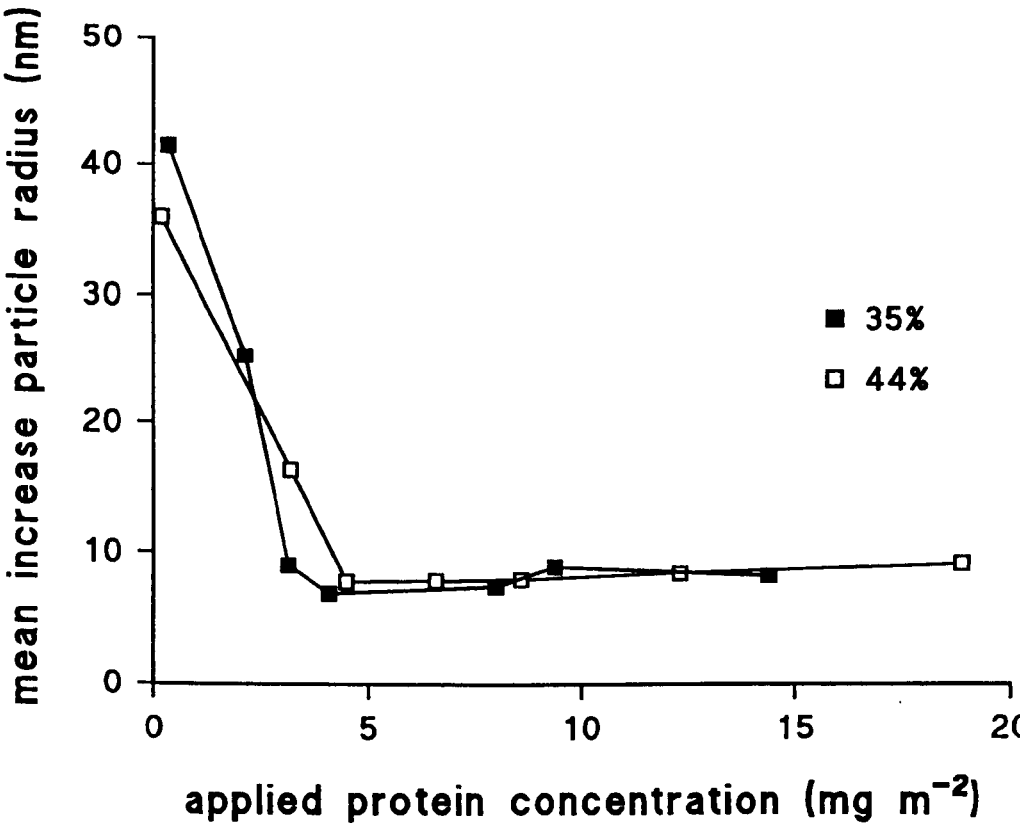

Fig. 6.6 Methylated β–cn adsorption to LB1 latex in the presence of 50mM NaCl.

The maximum layer thickness of the native, dephosphorylated, 35% methylated and 44% methylated β-cns on the positively charged and negatively charged latices are summarised in Table 6.1.

Similar aggregation occurred in the presence of salt with LB1 latex. This bridging flocculation has already been observed with β-cn[139,122]. Fig. 6.6 shows layer thicknesses after the aggregation phase was exceeded. Layer thicknesses of about 9nm were measured with both forms of methylated β-cn these thicknesses are considerably thinner than the native and dephosphorylated proteins (Table 6.1).

6.3.3 Electrophoretic mobility measurements

Electrophoretic mobilities were determined at 25°C in 20mM imidazole/HCl buffer pH7.0, containing 50mM NaCl. Only LB1 latex was used, since NaCl induced aggregation of amidine latex prior to protein addition. Mobility measurements for the methylated, dephosphorylated and native proteins are shown in Fig. 6.7, as a function of applied protein concentration. Adsorption of protein reduced the particle mobility as the surface of the latex complex took on the charge of its coating. Thus, the less highly negatively charged dephosphorylated β-cn produced the larger decrease in mobility. Electrophoretic mobility at saturation coverage of both methylated proteins was similar to that of native protein at $2.5 \times 10^{-8} m^2$ Vs. The values agree with the native protein obtained by Dalgleish *et al*[140] and Dickinson *et al*[141]. This suggests that the methylated proteins have an overall surface charge similar to that of native β-cn. Approximately twice the amount of methylated protein was required to reach plateau mobility compared with native β-cn. Since each individual methylated casein molecule will have less electrostatic charge (due to methylation of the free carboxyl groups) than

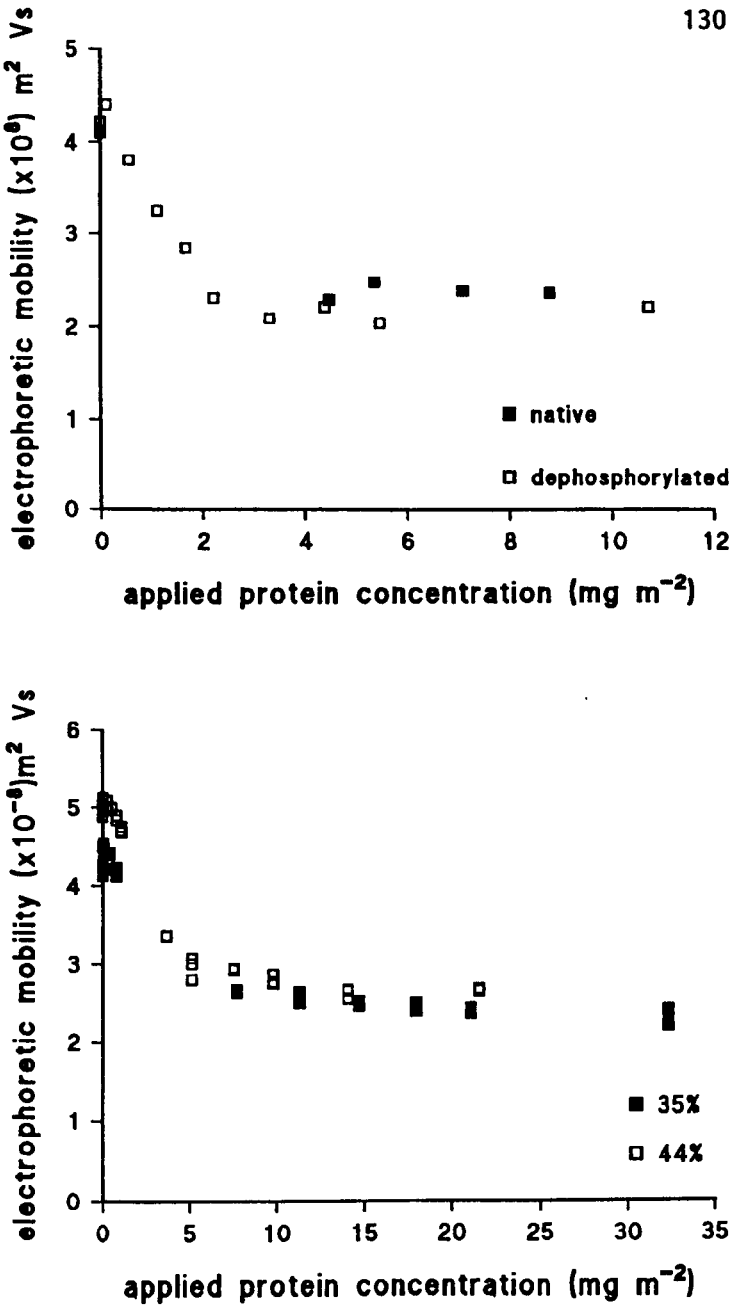

Fig. 6.7. Electrophoretic mobilities of casein–coated latex particles as a function of applied protein concentration.

Native and dephosphorylated β–cn results as Fig. 5.8 of chapter 5.

native β-cn, more protein is required in order to reach the same density of electrostatic charge.

6.4 Discussion

There are 23 free carboxyl groups in β-cn potentially available for esterification. Of these, 14 are located within the first 48 amino acids of the N-terminal region. The remaining 9 free carboxyl groups are distributed relatively uniformly throughout the rest of the molecule. Methylation reduces the net charge of the protein within the region of the molecule in which the free carboxyl groups are located, and also increases the molecule's hydrophobicity. This is shown by the fact that methylating 69% of the free carboxyl groups renders the protein completely insoluble in the imidazole buffer at pH7.0. Increasing the amount of methylation also reduces the proteins' electrical charge, which also contributes to the 69% methylated protein being insoluble.

It is important to realise that these methylated β-cn samples provided will not be "pure" samples. There will be a distribution of the amount of methylation in each of the samples, so that the "average" amount of methylation will be 35% or 44%[154]. In addition methylation will occur at different sites along the protein chain. Therefore, interpretation of the results can only be tentative and certain assumptions have to be made, namely that the majority of the molecules will be either 35 or 44% methylated, and that the positions of methylation are relatively uniform.

As indicated in Chapter 5, evidence is accumulating that the structure of adsorbed β-cn can be visualised in terms of a loop-and-train model with the loop being formed by the hydrophilic N-terminal region of the molecule and the train by the

remainder of the molecule which is, in general, considerably more hydrophobic. It would therefore be expected that methylation of the free carboxyl groups of those aspartate and glutamate residues in the loop region of the molecule would have a greater effect on layer thickness than of those in the remainder of the molecule which already lies relatively close to the surface of the latex. As the results presented in Figs. 6.3 and 6.4 show, the 44% methylated β-cn behaved as expected when its binding to the negatively charged LB1 latex was measured. The maximum layer thickness was 5nm less than that of the native protein and was approximately the same as that of dephosphorylated β-cn. In the case of dephosphorylated β-cn the net negative charge on the loop region was also reduced relative to that of the native protein, but in this case by enzymatic hydrolysis of the phosphates from the serine residues. This reduction in the net negative charge in the loop region reduces the repulsion between this end of the protein and the negatively charged latex surface, and thus allows the loop to lie closer to the interface. The binding isotherm of this 44% methylated derivative was very similar to that of the native and dephosphorylated proteins, being of the high affinity, hyperbolic type.

The layer thickness of both the native and dephosphorylated proteins was similar at 15 to 16nm on the positively charged amidine latex. However, that of the 44% methylated β-cn was dramatically reduced to only 6nm. The similarity of the protein layer thicknesses of the native and dephosphorylated proteins suggests that attraction between the positively charged surface and the negatively charged proteins is not as important as the repulsion between the negatively charged protein and LB1 latex. If this was the case it would be expected that the layer thickness of the more negatively charged native protein would be considerably less than that of either the

dephosphorylated or the 44% methylated forms. This is clearly not the case. It appears that with 44% methylated β-cn adsorption to positively charged latex, (after aggregation effects have been overcome), the effect of the increased amount of hydrophobicity is more important than electrostatic interactions. Hence, the loop section will have increased hydrophobicity due to methylation which apparently then leads to the loop lying closer to the surface.

The behaviour of the 35% methylated β-cn is more difficult to explain since when layer thicknesses of this derivative on both the positively and negatively charged surfaces were determined, they were found to be almost identical with those of the native protein. Therefore in this instance, the changes in the net negative charge of the protein did not effect the protein thickness. As stated earlier, not only the number but also the location of the methylated side-chains is probably important. Methylation of 35% of the free carboxyl groups is equivalent to esterification of 8 residues. If most of these were located in the train region of the molecule, they may have little effect on the behaviour of the loop and hence on the overall protein layer thickness. 44% methylation is equivalent to 10 free carboxyl groups esterified. Therefore, an increase of 2 in the number of methylated side chains has a dramatic effect on the behaviour of the adsorbed protein. This indicates that there is a fine threshold with regard to the effect which methylation has on the structure of the protein at the interface. It is worth noting that despite the 44% methylated protein binding to the negatively charged latex in a high affinity manner, the shape of the 35% methylated protein binding isotherm was sigmoidal, indicating that the affinity of this derivative was lower than that of the other forms. Chobert *et al*[136] have found a similar trend when studying the influence of the degree of ethyl-esterification on the emulsifying properties of β-cn. They

reported that the emulsifying activity of 37% modified β-cn was marginally better at pH7.0 than that of the native protein. However, increasing the extent of modification to 43% resulted in the emulsifying activity being more than halved. Also, the stability of the emulsion formed with the 37% ethyl-esterified protein was slightly poorer than the native protein. The 43% ethyl-esterified was considerably worse and indeed could not be measured due to emulsion collapse. More complete interpretation of these results requires information regarding the positions of esterification and the secondary structure of these derivatised proteins. Richardson[155] has studied the methyl-esterification of β-lg using CD and has found that methyl-esterification induces a change to more random structure. This suggests that methyl-esterified β-cn may also be in a more denatured form, which may mean that the β-cn derivatives are binding in this denatured form. This could explain why the increased hydrophobicity of the modified protein affects the adsorption to the latex surface. If the protein is denatured then the methyl-esterified carboxyl groups may be at the surface of the protein, and so freely accessible to interact with the latex surface. Therefore, the more methyl groups present, the greater the hydrophobic interactions with the latex surface. In this case it again appears that hydrophobic interactions are more important than electrostatic ones.

Chapter 7

Influence of Glycosylation and Surface Charge on the Binding of κ-cn to Latex Particles

7.1 Introduction

κ-Cn is unique amongst the casein proteins in its lack of calcium-sensitivity and in existing in both glycosylated and non-glycosylated forms. The relative amounts of glycosylation vary between individual animals and within the same animal during the course of a lactation. Even within the glycosylated fraction, there is considerable heterogeneity in the number of sugar residues attached to the protein molecules and, to a much more limited extent, in the degree of phosphorylation. The carbohydrate side chains consist of tri- and tetra-saccharide units of N-acetylneuraminic acid (NeuNAc), galactose and N-acetylhexosamine, O-glycosidically linked to serine and threonine residues in the C-terminal region of the protein[156]. Why κ-cn out of all the caseins should exist in these two major forms, and what effect glycosylation has on the physical properties of the protein, is not known.

The structure of bovine casein micelles has been reviewed recently[157]. Much of the κ-cn is believed to be located in the external surface or coat region of the micelle where it forms a "hairy" layer with the hydrophilic, C-terminal (glycosylated and phosphorylated) region projecting into the aqueous phase. This stabilises the individual micelles and prevents aggregation. The distribution of the glycosylated and the non-

glycosylated forms of the protein within the micelle is unclear. The glycosylated form may be selectively located on the outside of the micelle, or distributed uniformly throughout the micelle.

Light scattering studies on casein micelles have shown that addition of either rennin (chymosin) or of ethanol causes a decrease in the average radius of the micelles. This is followed by a pronounced increase in the average particle size due to aggregation of the individual micelles. The decrease in micellar radius as a result of rennin addition is due to the hydrolysis of the peptide bond between the Phe105-Met106 residues of the κ-cn molecule[158]. The release of the C-terminal caseinomacropeptide reduces the repulsion between the individual micelles and the subsequent aggregation is the basis of cheese manufacture. The decrease in micellar radius as a result of ethanol addition is more gradual. Aggregation of micelles occurs at ethanol concentrations above about 18%. These changes are believed to be due to the collapse of the "hairy" layer permitting aggregation to occur[159]. This ethanol-induced aggregation is important with regard to the production and stability of cream liqueurs. Despite the importance of the surface properties of κ-cn, no measurements of its behaviour in model systems have been reported. In order to investigate the influence of glycosylation on the physical properties of this technologically important protein, κ-cn has been fractionated into its major component forms. The binding of the various forms of the protein to polystyrene latex (used as a model colloidal system) was then determined. In addition, latices with different surface charges have been used in order to further elucidate the effect of charge on protein binding.

7.2 Materials and Methods

Positively charged amidine polystyrene latex (nominal diameter 76nm) was obtained from Interfacial Dynamics Corporation, Portland, Oregon, USA. Negatively charged LB1 (sulphonated) latex (nominal diameter 91nm) was purchased from Sigma Chemical Company Limited, Poole, Dorset, UK. Chromatography apparatus and columns were from Pharmacia Biotech, Milton Keynes, Bucks., UK. The chymosin (Maxiren 15) was obtained from Gist-Brocades. The concentrated chymosin was diluted before use (0.3g chymosin made up to 10g with H_2O).

Whole bovine κ-cn was purified from the milk of individual animals homozygous for the A or B variant of the protein by cation exchange chromatography[66]. After dialysis and freeze-drying, the κ-cn component was fractionated on a Hi-load 26/10 Q Sepharose HP anion exchange column. Whole κ-cn was dissolved at a protein concentration of 50mg ml^{-1} in bis-tris-propane buffer (5mM, pH7.0) containing 6M urea. 2-Mercaptoethanol was added at a concentration of 1μl mg^{-1} of protein and stirred for 1hr to reduce disulphide bonds. After filtering through a 0.22μm filter, 20ml (1g) of protein was applied to the column. Protein was eluted with a linear gradient of sodium chloride (0.15 to 0.3M in 51min.) in 5mM bis-tris-propane buffer containing 3.3M urea. Peak fractions were collected and pooled, and after dialysis against distilled water and freeze-drying, the purity and identity of the various κ-cn fractions was established by chromatography on a Mono Q FPLC column[160].

Hydrodynamic radii of the latex particles were determined using photon correlation spectroscopy (PCS). Stock latex suspensions were diluted in imidazole/HCl buffer (20mM, pH7.0) with and without 2-mercaptoethanol (0.1%). Stock protein

solutions were prepared in the same buffer with and without 2-mercaptoethanol (0.1%), the actual concentration of the protein solution being determined spectrophotometrically using known extinction coefficients. Binding studies and adsorption isotherms were carried out as detailed in Chapter 5.

Chymosin hydrolysis of κ-cn coated latices was performed by adding $CaCl_2$ at a concentration of 20mM before adding κ-cn. The hydrodynamic radius was determined prior to chymosin addition. The change in radius is then followed with time.

7.3 Results

The various glycosylated forms of the κ-cn A and B were reasonably well resolved on the Hi-load Q column as determined by FPLC of the individual fractions on a Mono Q column (Fig. 7.1). Overlap between the fractions was low in most cases (Fig. 7.2). Vreeman *et al* using DEAE-Sepharose[161,162], separated κ-cn B into five fractions which they numbered I to V. They also determined the NeuNAc and phosphate content of each of these fractions. For κ-cn A their fractions I, II, III, IV and V corresponded to fractions 2, 4, 5, 6 and 7 in this study. Fractions 2 and 3 were part of a double peak, so that fraction 3 was the same as 2. Fraction 1 from this separation was found by SDS-polyacrylamide gel electrophoresis not to be κ-cn, and was, therefore, discarded. For κ-cn B the corresponding fractions were 1, 2, 4, 5 and 6 (complete data not available for 6). Vreeman's fraction I was essentially the non-glycosylated form of κ-cn bearing a single phosphate group. The remaining fractions were found to have a somewhat heterogeneous composition. Fraction II was a mixture of equal amounts of non-glycosylated protein with 2 phosphate groups and protein

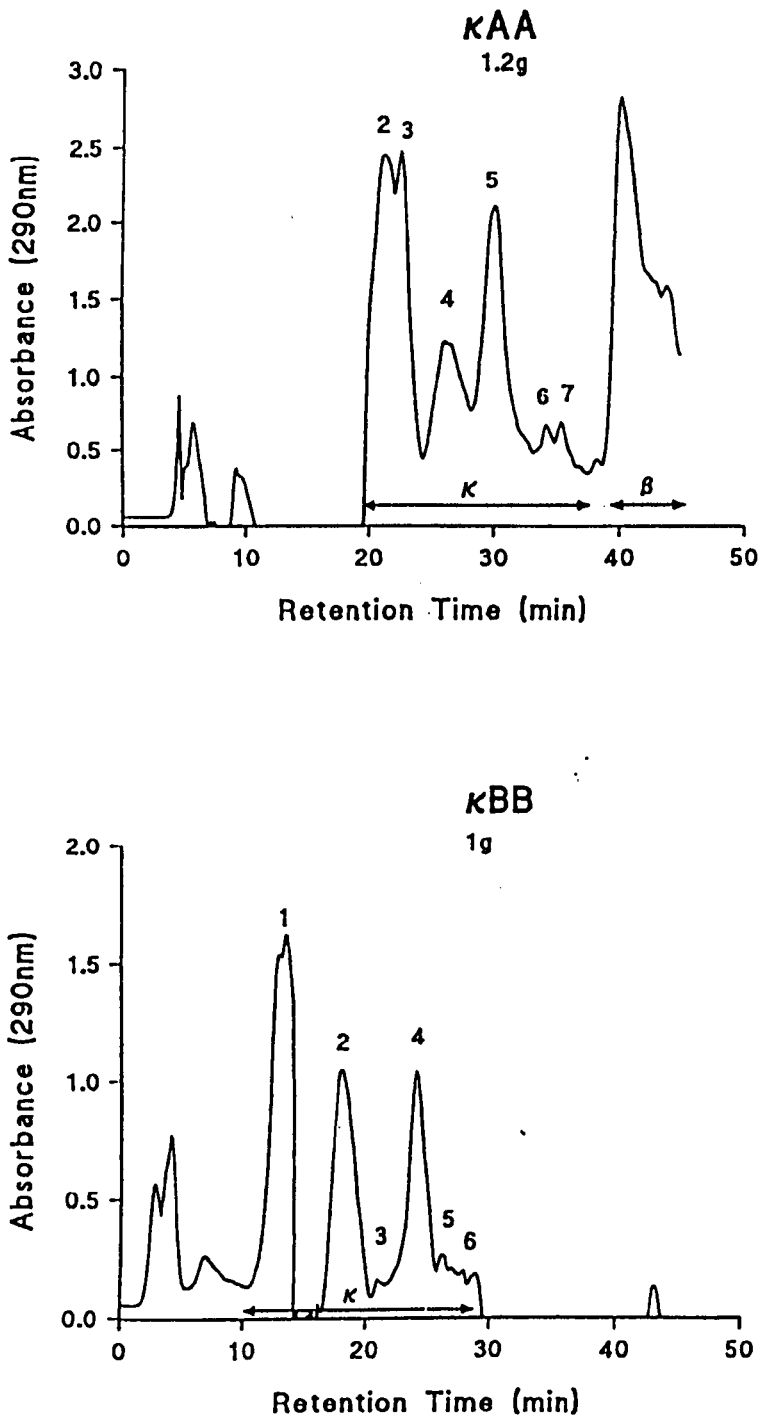

Fig. 7.1. Hi-load Q separation of glycosylated κ-cn.

Eluted using a gradient of 0.15-0.30M NaCl in 5mM bis-tris-propane pH7 containing 3.3M urea over 51min. at a flow rate of 6.5ml min^{-1}. Numbers are the same as the fraction numbers used in the text. The final peak obtained with κ-cn AA is β-cn.

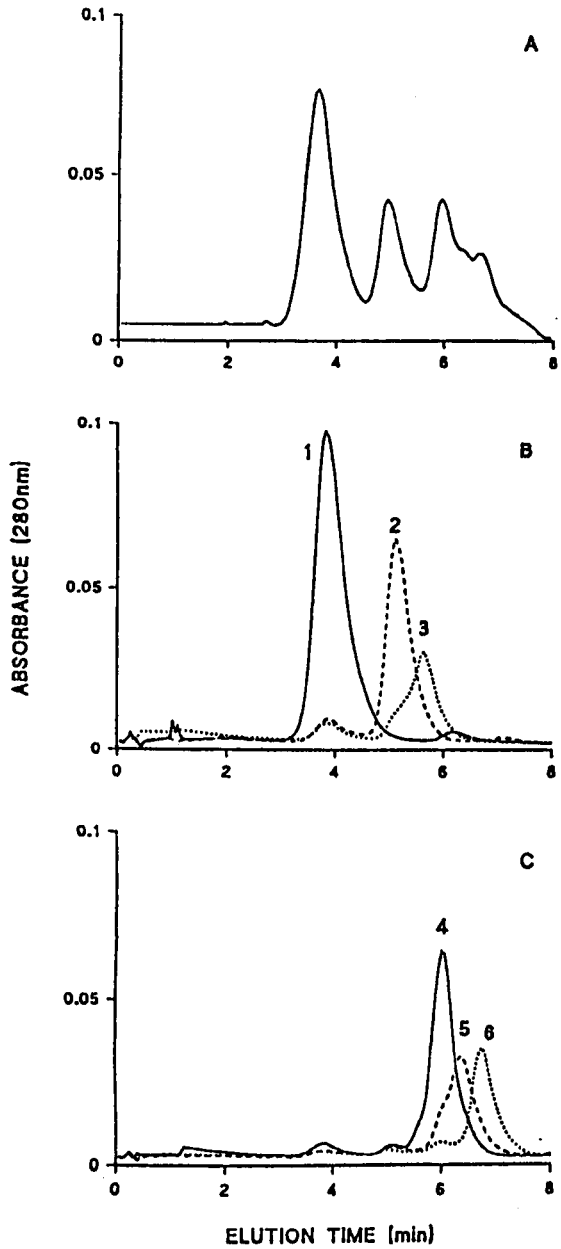

Fig. 7.2. Elution profiles from a Mono Q column of whole κ–cn B and the fractions obtained from the Hi–load Q column (B,C).

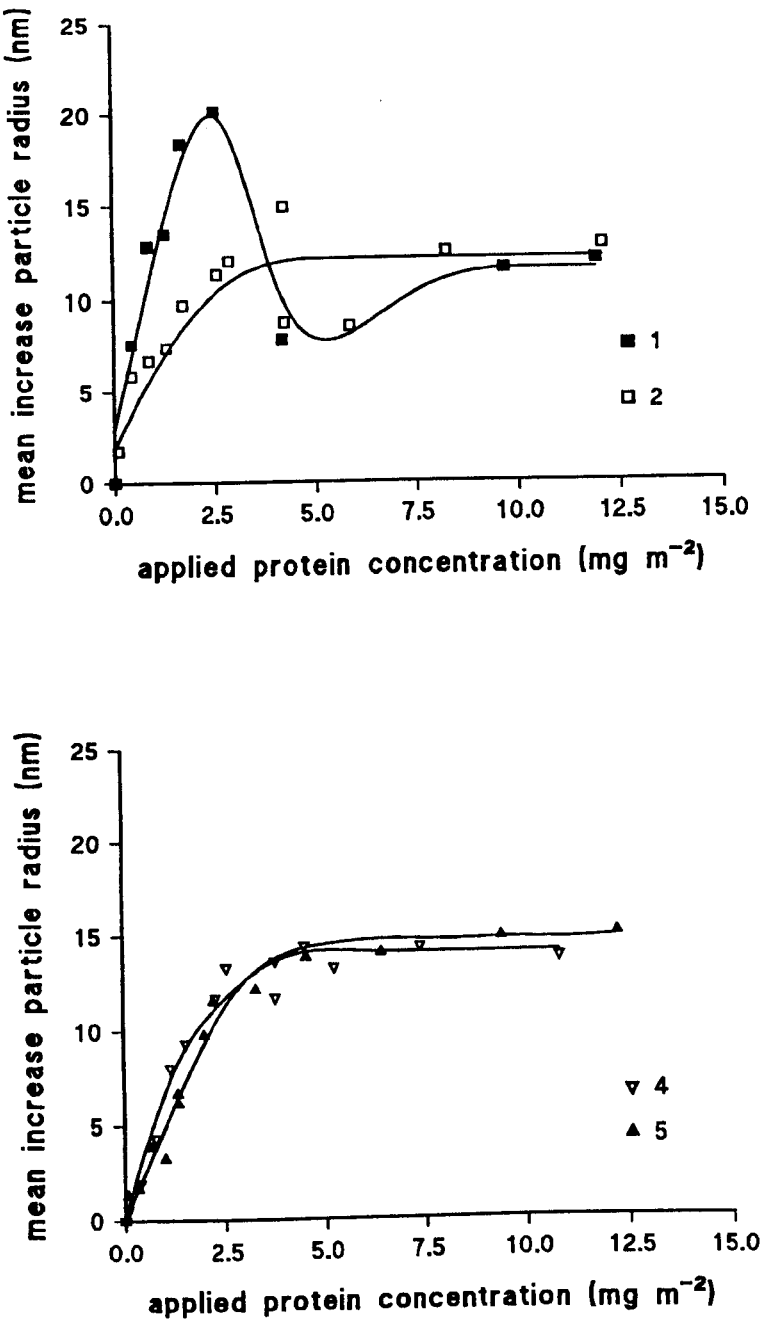

Fig. 7.3. Increase in the adsorbed layer thicknesses on negatively charged latex as a function of added protein concentration of κ–cn B fractions.

having 2 NeuNAc groups and a single phosphate group, III was a mixture of forms containing 3 NeuNAc groups and generally a single phosphate group, IV was a mixture of forms bearing 4 to 7 NeuNAc groups and mainly a single phosphate group and V had 6 to 9 NeuNAc groups and a single phosphate. The separation obtained here on the Hi-load Q column was very similar except for the separation of a further glycosylated fraction (results for this fraction are not shown). In general, the concentration of salt required to displace the protein from the ion exchange column increased with the degree of glycosylation.

The diameters of the uncoated LB1 and amidine latices as measured by PCS were 85 and 100nm respectively. The increase in the radius of the negatively charged LB1 latex as a function of added protein is shown for the various κ-cn B fractions (Fig. 7.3). At lower protein concentrations the thickness was apparently greater than at higher protein levels. This effect was only true for the non-glycosylated fraction 1. The cause of this effect is not known. It may have been due to some aggregated protein molecules bridging between latex particles at low protein concentrations since, when 2-mercaptoethanol was added to the protein in order to reduce disulphide bonds and so dissociate any aggregates of κ-cn, the effect was not observed (Fig. 7.4 and Fig. 7.5 shows the results for κ-cn B and A). Instead, the radius increased smoothly to a plateau value. The maximum thickness of the adsorbed protein layer on the LB1 latex increased marginally with the degree of glycosylation. The layer thickness of the non-glycosylated fraction (13nm for both phenotypes) was between 2.0 and 2.5nm less than that measured with the highly glycosylated fractions depending upon the κ-cn phenotype (Table 7.1). In general, the layer thickness with all of the κ-cn B fractions in the absence of 2-mercaptoethanol was 1 to 2nm less than that in its presence. This is

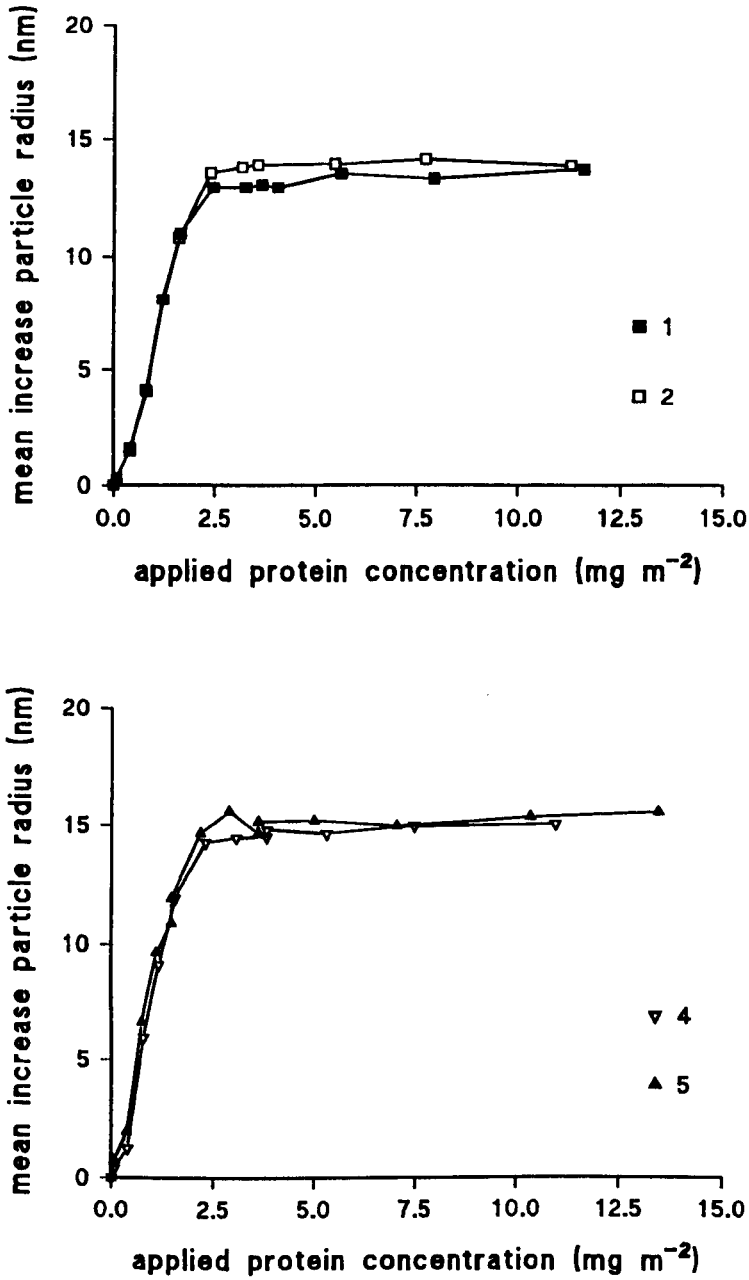

Fig. 7.4. Increase in the adsorbed layer thicknesses on negatively charged latex as a function of added protein concentration of κ–cn B fractions in the presence of 2–mercaptoethanol.

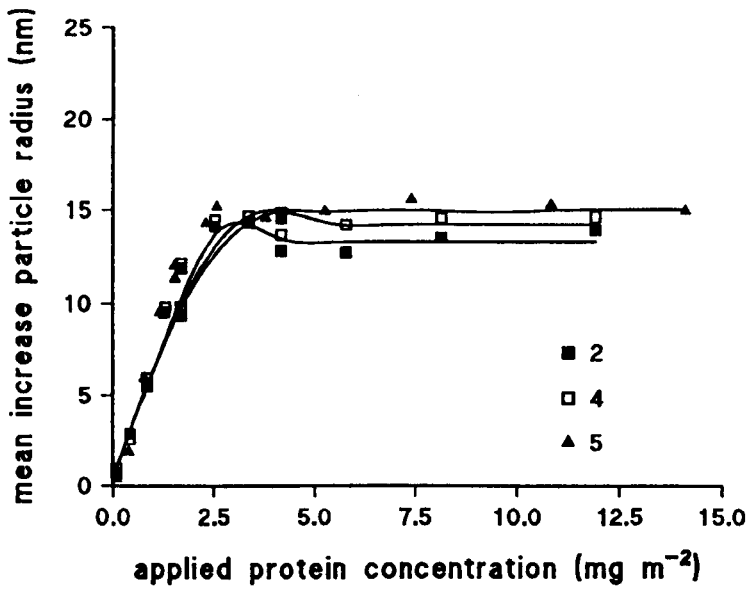

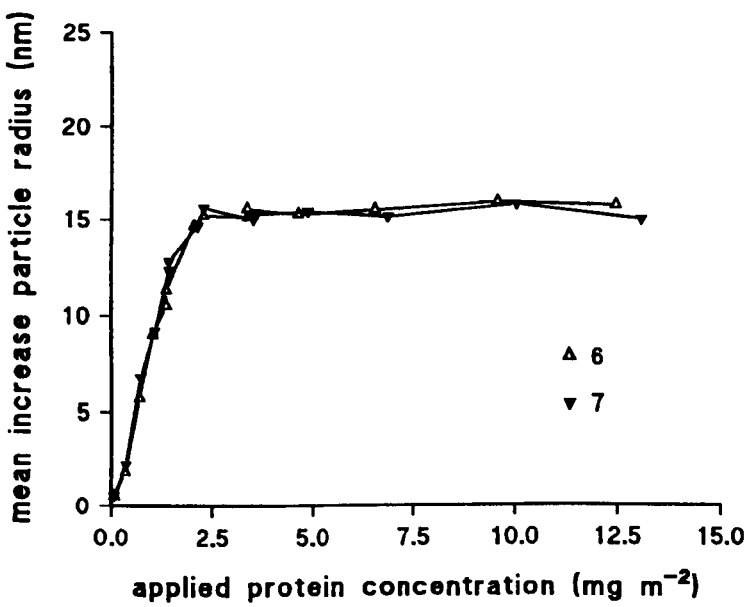

Fig. 7.5. Increase in the adsorbed layer thicknesses on negatively charged latex as a function of added protein concentration of κ–cn A fractions. In the presence of 2–mercaptoethanol.

Protein	Fraction number	Layer Thickness (nm)		Surface Coverage (mg m^{-2})	
		LB1	Amidine	LB1	Amidine
κ-cn A	2	13.0±1.0	11.5±1.5	3.5±0.2	3.0±0.5
	4	14.5±1.0	10.5±1.5	4.6±0.1	4.0±0.2
	5	15.0±1.2	12.0±1.5	2.5±0.7	5.2±0.5
	6	15.5±1.0	13.0±2.0	5.2±0.1	*
	7	15.5±1.0	13.0±1.7	3.2±0.2	3.5±0.5
κ-cn B	1	13.0±1.0	14.5±1.5	5.2±0.1	3.0±0.5
	2	14.0±1.0	11.0±1.5	3.9±0.1	1.5±0.2
	4	14.5±1.5	12.0±2.0	3.0±0.2	3.0±0.2
	5	15.0±1.0	12.5±2.0	3.0±0.1	1.7±0.5
Whole κ-cn	A	14.0±1.0	12.5±1.0	2.5±0.5	2.9±0.5
	B	13.0±1.6	12.0±3.0	2.0±1.0	2.1±0.5

Table 7.1. Layer thickness and surface coverage of κ-cn A and B fractions and whole κ-cn A and B on negatively charged LB1 and positively charged amidine latex.

* represents result not determined.

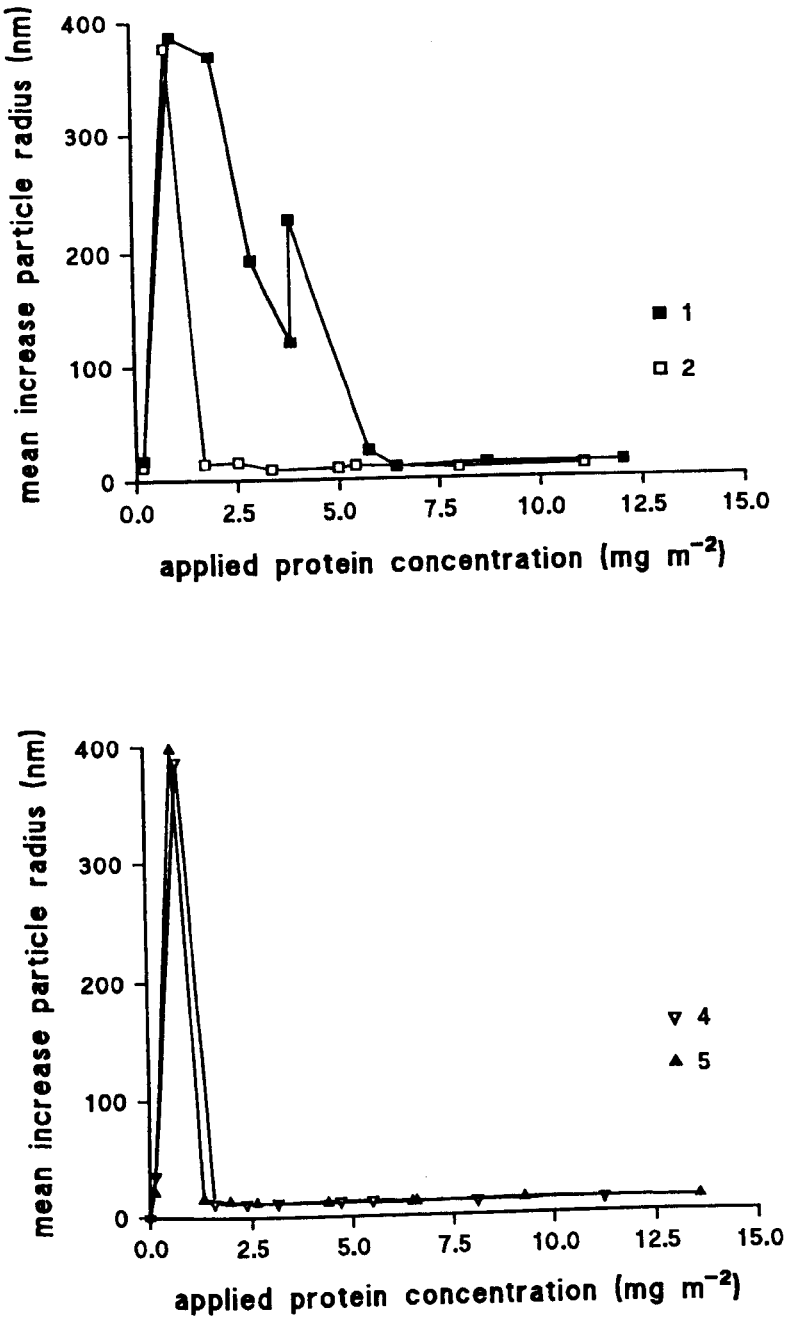

Fig. 7.6. Aggregation of positively charged amidine latex as a result of κ–cn B fractions in the presence of 2–mercaptoethanol. κ–cn A produces similar results.

presumably as a result of the relaxation in the secondary structure due to reduction of disulphide bridges.

Addition of low concentrations of any of the κ-cn fractions to diluted suspensions of the positively charged amidine latex resulted in aggregation of the latex particles even in the presence of 2-mercaptoethanol (Fig. 7.6). This suggests that the aggregation was due to protein molecules bridging between latex particles. These aggregates could not be disrupted by adding more protein, possibly due to the additional protein molecules being unable to penetrate into the aggregates, or more likely, to the tight binding of protein to the latex surface. This latter explanation is favoured, since if larger initial aliquots of protein solution were added, no aggregation was observed and thinner layers, similar to those on the LB1 latex, were measured. Fresh amidine latex dilutions had therefore to be used for each of the protein concentrations examined. The concentration of added protein required to overcome this bridging effect was not the same for all of the fractions. For κ-cn B, the amount of the non-glycosylated protein required to exceed this threshold was approximately four times greater than that of any of the glycosylated proteins. The trend was the same for κ-cn A, but the difference was not as dramatic. As with the negatively charged latex, the thickness of the non-glycosylated protein layer on amidine latex was between 1.5 and 2nm less than that observed with any of the other fractions (Fig. 7.7 and Fig. 7.8). Generally, the thicknesses of the absorbed protein layers on the positively charged latex were approximately 2nm less than that of the same fraction on the negatively charged latex. On the LB1 latex, all fractions of κ-cn A gave protein layers which were approximately 1nm thicker than those of κ-cn B fractions. On the amidine latex, the behaviour of the non-glycosylated fractions of both κ-cn phenotypes were

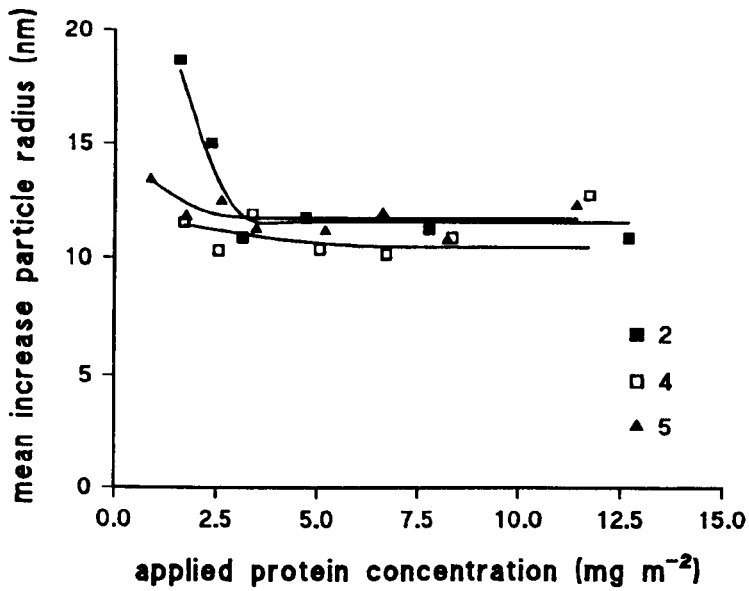

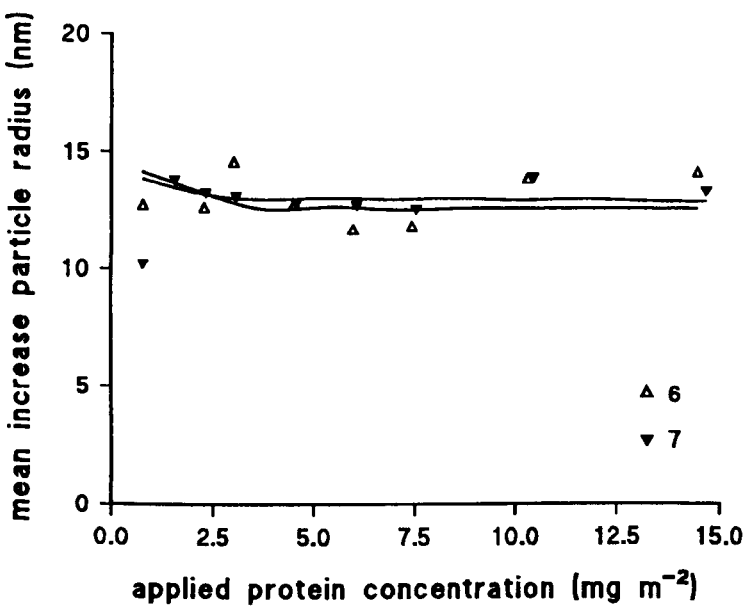

Fig. 7.7. Increase in the adsorbed layer thicknesses on positively charged amidine latex as a function of added protein concentration of κ–cn A fractions in the presence of 2–mercaptoethanol.

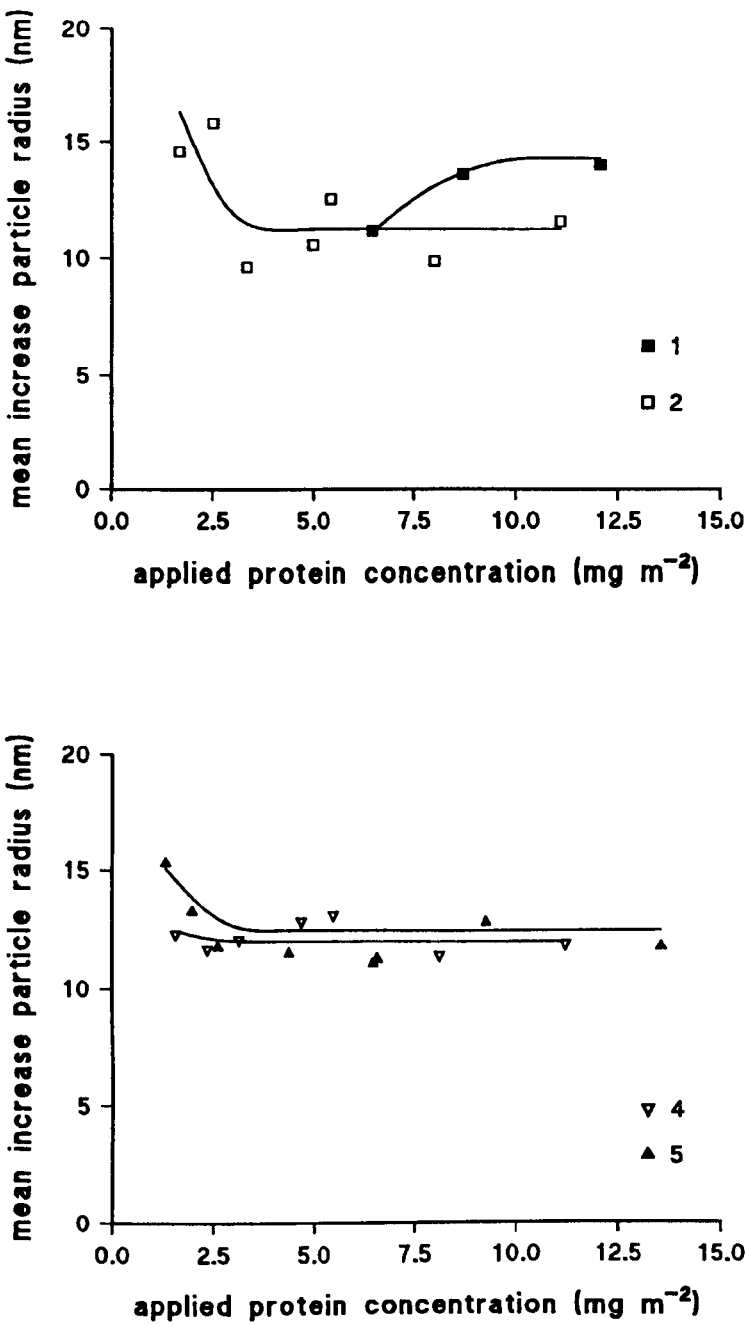

Fig. 7.8. Increase in the adsorbed layer thicknesses on positively charged amidine latex as a function of added protein concentration of the κ–cn B fractions in the presence of 2–mercaptoethanol.

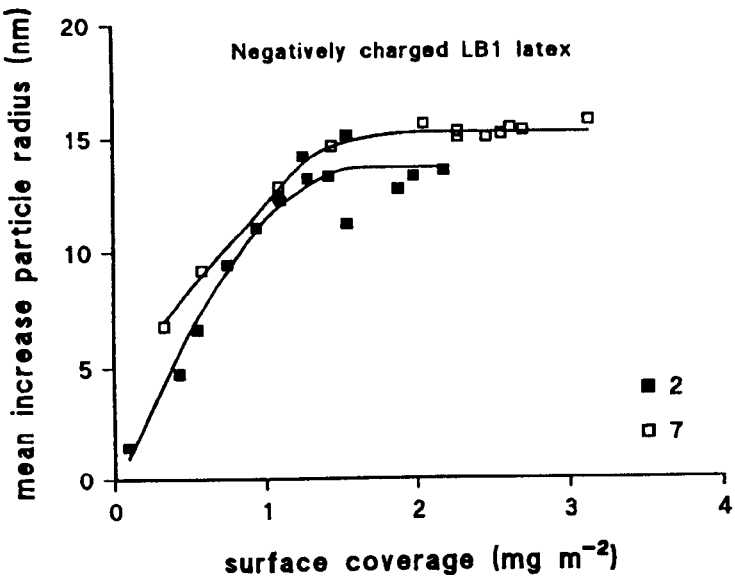

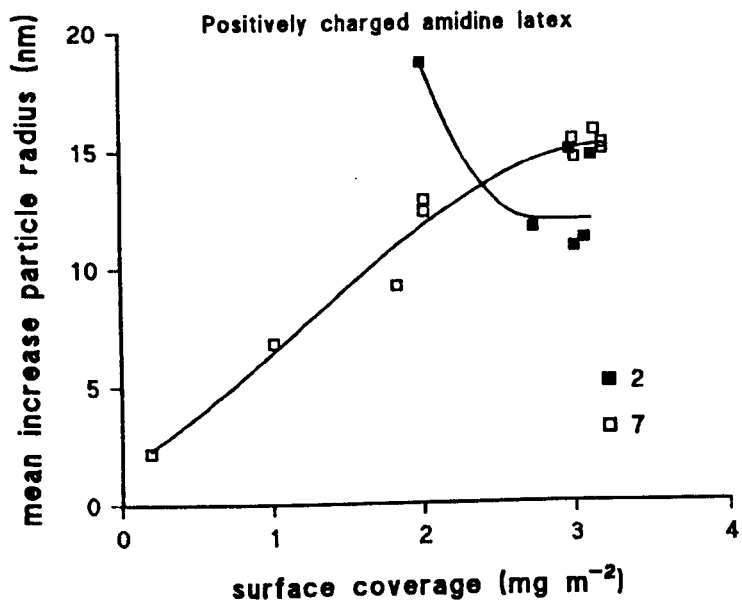

Fig. 7.9. Increase in adsorbed κ–cn A protein layer thicknesses as a function of surface coverage of fractions 2 – non–glycosylated and 7 – highly glycosylated.

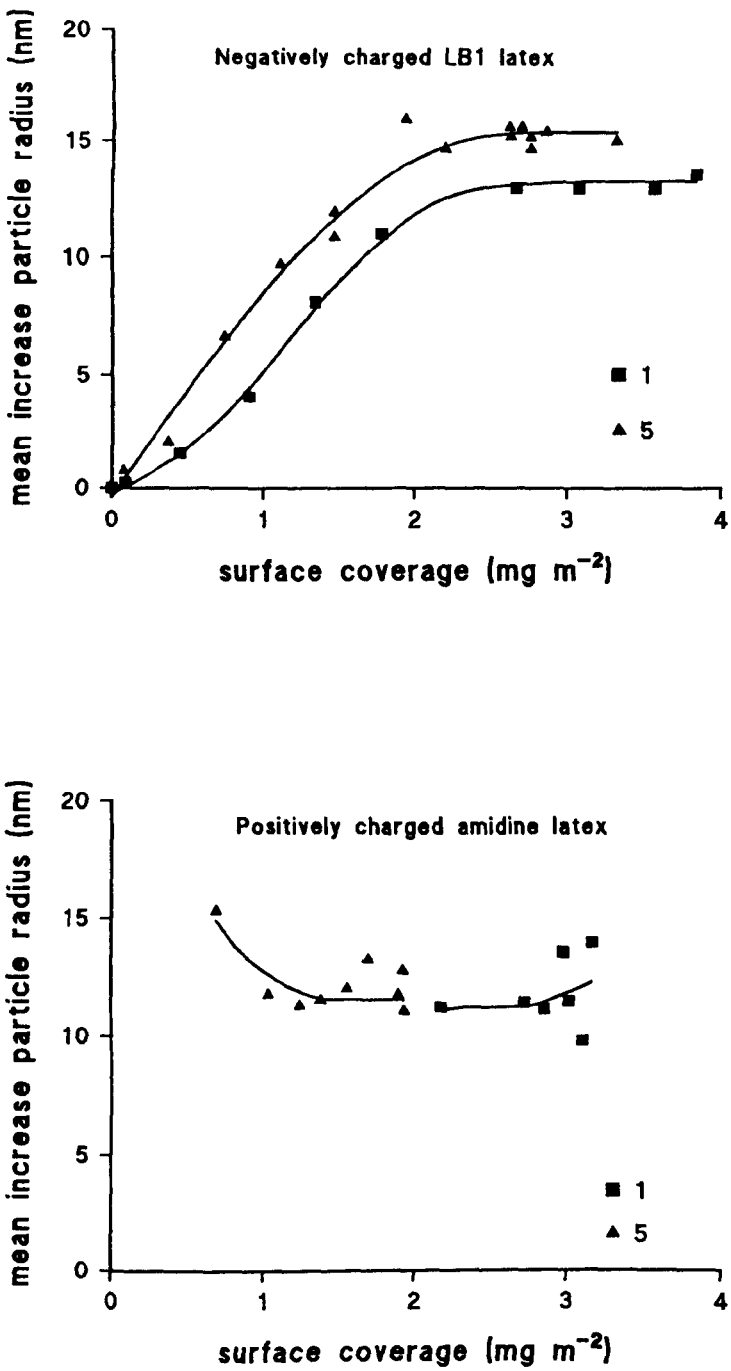

Fig. 7.10. Increase in adsorbed κ–cn B protein layer thicknesses as a function of surface coverage of fractions 1 – non–glycosylated and 5 – highly glycosylated.

similar, but the most highly glycosylated fractions gave protein layers about 1nm thicker with the κ-cn A phenotype. With amidine latex the error bars were much wider than with LB1 latex (±2 to 3nm compared with ±1 to 1.6nm). The thicknesses of the absorbed protein layers as a function of surface coverage of the non-glycosylated fractions and highly glycosylated fractions on the positively and negatively charged surfaces were compared (Fig. 7.9 and Fig. 7.10). Maximum layer thickness of the non-glycosylated fraction of κ-cn A and B on the negatively charged latex were achieved at approximately 3 and 1.5mg m^{-2} respectively and the highly glycosylated fractions of κ-cn A at 2mg m^{-2} and κ-cn B at 2.5mg m^{-2}. Due to aggregation of the positively charged latex in the presence of lower concentrations of protein, it was not possible to obtain exact values for this parameter. However, after the aggregation phase had been exceeded the maximum protein layer thickness was attained at 3.0 and 2.5mg m^{-2} for non-glycosylated and 3.2 and 1.5mg m^{-2} for highly glycosylated fractions of κ-cn A and B respectively. The affinity of non-glycosylated and highly glycosylated forms of κ-cn A and B for the two surfaces was similar, and at low protein concentrations all of the added protein was adsorbed to the surface (Fig. 7.11 and Fig. 7.12).

Similar experiments were performed with whole κ-cn A and B. The results are summarised in Table 7.1. κ-cn A and B gave a slightly thicker protein layer by 1.0-1.5nm, on the negative latex compared to positively charged latex. Layer thicknesses on LB1 latex are similar, with κ-cn A layers being slightly thicker than κ-cn B (Fig. 7.13). When adsorbed to amidine latex this difference in thickness was slightly less, with κ-cn A layers being about 0.5nm thicker than κ-cn B (Fig. 7.13). It should be noted that the results for κ-cn B have wide error bars which may mean that this is not

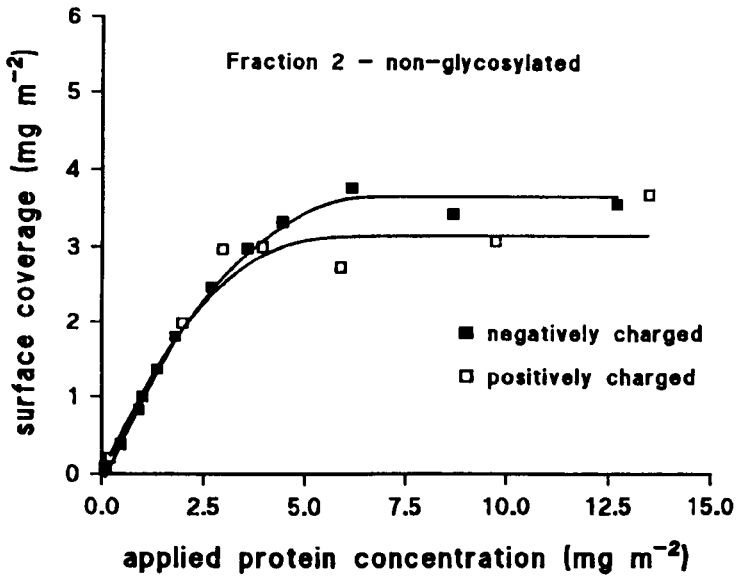

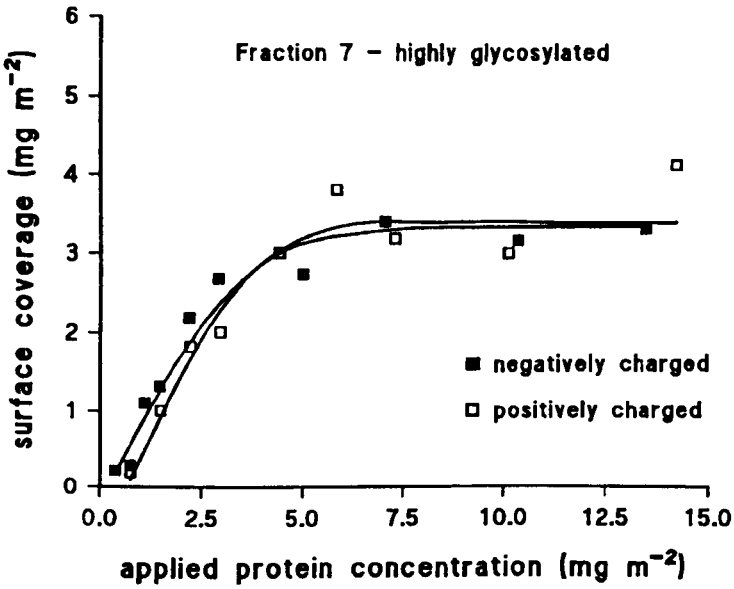

Fig. 7.11. Surface coverage as a function of added κ-cn A on the positively and negatively charged latices for fractions 2 and 7.

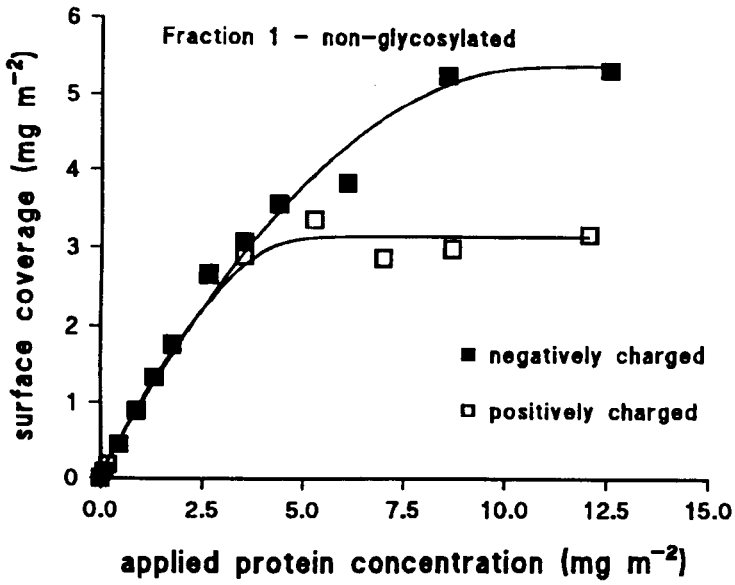

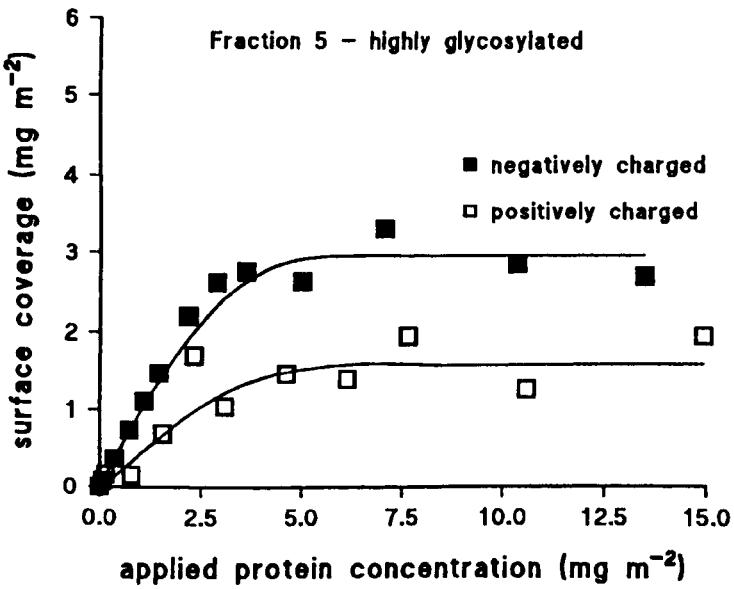

Fig. 7.12. Surface coverage as a function of added κ–cn B on positively and negatively charged latices for fractions 1 and 5.

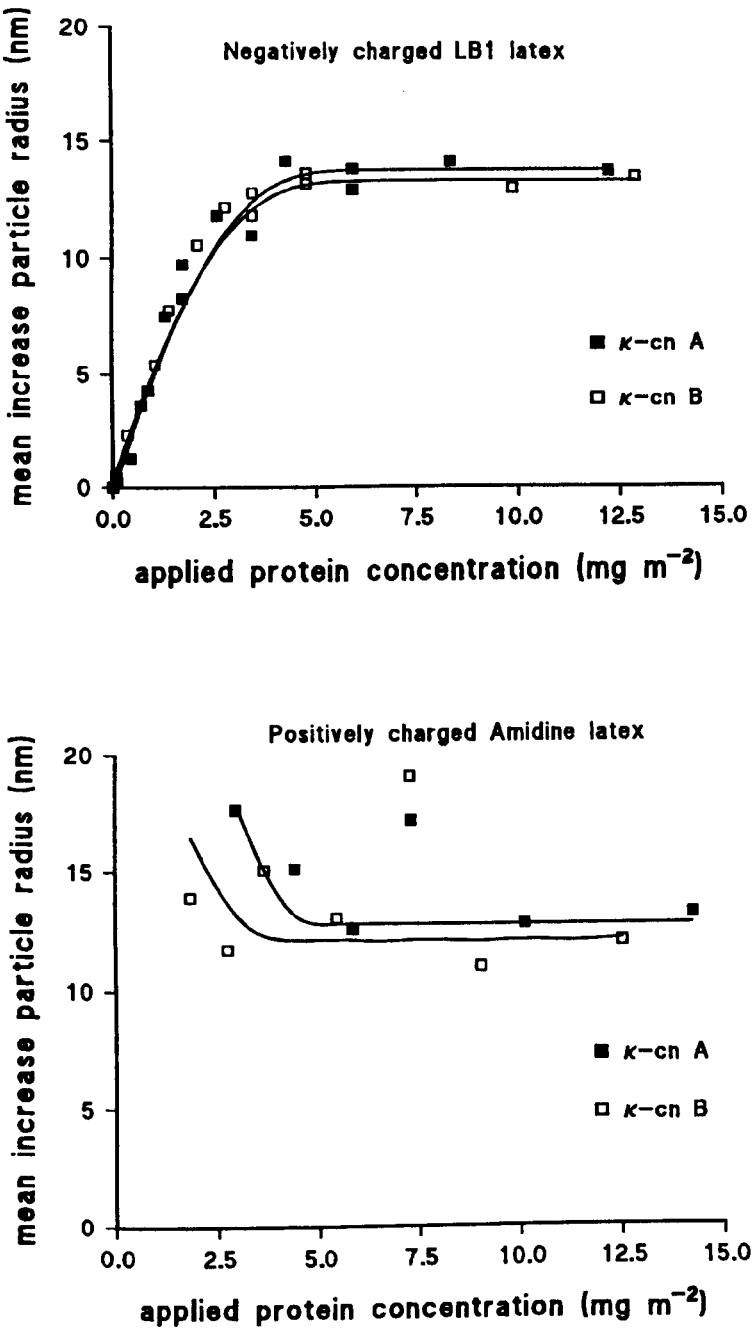

Fig. 7.13. Increase in the adsorbed layer thickness of whole κ-cn A and B on negatively charged LB1 latex and positively charged amidine latex as a function of applied protein concentration.

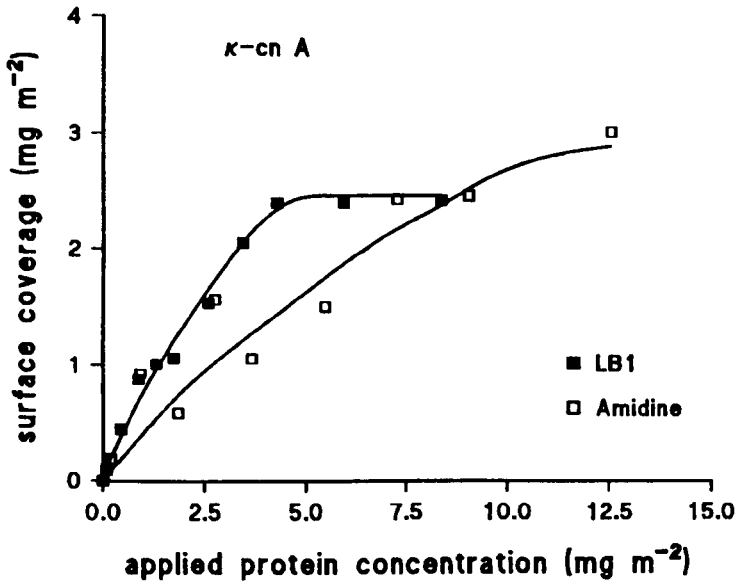

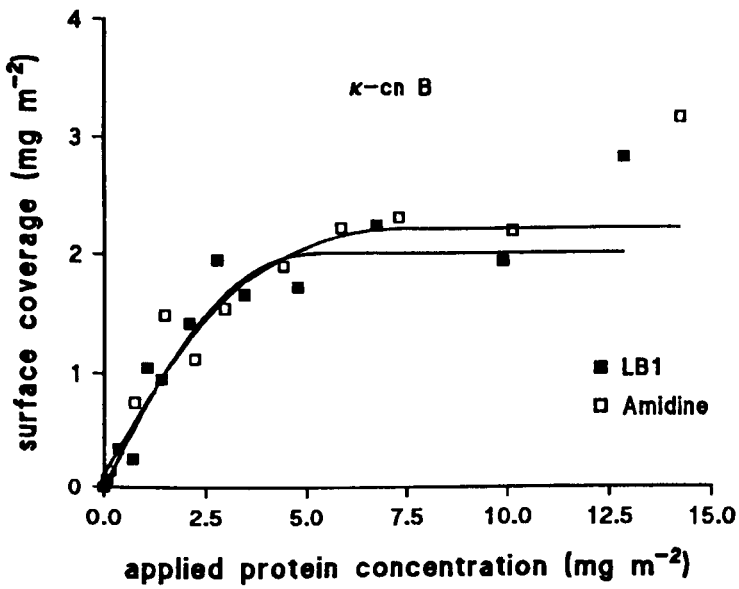

Fig. 7.14. Surface coverage as a function of added κ–cn on the positively and negatively charged latices for whole κ–cn.

a significant difference and the two points at ~7.5mg m^{-2} applied protein are probably due to scattering from some aggregates that are still present.

Surface coverage measurements showed only a slight difference between the amount of κ-cn A bound to LB1 and amidine latex, or κ-cn B binding to LB1 and amidine latex (Fig. 7.14). Surface coverages are slightly lower on the negatively charged surface than on the positively charged latex which is more apparent with κ-cn A. Also κ-cn A has a slightly higher surface coverage than κ-cn B. Indications of aggregation beginning to occur were detected at applied protein levels of 12.5mg m^{-2} and above, as shown by the elevated values of bound protein.

Having shown that κ-cn binds to the latex, attempts were made to cleave the adsorbed protein using chymosin. The amount of κ-cn added to the LB1 latex was sufficient to ensure high loading on the surface but also to minimise the amount of free protein in solution which would preferentially be cleaved by the enzyme. Ca^{2+} is necessary for maximum activity of the enzyme but the order of addition was found to be important. The effect of chymosin on negatively charged LB1 latex coated with whole κ-cn A or B is shown in Fig. 7.15. In order for there to be any change in particle size on addition of chymosin, Ca^{2+} had to be added to the latex prior to κ-cn adsorption. κ-cn A coated LB1 latex required approximately 4 times the amount of enzyme than κ-cn B, in order for a decline in layer thickness to reach a constant value (total decrease of 3-5nm).

7.4 Discussion

κ-cn is a relatively small protein which possesses an amphiphilic structure having a hydrophobic N-terminal domain and a polar C-terminal domain. At pH6.6

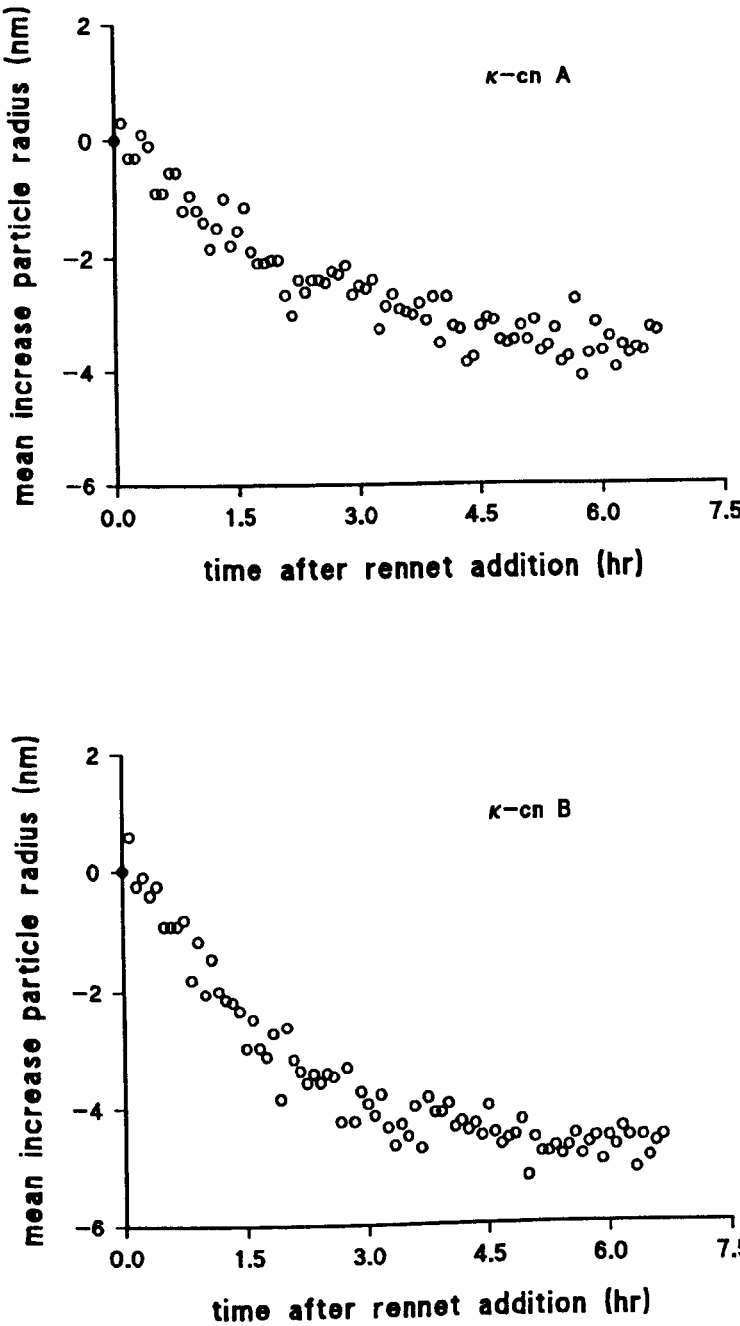

Fig. 7.15. Effect of chymosin on κ–cn A and κ–cn B coated LB1 latex.

36μl chymosin added to κ–cn A.

9μl chymosin added to κ–cn B.

the net charge of the polar domain of the non-glycosylated molecule is -10 or -11, but each additional NeuNAc residue contributes an additional negative charge. Since all of the glycosylation sites are located in the polar domain, the net negative charge in this region increases with glycosylation (Figs. 2.3 and 2.4).

These results can be compared with estimates of the dimensions of the stabilising κ-cn layer at the surface of the casein micelle. Since there is no conclusive evidence that the various forms of the micellar κ-cn are not uniformly distributed throughout the micelle, the micelle surface can be assumed to carry a mixture of both the glycosylated and non-glycosylated molecules. Addition of a critical level of ethanol causes the hairs to lie flat on the surface rather than remove them completely. These flattened hairs will still have a layer thickness. An estimate of the thickness of this flattened layer can be obtained from a number of other measurements made on adsorbed casein layers. Small-angle X-ray scattering studies of β-cn on LB1 latex[39] and neutron reflectivity measurements of β-cn at an oil-water interface[143] have shown that the protein layers consist of a dense region about 2 to 4nm thick with a more diffuse region extending a further 8 to 10nm from the surface. Trypsinolysis of adsorbed β-cn layers reduced the layer to a thickness of about 4 to 5nm[34,124]. Since κ-cn has a relatively unfolded structure like β-cn, the flattened κ-cn molecules would be expected to have similar dimensions to the dense region of β-cn *i.e.* at least 2nm. The average radius of casein micelles decreased by between 10 to 12nm as a result of addition of ethanol. If this decrease is added to the assumed flattened κ-cn layer thickness, then a total κ-cn layer thickness of 12 to 16nm results. The thicknesses of the κ-cn layers on the different surfaces reported here, ranging between 11 and 15.5nm depending on the degree of glycosylation, are in good agreement with this estimated

thickness. Recently Dalgleish[77] has studied the adsorption of whole κ-cn to polystyrene latex and has found a layer thickness of 13.7nm in the presence of 2-mercaptoethanol, which also agrees with these results.

Glycosylation was found to have a significant effect on the thicknesses of the adsorbed κ-cn layers. There are two possible reasons for the increased layer thickness of the glycosylated forms of the protein. Since glycosylation increases the negative charge in the C-terminal region of the protein, electrostatic repulsion between the C-terminal end of the κ-cn molecule and the negatively charged surface of the LB1 latex should be greater with the glycosylated forms. Conversely, electrostatic attractions between this end of the molecule and the positively charged amidine latex should also be greater with the glycosylated forms. In the absence of any other effects due to the NeuNAc residues, the glycosylated molecules should lie closer to the positively charged surface than the non-glycosylated protein. This did not occur with κ-cn A and, therefore, the increased hydrophilicity due to the presence of the NeuNAc groups must outweigh the electrostatic attraction effect.

κ-cn A possesses one more negative charge than κ-cn B. As a result it would be expected that there would be greater charge repulsion between the negatively charged LB1 latex and the κ-cn A molecules. This would mean that the layer thickness of κ-cn A should be greater, which it is. When the layer thicknesses on the positively charged amidine latex are compared, the highly glycosylated fractions of κ-cn A form layers which are thicker than those obtained with κ-cn B. κ-Cn A molecules also contain an extra glycosylation site[67], which would increase the molecule's hydrophilicity, and once again this seems to outweigh the electrostatic attractive forces. In addition the NeuNAc group is quite a bulky moiety, which may also lead to thicker

layers due to steric hindrance. Generally, with all κ-cn fractions (independent of phenotype), the thickness of the adsorbed protein layers on the positively charged surface was 2 to 3nm less than on the negatively charged latex. This reflects electrostatic interactions between the surfaces and the net negatively charged protein.

The density of packing of the non-glycosylated κ-cn B molecules was significantly higher than that of the most highly glycosylated form of the protein on both surfaces. This is probably due to their lower net negative charge and the absence of the bulky NeuNAc groups in the hydrophilic tail region. This difference is not as large in the case of κ-cn A, which may be due to the increased steric hindrance of the additional glycosylated molecule. The increased surface area which each protein molecule occupied on the positively charged surface (the contrary result of fraction 5 of κ-cn A cannot be explained) presumably results from interactions between negatively charged regions on the protein and positively charged groups on the latex and/or the decrease in electrostatic repulsion. This would permit the protein molecules to lie closer to the latex surface and may account for some, or all, of the 2 or 3nm differences in the layer thicknesses of κ-cn B on the differently charged surfaces. This also holds true when fractions of κ-cn A are compared with the corresponding fraction of κ-cn B. With κ-cn A the layer thickness and surface coverages on positively charged latex increase as the amount of glycosylation increases. These results again suggest that the steric hindrance caused by the additional NeuNAc residues outweighs the electrostatic attraction forces between the negatively charged NeuNAc residues and the positively charged latex.

The contribution of each of the fractions to the binding of whole κ-cn A and B can now be estimated. In milk of cows from the Hannah herd, κ-cn B milk has a

greater proportion of glycosylated molecules than does κ-cn A (58% glycosylation for κ-cn A and 63% for κ-cn B). These results agree with those of Ferron-Baumy *et al*[163] who found 60 to 67% glycosylation in bulk milk. On the negatively charged latex κ-cn A forms slightly thicker layers when compared with κ-cn B, presumably as a result of the extra repulsion between the more negatively charged κ-cn A. In the case of amidine latex, κ-cn A still produces a slightly thicker layer than does κ-cn B. This difference is not as significant as when the separate glycosylated fractions are used. This may be due to the higher proportion of glycosylated κ-cn molecules present in κ-cn B overcoming some of the electrostatic attraction between the protein and the positively charged latex, in a manner similar to that in which the degree of glycosylation effects the layer thickness in κ-cn A.

Dalgleish[77] has recently presented results on the adsorption of whole κ-cn to negatively charged polystyrene latex. He reported a protein layer thickness of 8.3nm without 2-mercaptoethanol and 13.7nm with 2-mercaptoethanol. Though the results in the presence of 2-mercaptoethanol agree with those presented here, the decrease in layer thickness in the absence of 2-mercaptoethanol is at variance with the results for κ-cn fractions 1 and 2 in Fig. 7.3. Results reported here show thicker layers in the absence of 2-mercaptoethanol causing a reduction in layer thickness presumably due to the breaking up the protein polymers. Since there is no indication which κ-cn phenotype was used in Dalgleish's work, it is possible that the κ-cn used contains both κ-cn A and B phenotypes. This may have some bearing on the results, as may the greater latex concentration and κ-cn concentration used by Dalgleish[77]. Aliquots of 100μg were used by Dalgleish[77], whereas aliquots ranging from 1.5-150μg were used in these studies. It could be that adding the protein in smaller amounts enabled

adsorption to the latex surface to be more uniform, as the protein had effectively a longer time to orientate on the latex surface. In addition, there is no indication as to how long the protein was left in contact with the latex prior to sizing. This also limits the time which the protein has to orientate at the latex surface.

The preliminary results on the effect of chymosin on the adsorbed layer thickness are interesting. The requirement for Ca^{2+} prior to κ-cn adsorption suggests that an ionic layer is formed around the latex particle, and that this affects the orientation of the protein at the latex surface, so exposing the susceptible Phe105-Met106 bond to chymosin attack. Further analysis of the peptides released during hydrolysis would give a better idea of the protein orientation at the latex surfaces. Dalgleish[77] found an increase in size (aggregation) due to chymosin, but no decrease in size prior to this aggregation was seen. However, there were no Ca^{2+} ions present in the buffer which could explain this difference. In the results reported here, no aggregation of the latex/protein complex after proteolysis was detected, even after 7hours. This agrees with work done by Dickinson[141] who found that κ-cn coated latex particles do not flocculate, suggesting that in order for aggregation to occur, interactions between other proteins and Ca^{2+} ions may be required.

The decrease in radius of 3-5nm suggests that, as with κ-cn coated PG liposomes subjected to trypsinolysis in Chapter 4, the macropeptide was released into solution, whilst the hydrophobic para-κ-casein remained adsorbed to the latex surface. This decrease is less than the 7.8nm reduction measured in renneting casein micelles[158].

The bridging by individual protein molecules between latex particles at low protein levels is not unique. Low concentrations of β-lg have previously been shown[123] to cause bridging between latex particles although the size of these aggregates were

smaller than those found with κ-cn. This could be because the particle latex concentration also has an effect on apparent size. With the exception of the slight overshoot in the layer thickness when κ-cn was adsorbed to the negatively charged latex and which may have been due to bridging, extensive bridging between particles was only observed with the positively charged latex. This reflects the fact that κ-cn can be regarded as having two "sticky" ends. The N-terminal region probably adsorbs to the surface mainly through hydrophobic interactions. The other, highly negatively charged, C-terminal region could interact with the positively charged surface through electrostatic attraction. However, glycosylation decreases the extent of aggregation and this argues against this form of binding and implies that, even here, hydrophobic interactions between the dangling chain and the free surface of another latex particle occur. If this is the case, increasing the extent of glycosylation will push the hydrophobic/hydrophilic balance of this region towards the hydrophilic, diminishing the strength of the hydrophobic interactions and the extent of bridging as was observed. At low protein levels, the density of loading is sufficiently low for interactions with both ends to occur. At higher levels the stronger hydrophobic interactions of the N-terminal regions predominate and the C-terminal regions extend into the aqueous phase.

Heating milk at temperatures above about 70°C results in the formation of disulphide bridges between the micellar κ-cn and the globular whey proteins. This is reflected in the rate at which the κ-cn molecules are cleaved by chymosin[164]. It has been reported that when milk was heated to high temperature, these interactions only appeared to influence the rate of release of the glycosylated macropeptide[163], although no explanation was given for the differences in reactivity. The results presented here, which show that the glycosylated molecule projects further from the surface, may in

part, explain this difference.

Chapter 8

Summary

The research described in this thesis concerns with the influence of charge on the adsorption of milk proteins to surfaces. A variety of charged surfaces were used *i.e.* negatively charged and zwitterionic liposomes prepared from phosphatidylglycerol (PG) and phosphatidylcholine (PC) respectively and positively and negatively charged polystyrene latices.

8.1 Adsorption of milk proteins to phosphatidylglycerol and phosphatidylcholine liposomes

Phospholipid bilayers are important cell constituents as they form the basic element of the cell membrane. Phospholipids are also added to some processed foods in order to act as emulsifiers. Protein-phospholipid interactions are therefore important with regard to the behaviour of these systems. Phospholipids can be organised into liposomes which are vesicles in which an aqueous volume is enclosed within a membrane composed of lipid molecules. Usually, the membrane consists of a bilayer of phospholipid molecules whose charged head groups project into the aqueous phase. The charge on the liposome surface can be changed by using different classes of phospholipids. PG has a head group with an overall negative charge, whilst PC is zwitterionic.

The milk proteins investigated were the disordered proteins, α_{s1}-, β- and κ-casein (-cn) and the globular whey protein β-lactoglobulin (β-lg). β-Cn was also enzymatically dephosphorylated with potato acid phosphatase in order to reduce the net

negative charge of the molecule.

Plots of the increase in particle radius as a function of added protein for the two types of liposome showed a consistent difference in both the shape of the plots and in the thickness of the adsorbed protein layers. In all cases protein layer thicknesses were less on PC than on PG liposomes. These results can largely be explained on the basis of the net charge on the liposome surface and the distribution of charge on the protein molecules. β-Cn is the most hydrophobic of the caseins and has a pronounced amphiphilic structure with the N-terminal 21 residues having a net negative charge of -12[63]. The remainder of the molecule has no net charge. Therefore, electrostatic charge repulsion should lead to thicker layers on the PG liposomes as the N-terminal region is pushed away from the surface. Due to the reduction in the net negative charge as a result of dephosphorylation protein layers were slightly thinner. There is also increased sigmoidicity in similar plots for dephosphorylated β-cn. This may have been due to the removal of some of the negative charge permitting the protein molecules to pack closer together before electrostatic repulsion on adjacent protein molecules pushes them out into the aqueous phase to their maximum extent.

The increase in the average size of the PG liposome preparation at higher concentrations of α_{s1}-cn was too great to be accounted for merely by extension of the protein from the surface. The most likely explanation is that the increase arises from protein bridging between liposomes. α_{s1}-Cn has a highly charged region near the centre of the molecule. At pH6.6 this region has a net negative charge of -20. On the PC surface the α_{s1}-cn apparently behaves like the other caseins with the unordered casein molecule lying relatively close to the surface. On the negatively charged PG surface however, charge repulsion appears to result in this negatively charged region

of the protein being displaced from the liposome surface. It apparently remains attached by one or both ends of the molecule. As protein loading increases, either one of the ends is displaced from the surface by competition with other casein molecules, or the concentration of the free ends reaches a level at which they link to other liposomes and form stable clusters. This is indicated by a large increase in particle size.

κ-Cn also has an amphiphilic structure with a hydrophilic C-terminal domain. At pH6.6, this region has a net negative charge of -16 or -17 (including the sialic acid residues). Therefore, it would be expected that the electrostatic repulsion would be greater between the negatively charged C-terminal "tail" and negatively charged PG head groups. This would result in the charged κ-cn "tail" being pushed further from the liposome surface resulting in much thicker layers on these liposomes.

In contrast to the random coil structure of the casein molecules, β-lg has a highly folded, globular structure. At pH6.2, β-lg exists as a dimer with a long axis of 6.93nm and a short axis of 3.58nm[103,104]. If β-lg was binding perpendicular to the PC liposome surface, a layer thickness of 6.93nm would be expected. The value of 7.5-8nm is within experimental error of this value. Again this may be due to charge repulsion between negatively charged portions of β-lg and the negatively charged liposome surface. Unlike the caseins, the charge distribution of the β-lg molecule is more difficult to predict due to its globular structure. Examination of the distribution of charge does not show the existence of any specific, highly charged regions[63].

When the binding of κ-cn and β-lg to PG liposomes was determined at pH4.4, a very large increase in particle size was observed. The isoelectric points of both proteins are at about pH5. Therefore, at pH4.4 the protein molecules will be largely

positively charged. This will result in greater attraction towards the negatively charged PG and may result in the protein acting as a bridge between liposome molecules resulting in a larger particle size.

8.2 Effect of cations on adsorption of native and dephosphorylated β-casein

Dephosphorylation decreased the thickness of adsorbed β-cn layers on LB1 by about 4-5nm. At low concentrations of both native and dephosphorylated β-cn the addition of NaCl to negatively charged LB1 latex suspensions resulted in a massive increase in particle size. This was probably due to Na^+ ions reducing the net negative charge on the proteins and surface allowing the proteins to bridge between uncoated portions neighbouring latex particles. At higher protein concentrations this bridging was overcome, since most of the latex surface would be coated with protein thus preventing this bridging phenomenon.

Addition of Ca^{2+} reduced the thickness of preadsorbed β-cn layers from 12 to 6nm. However, the effect of Ca^{2+} on the layer thickness of native β-cn is too great to be explained by simple ionic strength effects. The Ca^{2+} ions apparently bind primarily to the phosphate residues in the negatively charged "head". Once again, the electrostatic repulsion between the "head" and surface is reduced, which permits the "spring" to relax and also explains why dephosphorylated β-cn is less sensitive to Ca^{2+} ions.

8.3 Effect of protein modification on the adsorption to positively and negatively charged latices

The 23 free carboxyl residues of β-cn were methyl-esterified to an extent of 35,

44 and 69%. It is not known which residues are methylated in each of the modified samples but as with dephosphorylation, methylation reduces the net negative charge on the protein. However, unlike dephosphorylation the sites of methylation occur relatively uniformly throughout the protein molecule. In addition methylation increases the hydrophobicity of the molecule. This explains why the 69% methylated β-cn is insoluble in the imidazole buffer at pH7.0.

When the binding of the 44% methylated β-cn to negatively charged LB1 latex was investigated the layer thickness was less than that of native β-cn. As with dephosphorylated β-cn, the net negative charge on the loop region was probably less than that of the native β-cn molecule. This reduction in the net negative charge in the loop region reduces the repulsion between this end of the protein and the negatively charged latex surface and allows the loop to lie closer to the surface.

Addition of low concentrations of native or modified β-cn to positively charged amidine latex resulted in massive aggregation. Once again, this was probably due to a bridging effect with the negatively charged portions of the proteins forming a bridge between the positively charged latices and causing a large increase in particle size. Once the latex surface is sufficiently coated with protein this bridging effect cannot occur.

On the positively charged amidine latex, the layer thicknesses of native and dephosphorylated β-cn were similar at 15 to 16nm. However, the layer thickness of the 44% methylated β-cn was dramatically reduced to only 6nm. This suggests that the adsorption of the 44% methylated β-cn to the positively charged latex is affected more by the increased hydrophobicity resulting from the methylation which would cause the protein to lie closer to the latex surface, than by the reduction in the net

negative charge which would have the opposite effect.

The behaviour of the 35% methylated β-cn which gave layer thicknesses similar to native β-cn on both positively and negatively charged surfaces, was more difficult to explain. Methylation of 35% of the free carboxyl groups in the β-cn molecule is equivalent to the modification of 8 residues. If most of these were located in the "train" segment of the molecule, they may have little effect on the behaviour of the loop and hence on the overall protein layer thickness. Methylation of 44% of the free carboxyl groups is equivalent to an extra 2 residues being esterified. This has a dramatic effect on the behaviour of the adsorbed protein and this indicates that there is a fine threshold with regard to the effect which methylation has on the structure of the protein at the interface.

The effect of glycosylation on the adsorption of κ-cn was also investigated by fractionating the naturally occurring protein variants into samples having varying degrees of glycosylation. Although not chemically modified in the laboratory, it is still included in this section as a protein modification. Glycosylation occurs on threonine residues in the N-terminal macropeptide region. Therefore, the flexible macropeptide becomes increasingly more negatively charged as the amount of glycosylation increases.

When the binding of the κ-cn A and B fractions to negatively charged LB1 latex was determined, the addition of 2-mercaptoethanol was seen to cause a reduction in protein layer thickness. This was probably due to 2-mercaptoethanol disrupting κ-cn polymers so that monomeric κ-cn adsorbed to the surface. With both κ-cn phenotypes, the protein layer thickness increased with the extent of glycosylation. Again this was probably due to electrostatic repulsion between the negatively charged surface and the

negatively charged macropeptide region of κ-cn. In the absence of any other non-electrostatic effects due to NeuAc residues, the layer thicknesses on the positively charged amidine latex should decrease with increasing glycosylation due to increasing electrostatic attraction between the positively charged surface and negatively charged region of κ-cn. This did not occur with κ-cn A. Therefore, the increased hydrophilicity due to the presence of the NeuAc groups must outweigh the electrostatic attraction effect. This balance also explains why whole κ-cn A forms slightly thicker layers than κ-cn B on the positively charged amidine latex. κ-Cn A has one more negative charge which should result in thinner layers. However, it also has an extra NeuAc group and once again, the increased hydrophilicity outweighs the electrostatic attraction effect.

The research in this thesis has shown the role which charge plays in the adsorption behaviour in the liposome/latex-protein system. This may be important not only with respect to the long-term stability of food systems but also in the use of liposomes as drug carrier systems.

References

1 KRUYT, H.R. (Ed.) (1952) *Colloid Science. Vol. I. Irreversible Systems*, Elsevier, Amsterdam.

2 DICKINSON, E. and STAINSBY, G. (Eds.) (1982) *Colloids in food*, Applied Science Publishers, London and New York.

3 LYKLEMA, J. (1991) *Fundamentals of Interface and Colloid Science. Vol. I Fundamentals*, Academic Press, London.

4 WALSTRA, P. (1993) In *Food Colloids and Polymers : Stability and Mechanical Properties*, (eds. E. Dickinson and P. Walstra) Royal Society of Chemistry, Cambridge, UK, p3.

5 MEIER, D.J. (1967) *Journal of Physical Chemistry*, **71**, 1861.

6 HESSELINK, F.Th. (1969) *Journal of Physical Chemistry*, **73**, 3488.

7 FISCHER, E.W. (1958) *Kolloid-Zeitschrift*, **160**, 120.

8 FLORY, P.J. and KRIGBAUM, W.R. (1950) *Journal of Chemical Physics*, **18**, 1086.

9 FLEER, G.J. and SCHEUTJENS, J.M.H.M. (1992) In *Coagulation and Flocculation : Theory and Applications*, (Ed. B. Dobias) Dekker, New York.

10 FLEER, G.J. and LYKLEMA, J. (1974) *Journal of Colloid and Interface Science*, **46**, 1.

11 VRIJ, A. (1976) *Pure and Applied Chemistry*, **48**, 471.

12 BERGENSTÅHL, B. (1988) In *Gums and Stabilizers for the Food Industry*, (Eds. G.O. Phillips, P.A. Williams and D.J. Wedlock) IRL Press, Oxford, **4**, p363.

13 MACRITCHIE, F. (1977) *Journal of Colloid and Interface Science*, **61**, 223

14 DICKINSON, E. and MATSUMURA, Y. (1991) *International Journal of Biological Macromolecules*, **13**, 26.

15 DICKINSON, E., ROLFE, S.E. and DALGLEISH, D.G. (1990) *International Journal of Biological Macromolecules*, **12**, 189.

16 DALGLEISH, D.G. (1991) In *Food Polymers, Gels and Colloids*, (Ed. E. Dickinson) Royal Society of Chemistry, Cambridge, UK, p485.

17 COURTHAUDON, J-L., DICKINSON, E. and CHRISTIE, W.W. (1991) *Journal of Agricultural and Food Chemistry*, **39**, 1365.

18 COURTHAUDON, J-L., DICKINSON, E. and DALGLEISH, D.G. (1991) *Journal of Colloid and Interface Science*, **145**, 390.

19 DICKINSON, E and GELIN, J-L. (1992) *Colloids and Surfaces*, **63**, 329.

20 WILDE, P.J. and CLARK, D.C. (1993) *Journal of Colloid and Interface Science*, **155**, 48.

21 DICKINSON, E. and WOSKETT, C.M. (1989) In *Food Colloids*, (Eds. R.D. Bee, P. Richmond and J. Mingins) Royal Society of Chemistry, Cambridge, p74.

22 DARLING, D.F. and BIRKETT, R.J. (1987) In *Food Emulsions and Foams*, (ed. E. Dickinson) Special Publication No. 58, Royal Society of Chemistry, London, p1.

23 KROG, N., BARFOD, N.M. and BUCHHEIM, W. (1987) In *Food Emulsions and Foams*, (Ed. E. Dickinson) Special Publication No. 58, Royal Society of Chemistry, London, p144.

24 DICKINSON, E., ROLFE, S.E. and DALGLEISH, D.G. (1989) *Food Hydrocolloids*, **3**, 193.

25 DALGLEISH, D.G., EUSTON, S.E., HUNT, J.A. and DICKINSON, E. (1991) In *Food Polymers, Gels and Colloids*, (Ed. E. Dickinson) Royal Society of Chemistry, Cambridge, p485.

26 DICKINSON, E., ROLFE, S.E. and DALGLEISH, D.G. (1988) *Food Hydrocolloids*, **2**, 397.

27 COURTHAUDON, J-L., DICKINSON, E., MATSUMURA, Y. and CLARK, D.C. (1991) *Colloids and Surfaces*, **56**, 293.

28 GRAHAM, D.E. and PHILLIPS, M.C. (1979) *Journal of Colloid and Interface Science*, **70**, 403.

29 GRAHAM, D.E. and PHILLIPS, M.C. (1979) *Journal of Colloid and Interface Science*, **70**, 415.

30 GRAHAM, D.E. and PHILLIPS, M.C. (1979) *Journal of Colloid and Interface Science*, **70**, 427.

31 DICKINSON, E. and STAINSBY, G. (Eds.) (1982) *Colloids in food*, Applied Science Publishers, London and New York, p308.

32 LEAVER, J. and DALGLEISH, D.G. (1990) *Biochimica et Biophysica Acta*, **1041**, 217.

33 DALGLEISH, D.G. and LEAVER, J. (1991) In *Food Polymers, Gels and Colloids*, (Ed. E. Dickinson) Royal Society of Chemistry, Cambridge, U.K., p113.

34 DALGLEISH, D.G. and LEAVER, J. (1991) *Journal of Colloid and Interface Science*, **141**, 288.

35 MURRAY, E.K. (1987) In *Food Emulsions and Foams*, (Ed. E. Dickinson) Royal Society of Chemistry, Cambridge, UK, p170.

36 HUNTER, J.R., KILPATRICK, P.K. and CARBONELL, P.G. (1991) *Journal of Colloid and Interface Science*, **142**, 429.

37 DICKINSON, E. (1992) *Journal Chemical Society Faraday Transactions*, **88**, 2973.

38 ELGERSMA, A.V., ZSOM, R.L.J., NORDE, W. and LYKLEMA, J. (1990) *Journal of Colloid and Interface Science*, **138**, 145.

39 MACKIE, A.R., MINGINS, J and NORTH, A.N. (1991) *Journal of Chemical Society Faraday Transactions*, **87**, 3043.

40 BRUNNER, J.R. (1977) In *Food Proteins*, (Eds. J.R. Whitaker and S.R. Tannenbaum) AVI Publishing Company, Inc. Westport, Connecticutt, USA, p175.

41 WHITE, J.C.D. and DAVIES, D.T. (1958) *Journal of Dairy Research*, **25**, 236.

42 ASCHAFFENBURG, R. and DREWRY, J. (1957) *Nature*, **180**, 376.

43 THOMPSON, M.P., KIDDY, C.A., PEPPER, L. and ZITTLE, C.A. (1962) *Nature*, **195**, 1001.

44 GROSCLAUDE, F., PUJOLLE, J., GARNIER, J. and RIBADEAU DUMAS, B. (1966) *Annalis de Biologie Animale Biochimie et Biophysique*, **6**, 215.

45 EIGEL, W.N., BUTLER, J.E., ERNSTROM, C.A., FARRELL, H.M., HARWALKAR, V.R., JENNESS, R. and WHITNEY, R. McL (1984) *Journal of Dairy Science*, **67**, 1599.

46 ASCHAFFENBURG, R. (1961) *Nature*, **192**, 431.

47 PETERSON, R.F. and KOPFLER, F.C. (1966) *Biochemical and Biophysical Research Communications*, **22**, 388.

48 ASCHAFFENBURG, R., SEN, A. and THOMPSON, M.P. (1966) *Comparative Biochemistry and Physiology*, **25**, 177.

49 ASCHAFFENBURG, R., SEN, A. and THOMPSON, M.P. (1968) *Comparative Biochemistry and Physiology*, **25**, 177.

50 NEELIN, J.M. (1964) *Journal of Dairy Science*, **47**, 506.

51 SCHMIDT, D.G. (1964) *Biochimica et Biophysica Acta*, **90**, 411.

52 WOYCHIK, J.H. (1964) *Biochemical and Biophysical Research Communications*, **16**, 267.

53 Di STASIO, L. and MERLIN, P. (1979) *Rivista Zootecnica*, **2**, 64.

54 SEIBERT, B., ERHARDT, G. and SENFT, B. (1987) *Animal Genetics*, **18**, 269.

55 ERHARDT, G. (1989) *Journal of Animal Breeding and Genetics*, **106**, 255.

56 McKENZIE, H.A. (1967) *Advances in Protein Chemistry*, **22**, 55.

57 GROSCLAUDE, F., GARNIER, J., RIBADEAU DUMAS, B. and JEUNET, R. (1964) *Compte Rendu de l'Académie des Sciences*, **259**, 1569.

58 KING, J.W.B., ASCHAFFENBURG, R., KIDDY, C.A. and THOMPSON, M.P. (1965) *Nature*, **206**, 324.

59 LARSEN, B. and THYMANN, M. (1966) *Acta Veterinaria Scandinavica*, **7**, 189.

60 WAKE, R.G. and BALDWIN, R.L. (1961) *Biochimica et Biophysica Acta*, **47**, 225.

61 SWAISGOOD, H.E. (Ed.) (1975) In *Methods of Gel Electrophoresis of Milk Proteins*, American Dairy Science Association.

62 THOMPSON, M.P. (1970) *Journal of Dairy Science*, **53**, 1341.

63 SWAISGOOD, H.E. (1982) In *Developments in Dairy Chemistry 1.*, (ed. P. Fox) Applied Science, London, p1.

64 ASCHAFFENBURG, R. (1964) *Biochimica et Biophysica Acta*, **82**, 188.

65 MICHALAK, W. (1967) *Journal of Dairy Science*, **50**, 131.

66 LEAVER, J. and LAW, A.J.R. (1992) *Journal of Dairy Research*, **59**, 557.

67 SWAISGOOD, H.E. (1973) *CRC Critical Reviews Food Technology*, **3**, 375.

68 DOI, H., KAWAGUCHI, N., IBUKI, F. and KANAMORI, M. (1979) *Journal of Nutritional Science and Vitaminology*, **25**, 95.

69 TRAN, V.D. and BAKER, B.E. (1970) *Journal of Dairy Science*, **53**, 1009.

70 FIAT, A-M., ALAIS, C and JOLLÈS, P. (1972) *European Journal of Biochemistry*, **27**, 408.

71 JOLLÈS, P. and FIAT, A-M. (1979) *Journal of Dairy Research*, **46**, 187.

72 KANAMORI, M., KAWAGUCHI, N., IBUKI, F. and DOI, H. (1980) *Agricultural and Biological Chemistry*, **44**, 1855.

73 CHOU, P.Y. and FASMAN, G.D. (1974) *Biochemistry*, **13**, 211.

74 CHOU, P.Y. and FASMAN, G.D. (1974) *Biochemistry*, **13**, 222.

75 CHOU, P.Y. and FASMAN, G.D. (1977) *Journal of Molecular Biology*, **115**, 135.

76 SWAISGOOD, H.E. (1992) In *Advanced Dairy Chemistry. Volume 1 : Proteins*, (Ed. P.F. Fox) Elsevier Science Publishers Ltd., Barking, Essex, U.K., p63.

77 DALGLEISH, D.G. (1993) *Colloids and Surfaces B : Biointerfaces*, **1**, 1.

78 HERSKOVITS, T.T. (1966) *Biochemistry*, **5**, 1018.

79 HOLT, C. and SAWYER, L. (1993) *Journal of the Chemical Society Faraday Transactions*, **89**, 2567.

80 CHURCH, F.C., CATIGNANI, G.L. and SWAISGOOD, H.E. (1981) *Journal of Dairy Science*, **64**, 724.

81 FOX, P.F. (1969) *Journal of Dairy Science*, **52**, 1214.

82 FOX, P.F. and GUINEY, J. (1973) *Journal of Dairy Research*, **40**, 229.

83 ANDREWS, A.L., ATKINSON, D., EVANS, M.T.A., FINER, E.G., GREEN, J.P.,PHILLIPS, M.C. and ROBERTSON, R.N. (1979) *Biopolymers*, **18**, 1105.

84 REIMERDES, E.H. and HERLITZ, E. (1979) *Journal of Dairy Research*, **46**, 219.

85 HILL, R.J. and WAKE, R.G. (1969) *Nature*, **221**, 635.

86 DELFOUR, A., JOLLÈS, J., ALAIS, C and JOLLÈS, P. (1965) *Biochemical and Biophysical Research Communications*, **19**, 452.

87 JOLLÈS, J., ALAIS, C and JOLLÈS, P. (1968) *Biochimica et Biophysica Acta*, **168**, 591.

88 LOUCHEUX-LEFEBVRE, M-H., AUBERT, J.P. and JOLLÈS, P. (1978) *Biophysical Journal*, **23**, 323.

89 SWAISGOOD, H.E., BRUNNER, J.R. and LILLEVIK, H.A. (1964) *Biochemistry*, **3**, 1616.

90 JANOLINO, V.G. and SWAISGOOD, H.E. (1975) *Journal of Biological Chemistry*, **250**, 2532.

91 PHILLIPS, N.I., JENNESS, R. and KALAN, E.B. (1967) *Archives Biochemistry and Biophysics*, **120**, 192.

92 McKENZIE, H.A., RALSTON, G.B. and SHAW, D.C. (1972) *Biochemistry*, **11**, 4539.

93 PREAUX, G. and LONTIE, R. (1972) *Archives Internationales de Physiologie et de Biochimie*, **80**, 980.

94 DECKMYN, H. and PREAUX, G. (1978) *Archives Internationales de Physiologie et de Biochimie*, **86**, 938.

95 GREEN, D.W., ASCHAFFENBURG, R., CAMERMAN, A., COPPOLA, J.C., DIAMOND, R.D., DUNNILL, P., SIMMONS, R.M., KOMOROWSKI, E.S., SAWYER, L., TURNER, E.M.C. and WOODS, K.F. (1979) *Journal of Molecular Biology*, **131**, 375.

96 PAPIZ, M.Z., SAWYER, L., ELIOPOULOS, E.E., NORTH, A.C.T., FINDLAY, J.B.C., SIVAPRASADARAO, R., JONES, T.A., NEWCOMER, M.E. and KRAULIS, P.J. (1986) *Nature*, **324**, 383.

97 PAYENS, T.A.J. and VAN MARKWIJK, B.W. (1963) *Biochimica et Biophysica Acta*, **71**, 517.

98 TALBOT, B and WAUGH, D.F. (1970) *Biochemistry*, **9**, 2807.

99 DALGLEISH, D.G. and PARKER, T.G. (1980) *Journal of Dairy Research*, **47**, 113.

100 PARKER, T.G. and DALGLEISH, D.G. (1981) *Journal of Dairy Research*, **48**, 71.

101 HORNE, D.S. and DALGLEISH, D.G. (1980) *International Journal of Biological Macromolecules*, **2**, 154.

102 DICKSON, I.R. and PERKINS, D.J. 1971) *Biochemistry Journal*, **124**, 235.

103 PIEZ, K.A., DAVIE, E.W., FOLK, J.E. and GLADNER, J.A. (1961) *Journal of Biological Chemistry*, **236**, 2912.

104 M'KENZIE, H.A. (Ed.) (1971) In *Milk Proteins, Chemistry and Molecular Biology II*, Academic Press, New York, p308.

105 KLOSTERGAARD, H. and PASTERNAK, R.A. (1957) *Journal of American Chemical Society*, **79**, 5671.

106 KUMOSINSKI, T.F. and TIMASHEFF, S.N. (1966) *Journal of American Chemical Society*, **88**, 5635.

107 MACKIE, A.R., MINGINS, J. and DANN, R. (1991) In *Food Polymers, Gels and Colloids*, (Ed. E. Dickinson) Royal Society of Chemistry, Cambridge, p96.

108 TOWNEND, R., KERSKOVITS, T.T., TIMASHEFF, S.N. and GORBUNOFF, M.J. (1969) *Archives Biochemistry and Biophysics*, **129**, 567.

109 TANFORD, C. and NOZAKI, Y. (1959) *Journal of Biological Chemistry*, **234**, 2874.

110 TANFORD, C. and TAGGART, V.G. (1961) *Journal of American Chemical Society*, **10**, 2738.

111 TIMASHEFF, S.N., MESCANTI, L., BASCH,.J.J. and TOWNEND, R. (1966) *Journal of Biological Chemistry*, **241**, 2496.

112 BASCH, J.J. and TIMASHEFF, S.N. (1967) *Archives of Biochemistry and Biophysics*, **118**, 37.

113 TIMASHEFF, S.N., TOWNEND, R. and MESCANTI, L. (1966) *Journal of Biological Chemistry*, **241**, 1863.

114 TOWNEND, R., KUMOSINSKI, T.F. and TIMASHEFF, S.N. (1967) *Journal of Biological Chemistry*, **242**, 4538.

115 HAMBLING, S.G., McALPINE, A.S. and SAWYER, L. (1992) In *Advanced Dairy Chemistry Volume 1 Proteins*, (Ed. P.F. Fox) Elsevier Science Publishers Limited, Barking, Essex, UK, p141.

116 KOPPEL, D.E. (1972) *Journal of Chemical Physics*, **57**, 4814.

117 GUNSTONE, F.D., HARWOOD, J.L. and PADLEY, F.B. (Eds.) (1986) In *The Lipid Handbook*, Chapman and Hall, London, p29.

118 GUNSTONE, F.D., HARWOOD, J.L. and PADLEY, F.B. (Eds.) (1986) In *The Lipid Handbook*, Chapman and Hall, London, p327.

119 PASTOR, R.W., VENABLE, R.M. and KARPLUS, M. (1991) *Proceedings of National Academy Science USA*, **88**, 892.

120 McDOUGAL, I.R. (1978) *Scottish Medical Journal*, **23**, 6.

121 BONTÉ, F. and JULIANO, R.L. (1986) *Chemistry and Physics of Lipids*, **40**, 359.

122 DALGLEISH, D.G. (1990) *Colloids and Surfaces*, **46**, 141.

123 PRICE, J.C., GRIFFIN, W.G. and GRIFFIN, M.C.A. (1991) *Biochemical Society Transactions*, **19**, 508.

124 LEAVER, J. and HORNE, D.S. (1993) In *Food Colloids and Polymers: Stability and Mechanical Properties*, (Eds. E. Dickinson and P. Walstra) Royal Society of Chemistry, London, p332.

125 ARMSTRONG, J.M^{c}D., M^{c}KENZIE, H.A. and SAWYER, W.H. (1967) *Biochimica et Biophysica Acta*, **147**, 60.

126 BINGHAM, E.W., FARRELL Jr., H.M. and CARROLL, R.J. (1972) *Biochemistry*, **11**, 2450.

127 HUNDRIESER, K.E., CLARK, R.M. and JENSEN, R.G. (1985) *American Journal of Clinical Nutrition*, **41**, 988.

128 NEW, R.R.C. (Ed.) (1990) In *Liposomes: A Practical Approach*, Oxford University Press, Oxford, p105.

129 JULLIEN, S., VERTUT-CROQUIN, A., BRAJTBURG, J. and BOLARD, J. (1988) *Analytical Biochemistry*, **172**, 197.

130 HERNÁNDEZ-CASELLES, T., VILLALAÍN, J. and GÓMEZ-FERNÁNDEZ, J.C. (1990) *Journal of Pharmacy and Pharmacology*, **42**, 397.

131 BRANDL, M., BACHMANN, D., DRECHSLER, M. and BAUER, K.H. (1990) *Drug Development and Industrial Pharmacology*, **16**, 2167.

132 CHIANCONE, E. and GATTONI, M. (1991) *Journal of Chromatography*, **539**, 455.

133 HAUSER, H. and PHILLIPS, M.C. (1979) In *Progress in Surface and Membrane Science*, (Eds. D.A. Cadenhead and J.F. Danielli) Academic Press, New York, **13**, p297.

134 CORNELL, D.G. (1982) *Journal of Colloid and Interface Science*, **88**, 536.

135 MULDER, H and WALSTRA, P. (1974) *The Milk Fat Globule*, Commonwealth Agricultural Bureaux, Farnham Royal, Bucks. England.

136 CHOBERT, J-M., TOUATI, A. BERTRAND-HARB, C., DALGALARRONDO, M., NICOLAS, M-G. and HAERTLÉ, T. (1990) *Journal of Agricultural and Food Chemistry*, **38**, 1321.

137 CAYOT, P., COURTHAUDON, J-L. and LORIENT, D. (1991) *Journal of Agricultural and Food Chemistry*, **39**, 1369.

138 BRADFORD, M.M. (1976) *Analytical Biochemistry*, **72**, 248.

139 DICKINSON, E., ROBSON, E.W. and STAINSBY, G. (1983) *Journal of Chemical Society Faraday Transactions*,**79**, 2937.

140 DALGLEISH, D.G., DICKINSON, E. and WHYMAN, R.H. (1985) *Journal of Colloid and Interface Science*, **108**, 174.

141 DICKINSON, E., WHYMAN, R.H. and DALGLEISH, D.G. (1987) In *Food Emulsions and Foams*, (Ed. E.Dickinson) Royal Society of Chemistry, London, p40.

142 KUMOSINSKI, T.F., BROWN, E.M. and FARRELL, H.M. (1993) *Journal of Dairy Science*, **76**, 931.

143 DICKINSON, E., HORNE, D.S., PHIPPS, J.S. and RICHARDSON, R.M. (1993) *Langmuir*, **9**, 242.

144 de GENNES, P.G. (1976) *Journal of Physics*, **37**, 1443.

145 de GENNES, P.G. (1980) *Macromolecules*, **13**, 1069.

146 MORR, C.V. (1982) In *Developments in Dairy Chemistry - 1*, (Ed. P.F. Fox) Applied Science Publications, London, p375.

147 MODLER, H.W. (1985) *Journal of Dairy Science*, **68**, 2195.

148 WEBB, B.H. and WHITTIER, E.O. (1970) *By-products from milk*, AVI Publishing, Westport, C.T.

149 KESTER, J.J. and RICHARDSON, T. (1984) *Journal of Dairy Science*, **67**, 2757.

150 DUFOUR, E. and HAERTLÉ, T. (1991) *Biochimica et Biophysica Acta*, **1079**, 316.

151 MEANS, G.E. and FEENEY, R.E. (1968) *Biochemistry*, **7**, 2192.

152 FRAENKEL-CONRAT, H. and OLCOTT, H.S. (1945) *Journal of Biological Chemistry*, **161**, 259.

153 WILCOX, P.E. (1967) *Methods in Enzymology*, **11**, 605.

154 BERTRAND-HARB, C., CHOBERT, J-M, DUFOUR, E. and HAERTLÉ, T. (1991) *Sciences des Aliments*, **11**, 641.

155 RICHARDSON, T. (1985) *Journal of Dairy Science*, **68**, 2753.

156 EIGEL, W.N., BUTLER, J.E., ERNSTROM, C.A., FARRELL, H.M., HARWALKAR, V.R., JENNESS, R. and WHITNEY, R.McL. (1984) *Journal of Dairy Science*, **67**, 1599.

157 HOLT, C. (1992) In *Advances in Protein Chemistry*, (eds. C.B. Anfinsen, J.T. Edsall, F.M. Richards and D.S. Eisenberg) Academic Press, New York, **43**, p63.

158 WALSTRA, P., BLOOMFIELD, V.A., WEI, G.J. and JENNESS, R. (1981) *Biochimica et Biophysica Acta*, **669**, 258.

159 HORNE, D.S. (1984) *Biopolymers*, **23**, 989.

160 DAVIES, D.T. and LAW, A.J.R. (1987) *Journal of Dairy Research*, **54**, 369.

161 VREEMAN, H.J., BOTH, P., BRINKHUIS, J.A. and Van der SPEK, C.A. (1977) *Biochimica et Biophysica Acta*, **491**, 93.

162 VREEMAN, H.J., VISSER, S., SLANGEN, C.J. and VANRIEL, J.A.M. (1986) *Biochemical Journal*, **240**, 87.

163 FERRON-BAUMY, C., MOLLÉ, D., GARRIC, G. and MAUBOIS, J.L. (1992) *Lait*, **72**, 165.

164 REDDY, I.M. and KINSELLA, J.E. (1990) *Journal of Agricultural and Food Chemistry*, **38**, 50.